

## 23. GEOCHEMISTRY AND PETROLOGY OF VOLCANIC ASHES RECOVERED FROM SITES 881 THROUGH 884: A TEMPORAL RECORD OF KAMCHATKA AND KURILE VOLCANISM<sup>1</sup>

L.-Q. Cao,<sup>2</sup> R.J. Arculus,<sup>2,3</sup> and B.C. McKelvey<sup>2</sup>

### ABSTRACT

One hundred and fifty-four ash layers were sampled during ODP Leg 145 at Sites 881, 882, 883, and 884, in the northwest Pacific. The Miocene to Recent ashes are interpreted to be explosive eruption products of the Kurile-Kamchatka arc system. On the basis of number and thickness of ash layers within given time intervals, it appears that at least five major pulses of subaerial volcanism occurred during the last 3 Ma, with a remarkable increase in the number and thickness of layers commencing at ~2.6 Ma. Ash layers are absent in the age interval 34.4 to 6.3 Ma, but are present in the lower Oligocene to middle Eocene. High Ba/Nb (~200) of the Paleogene ashes is consistent with derivation from an island arc rather than mid-ocean ridge or hot-spot source.

Several huge explosive events are inferred, with the thickest ash layer  $\leq 2.5$  meters at Site 884. Dry clay-free ash colors are without exception light- to yellowish grays (hue 2.5Y). The ashes consist of microlites (plagioclase, clinopyroxene, quartz, and Fe-Ti oxides) and vitric shards. Elongate ( $\approx 5$  to  $\approx <100$  mm), tubular, and bubble wall fragments are ubiquitous and were probably derived from plinian eruption cloud fallout at distances in excess of the present 600 km from the active arc.

Major element analyses of about 2000 individual vitric shards were obtained by electron microprobe, and the abundances of a range of large ion lithophile (including rare earth) and high field strength trace elements have been determined for a subset of about 100 ash layers by inductively coupled plasma source mass spectrometry.  $^{143}\text{Nd}/^{144}\text{Nd}$  and  $^{87}\text{Sr}/^{86}\text{Sr}$  were determined for an acid-leached subset of 40 of these vitric shards.

A compositional spectrum from basaltic andesite through dacite to rhyolite exists in these ash layers, but the majority of them are rhyolitic. An extensive range from low- through medium- to high-K compositions is present, but all are tholeiitic on the basis of the  $\text{FeO}^*/\text{MgO}$  vs. wt%  $\text{SiO}_2$  criterion. On the basis of distinctive major and trace element characteristics for the Miocene and younger ashes, we recognize 12 compositional groupings. These range in terms of rare earth element (REE) abundances from light REE-depleted through relatively unfractionated to light REE-enriched compared with chondrites. The degree of relative light REE enrichment is positively correlated with the K content. Negative Eu anomalies are characteristic of the majority of the samples. Most of the samples overlap the isotopic range of the currently active Kamchatka-Kurile arc with  $\epsilon_{\text{Nd}}$  of  $\sim +8$  and  $^{87}\text{Sr}/^{86}\text{Sr} = 0.7031$  to 0.7038, but some samples range to a lower  $\epsilon_{\text{Nd}}$  of +3 and  $^{87}\text{Sr}/^{86}\text{Sr}$  of  $\sim 0.7045$ .

Nine trace elements (Rb, Ba, Th, U, La, Ce, Y, Yb, and Lu) are particularly useful for discriminating between the compositional groups within the ashes, and for comparison with the major subaerial volcanic belts in the Kurile-Kamchatka arc system. Some strong variations in abundances and ratios (Rb/Ba, Th/U) were noted and may prove to be diagnostic of particular geographic sources.

### INTRODUCTION

Spatial variation of chemical composition and physical parameters such as volumes of erupted materials within island arcs were recognized by Kuno (1959) and Sugimura, (1960). Appreciation of the fundamental role of island arc magmatism in the genesis of the continental crust (Taylor, 1967) stimulated a search for evidence of temporal controls on petrogenesis leading to suggestions that nascent low-alkali through intermediate- to highly alkaline "mature" systems correlated with changes in crustal character from intraoceanic to continental (Baker, 1968; Gill, 1970). Within any individual arc however, the typically incomplete or poor onland exposures render deciphering the temporal record an awkward task and restrict our view to a narrow period of development. Experience has shown that lengthy records of arc activity, either as ash- or volcaniclastic-rich turbidite layers, can be obtained by drilling deposits in the marine realm that are optimally placed to avoid disturbance and reworking with reasonable penetration thicknesses. Disadvantages include the difficulty of precisely identifying the sources of these materials, technical drilling problems with the recovery of coarse clastic sequences, the possibil-

ity of incomplete records through erosion and nondeposition, and the problems of diagenetic change as a result of exposure to seawater.

Concentrations of ash and distinct ash layers can persist despite slumping and/or erosion by bottom currents and bioturbation. We have found that fresh volcanic glass can persist in layers up to 35 Ma old, and even some older. Single eruptive episodes were probably responsible for homogeneous layers (type I of Huang, 1980) whereas multiple eruptions from different sources or mixed magmas are most likely the origin of heterogeneous layers (type II of Huang, 1980). Shards, tubular-elongate micropumice, bubble wall, and U- to Y-shaped fragments are common and probably associated with Plinian eruptions. Apparently pristine igneous trends can be distinguished from analysis of many of these materials, and magmatic Sr isotopic ratios have been recovered with comparatively mild leaching treatment of glass shards.

During late 1988 through late 1992, the Ocean Drilling Program (ODP) successfully recovered extensive cores of volcaniclastic materials overlying basement from a number of sites within ash fallout/pumice drift range of convergent margins of the western Pacific. The areas targeted by these studies include the Sulu and Celebes Seas (Pouclet et al., 1991), Izu-Bonin forearc (Arculus and Bloomfield 1992; Fujioka et al., 1992), Izu-Bonin backarc (Rodolfo et al., 1992), Japan Sea (Pouclet et al., 1992; Pouclet and Scott, 1992), and Vanuatu (Baker et al., 1994). More generalized regional comparisons have also been documented by Cambray (1991). Allied with the results of analytical and interpretative efforts targeted on cores obtained during the predecessor efforts of the Deep Sea Drilling Project (DSDP) in some of these systems, we now have an improved appreciation for the factors that appear to be critical in controlling aspects of the geochem-

<sup>1</sup> Rea, D.K., Basov, I.A., Scholl, D.W., and Allan, J.F. (Eds.), 1995. *Proc. ODP, Sci. Results*, 145: College Station, TX (Ocean Drilling Program).

<sup>2</sup> Department of Geology and Geophysics, University of New England, Armidale, New South Wales 2351, Australia.

<sup>3</sup> Present address: Department of Geology, Australian National University, Canberra, ACT 0200, Australia.

istry. Some of the questions and issues that have been addressed by these efforts include a number that have long been important in studies of supra-subduction zone magmatism:

1. Are there any temporal changes in the geochemistry of arc magmas;
2. If so, are these regular, erratic, or blends of these end-member behaviors;
3. Can we detect crustal growth using geochemical parameters believed to correlate at least globally with crustal thicknesses;
4. Can changes in the style of eruptive activity and/or geochemistry be attributed to distinct tectonic events;
5. Is there interarc synchronicity of major periods of explosive activity;
6. Do episodes of major explosive activity in arcs correlate with climate change?

The advanced piston coring techniques deployed during Leg 145 were successfully used to recover substantial distal records of volcanic activity of the Kurile-Kamchatka arc in sediments ranging in age from middle Eocene to Holocene on the inbound Pacific plate. Recoveries approaching 100% at Sites 881, 882, 883, and 884 provide an unique record of subaerial explosive volcanism in the northwestern Pacific Ocean. About 360 ash layers, ranging from less than 1 cm to more than 370 cm in thickness, were observed at Holes 881A, 881B, and 881C drilled about 700 km southeast of the southern tip of Kamchatka (at  $47^{\circ}6'N$ ,  $169^{\circ}29'E$ ), and at Holes 882A, 883B and 884B drilled on the upper part of Detroit Seamount (at  $50^{\circ}51'N$ ,  $167^{\circ}168'E$ ) about 700 km east southeast of Petropavlovsk (Fig. 1). Site 881 also represented the northernmost continuation of a north-south traverse initiated on DSDP Leg 86 (Heath, Burckle, et al., 1985), and the Detroit Seamount sites can be compared with the shorter recovery from the Meiji Seamount DSDP Leg 19 Site 192 (Creager, Scholl, et al., 1973) (Fig. 1).

A strategy of sampling based on representative downhole coverage was adopted, and about 40% of the recorded ash layers (totaling 130 out of ~325 ash layers) were collected for mineralogical, bulk major element, trace element, and isotopic analysis. In order to place the geochemical aspects of the study in context, a general understanding of stratigraphic and lithological characteristics of the volcanic ash layers is essential, requiring detailed information for every ash layer such as magnetic susceptibility, age, depth, thickness, color (dry and wet), morphologies of vitric shards, and surrounding lithology.

In this study, we report major-element analyses of individual glass shards obtained by electron microprobe (EMP), bulk layer analyses of trace elements by inductively coupled plasma source mass spectrometry (ICP-MS),  $^{143}\text{Nd}/^{144}\text{Nd}$  and  $^{87}\text{Sr}/^{86}\text{Sr}$  for acid-leached bulk glass samples, and representative EMP analyses of microlites of plagioclase, pyroxene, Fe-Ti oxides, biotite, and amphibole. With these data, we attempt to track compositional changes through time. Identification of possible ash sources on the basis of geochemical comparisons with published analyses for the different volcanic belts in Kurile-Kamchatka is at an early stage. We regard this as a preliminary effort in view of the wealth of samples yet to be studied and the variety of integrative analytical approaches still required.

## GENERAL GEOLOGY AND PREVIOUS STUDIES

The general prevailing wind and current directions coupled with the relative inactivity of the western Aleutian arc lead us to believe that the predominant source of the ash layers recovered at Sites 881 to 884 is the Kurile-Kamchatka arc system. We note that prominent although sparse ash layers derived from the Honshu-Kurile arc system were reported by Natland (1993) at Site 810 on the Shatsky Rise, at present located at some 1600 km from the arc. Thus, in terms only of distance of travel, a Kurile-Kamchatka source is plausible. In addition, the general overlap of compositions recovered at Site 881

vs. Sites 882–884, including the distinctively potassic groups, are more likely to have been derived collectively from the nearest potentially active arc source.

The considerable body of literature published on the Kurile-Kamchatka arc system by Russian scientists since the 1950s relates to regional geology, geophysical characteristics, petrology, geochemistry, and physical volcanology (Fedotov and Masurenkov, 1991). The Kurile-Kamchatka arc has a total length of 2000 km and is about 400 km wide on the Kamchatka peninsula. Three major, active subaerial volcanic belts are distributed parallel to the Kurile-Kamchatka trench in the peninsula. These belts, located at different tectonic positions above the Kurile-Kamchatka subduction zone, are (1) Sredinny (or Central) Range (SR); (2) Central Kamchatka Depression (CKD); and (3) East Kamchatka (EK), at distances of 400, 310, and 250 km from the trench, respectively. Some consider EK to comprise a northern and southern portions (Fedotov and Masurenkov, 1991). The most active island arc volcano in the world (Klyuchevskoy) is currently located within the CKD (Kersting and Arculus, 1994), together with a number of other highly explosive volcanoes. From north to south, these are Sheveluch, Klyuchevskoy, Bezymianny, and Tolbachik. The plinian eruption plume of the September–October 1994 eruption of Klyuchevskoy was witnessed by Space Shuttle astronauts to extend >2000 km to the southeast of the volcano.

The Kamchatka Peninsula is an amalgamation of accreted continental fragments, island arcs, and obducted oceanic crust including seamounts, which range from Jurassic to Cretaceous in age (Watson and Fujita, 1985). It appears that accretion began about 150 Ma ago in the western part of the peninsula, with the eastern side being the latest addition during the Miocene (Fedorchuk et al., 1993). The western part of Kamchatka is the eastern margin of the continental microplate of the Okhotsk block (Jolivet et al., 1988), which started to collide with Eurasia in the Late Jurassic. Closure continued until the Late Cretaceous.

Shantser and Shapiro (1988) proposed a detailed temporal development of Kurile-Kamchatka volcanism. Two main stages of evolution of volcanism are identified: the first stage commenced in the Late Cretaceous to the very beginning of the Paleocene (~70 to ~65 Ma), with volcanism exclusively in a submarine environment. The second stage commenced in the Paleocene and was dominated by subaerial volcanism. Three phases are identified in the second stage: (1) Paleocene-Eocene (63.5 to ~36.5 Ma): subaerial volcanism occurred in the West Kamchatka Trough, to the west of the SR (Moroz, 1988; Gnibidenko et al., 1972). This region is also known as the western Kamchatka alkaline province (Erlich, 1971). (2) Oligocene-Miocene (36.5 to ~5 Ma): subaerial volcanism was located in the present-day SR and South Kamchatka. Moroz (1988) argued that both of these belts form a continuous volcano-tectonic structure called the Kamchatka-Koryakskii anticlinorium. (3) Pliocene (5.1 to ~1.8 Ma): all of the modern subaerial volcanic belts were fully developed during this period, with a predominance of low- and medium-K series lavas.

Ash distribution and composition of some of the largest (plinian) Holocene eruptions were reported by Kir'yanov and Rozhkov (1990) and Kir'yanov et al. (1990). Airfall deposits are traceable over tens of thousands of square kilometers and several are known to have travelled toward the region of the Detroit Seamount, including, for example, the 7.7 ka caldera-forming Karymskii eruption and the 1.45 ka eruption of Opala. Bulk compositions of these major Holocene eruptions are generally andesite-dacite.

Lithological characteristics and bulk major element and selected trace element analyses of ash layers recovered at Site 192 (Fig. 1) have been reported by Creager, Scholl, et al. (1973) and Scheidegger et al. (1980) respectively. From 0 to 140 meters below seafloor (mbsf), which is equivalent in age to the late Pliocene, the abundant ash layers range up to 30 cm in thickness, and are composed of colorless to light brown glass and microlites of feldspar, pyroxene, and oxide minerals. Compositions range from dacite to rhyolite, with the majority of medium-K character, but a minority are high-K.

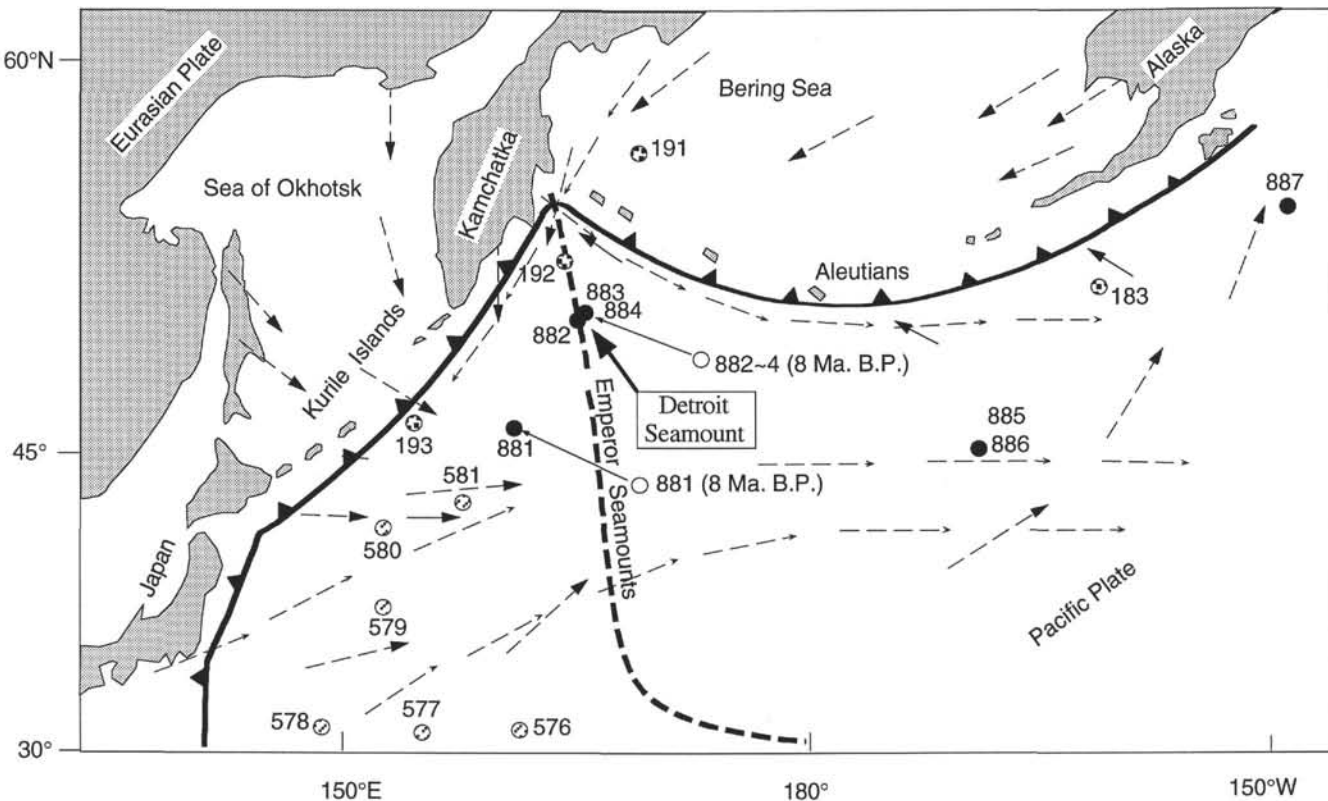


Figure 1. Map of the northwestern Pacific showing the locations of DSDP Legs 19 (Sites 183, 191–193) and 86 (Sites 576–581) and ODP Leg 145 Sites (solid circles). Other notations are the winter wind directions (dashed lines with large arrow heads), current directions (dashed lines with small arrow heads), directions of plate motion (solid line and arrow head), and reconstructed positions (arrow from open circles to present location) of Leg 145 Sites 881–884 for the past 8 m.y.

## **ANALYTICAL PROCEDURES**

At the University of New England (UNE), all the samples were examined under a petrographic microscope to determine the morphologies and sizes of the shards, noting in particular all samples containing a sufficient number large enough to analyze (at least 10 mm in diameter), and any significant organic and clay contamination. Ash samples were carefully washed with distilled water and dried at 105°C, affixed in an epoxy mounting ring, polished, and carbon coated.

The major element chemical composition of each vitric shard was obtained at UNE using a JEOL Model JSM35 electron microprobe with a KEVEX Si-Li energy dispersive spectrometer (EDS). Nine elements (Si, Ti, Al, Fe, Mn, Mg, Ca, K, and Na) were analyzed. Standard natural and synthetic glasses from the Smithsonian Institution were analyzed concurrently with excellent agreement between our analyses and the published values. Our experience with the UNE EMP is that the precision of multiple analyses of homogeneous glass standards produces concentration values within the expected range of X-ray counting statistics, and is a function of elemental abundance and counting time. Comparisons of analyses obtained with this instrument and a wavelength-dispersive (WDS) EMP (Camebax) at the University of Michigan (UM) and the Australian National University are generally excellent, although we prefer the EDS system because it minimizes sample damage in hydrous,  $\text{SiO}_2$ -rich glasses. For example, a comparison of the Na concentrations obtained by Arculus and Bloomfield (1992) for the ODP Leg 125 Izu-Bonin vitric shards using the EMP at UM, with values obtained at UNE, show significant differences involving up to 50% loss with the higher beam currents employed during WDS analysis. This loss occurred despite the use of a defocused and rastered beam spot. Operating conditions at UNE were 15 kV accelerating voltage, 10 nA beam current, and 100 s count time.

Many of the major element analyses total <100%. We believe this results from variable degrees of hydration of the glasses because

totals close to the nominal 100% were obtained concurrently with the essentially anhydrous Smithsonian glass standards. We did not detect any consistent correlations between the abundances of potential additions through seawater of major elements such as K or trace elements such as Sr, and the degree of apparent hydration (difference between the analytical total and 100%) of the glasses.

A subset of 100 samples was analyzed by ICP-MS at Monash University. Because of time limitations, we chose to study layers initially from the southern (881) and one of the Detroit Seamount Sites (882). With the ICP-MS technique, we obtained abundances for ~36 trace elements, including the rare earth elements (REE). We routinely ran a number of standard rocks as unknowns with generally excellent agreement with the accepted values. Data for the transition elements, however, such as Sc, V, Cr, Co, and Ni, seem to be less reliable by the ICP-MS technique given the relatively poor reproducibility observed.

Sample preparation involved digestion of  $0.1 \pm 0.03$  g of distilled water-washed ash sample for 24 to 48 hours in screw-top Teflon bombs at  $100^\circ$ – $120^\circ\text{C}$  in a mixture of distilled HF (4 mL) and distilled  $\text{HNO}_3$  (2 mL). Sample solutions were slowly dried with heatlamps, and converted from fluorides to nitrates with additions of concentrated  $\text{HNO}_3$ . Samples were then taken into solution with 50 g of 2%  $\text{HNO}_3$  (made from sub-boiled, distilled concentrated  $\text{HNO}_3$  and 18.2 MΩ Millipore  $\text{H}_2\text{O}$ ). Aliquots of this solution were run at a total dilution factor of  $\approx 2000$ . All samples were made up with 100 ppb In to serve as an internal standard for drift correction. One analytical blank and 5 standard solutions (based on U.S. Geological Survey standard rocks) were typically prepared for each run. An initial calibration was performed using synthetic standards and finalized with a set of laboratory and international standards. Total analytical blanks are typically  $< 20$  ppb for most elements except for Sc, Cr, Cu and Ni (which are  $< 500$  ppb). Errors are  $\pm 15$ – $20$  relative % for Sc, Ga, Ge, Pr, Gd, Th, and U depending on abundances,  $\pm 5$ – $10$  relative

% for the other REE and  $\pm$  3–15 relative % for all other trace elements analyzed.

Prior to separation of the Sr and Nd fractions for isotopic studies, we employed a relatively mild leaching process with HCl that we found was effective in returning consistent isotopic ratios without any sign of seawater contamination for glass shards from Legs 60 and 125 (W. Chen and R.J. Arculus, unpubl. data). The success of this procedure implies some addition of seawater Sr to the glasses, but at this stage we have not quantified the effect. Subsequently, we used standard techniques with ion-exchange separation columns for Sr and Nd at UNE, followed by thermal ionization mass spectrometry (VG 354 spectrometer) for Sr and Nd isotope ratios at the Center for Isotope Studies at North Ryde in Sydney. Reference standards throughout the course of analysis averaged values of  $^{87}\text{Sr}/^{86}\text{Sr} = 0.71027 \pm 1$  for NBS 987, and  $^{143}\text{Nd}/^{144}\text{Nd} = 0.51111 \pm 10$  for the O'Nions Nd standard. The  $^{87}\text{Sr}/^{86}\text{Sr}$  was normalized to  $^{86}\text{Sr}/^{88}\text{Sr} = 0.1194$ ,  $^{143}\text{Nd}/^{144}\text{Nd}$  was normalized to  $^{146}\text{Nd}/^{144}\text{Nd} = 0.7219$ , and  $\epsilon_{\text{Nd}}$  values were calculated assuming an average chondritic value of  $^{143}\text{Nd}/^{144}\text{Nd}$  at present of 0.512638.

## STRATIGRAPHY AND LITHOLOGY

The majority of the ash layers occur within the predominantly upper Miocene to Pleistocene clayey diatom ooze of the northwest Pacific (Fig. 2; Tables 1, 2, 3, and 4). Ages were estimated based on the stratigraphic positions of radiolarian and diatom datum levels in the vicinity of the ash layers provided by the Leg 145 Shipboard Scientific Party (Rea, Basov, Janecek, Palmer-Julson, et al., 1993). The most detailed estimation of the age of each ash layer was completed by interpolations assuming linear sedimentation rates in the different depth ranges; thus, the exact age (the accuracy is limited to 0.01 Ma) may not be reliable for fine stratigraphic dating, but it is still considered accurate enough to provide general correlations for each ash layer.

For Site 884 (Fig. 2D), it appears from the number and thickness of ash layers that there are pulses of increased explosive activity: 0.0 to  $\sim$ 0.2, 0.3 to  $\sim$ 0.4, 0.8 to  $\sim$ 1.0, and 1.5 to  $\sim$ 1.8 Ma during the Pliocene-Pleistocene-Holocene. Not all of these pulses of activity are obvious in the recovery at Sites 882 (Fig. 2B) and 883 (Fig. 2C), but do appear at Site 881 (Fig. 2A) with an additional pulse at 2.4 to  $\sim$ 2.6 Ma. Within any given pulse, the volcanic ashes are characterized by a wide compositional spectrum from basaltic andesite to rhyolite (Fig. 3), a wide range of potassium abundances (Fig. 4), and a wide range of La/Y ratios (Fig. 5). It is notable that these pulses of volcanism during the Pleistocene and Pliocene are also recognized in the Japan arc system (Pouplet and Scott, 1992).

A marked paucity of ash layers is noted during the period of 6.3 to  $\sim$ 34.4 Ma, but partly to completely altered ashes, now seen as yellow palagonite and smectite, reappear below lower Oligocene to middle Eocene nannofossil chalks and claystone (34.4–45 Ma), much of which is reworked and slumped (Rea, Basov, Janecek, Palmer-Julson, et al., 1993). There is a distinct difference in compositional mode between the ash layers younger than 6.3 Ma and those older than 34.4 Ma. The former are dominated by rhyolite while the latter are predominantly basaltic andesite.

Several remarkably thick ash layers are present at Sites 881 through 884. All of these huge ash layers are rhyolite in composition, light gray in color (dry sample), and characterized by sharply pointed, fragile, elongate vitric shards, which are consistent with air fall rather than pumice rafting. The thick layers are present as follows: (1) 110 cm thick between Sections 145-881A-1H-4 and -5, but curiously thinned or patchily represented in Holes 881B and 881C; (2) 130 cm thick in Section 145-884B-6H-2; (3) 40 cm thick in Section 145-884B-7H-2; (4) 50 cm thick in Section 145-884B-8H-7; (5) 180 cm thick between Sections 145-884B-9H-5 and -7; (6) 120 cm thick between sections 145-884B-9H-7 and 145-884B-10H-1; (7) 250 cm thick between Sections 145-884C-6H-4 and -5; (8) 140 cm thick between Sections 145-

884C-9H-3 and -4. Shipboard correlations between different holes were successful for Site 881 but not reported for Sites 882, 883, and 884, and, at present, we do not have sufficient chemical data to identify correlations within and among the different holes at these sites.

The correlation of distance of transport of tephra from an eruption source with physical parameters such as mean and maximum shard diameters and crystal/glass modal proportions have been well documented (Sparks and Walker, 1977; Walker, 1980; Carey and Sigurdsson, 1980; Kyle et al., 1981; Rose and Chesner, 1987). The mean diameters of vitric shards from Sites 881 through 884 are all  $\sim$ 30  $\mu\text{m}$  (phi value = 5), implying a source distance  $>$ 500 km (Rose and Chesner, 1987).

Two color assignments were made for the ashes. The first, for all of the layers, was recorded by the Leg 145 Shipboard Scientific Party, who estimated the color for wet samples, possibly with variable modulation by clay and ooze. In detail, the determination was variably made with the standard Munsell notation or more qualitatively (Rea, Basov, Janecek, Palmer-Julson, et al., 1993). Another set of colors, recorded by the authors for the restricted sample set, is assigned to dried, clay-free ash samples that had been carefully washed with distilled water. The revised standard soil color charts of Oyama and Takehara (1967), equivalent to Munsell, were used. It is interesting to note that all dry ash samples are characterized by the gray-dominated hue 2.5Y with no exception, although the wet (possible clay- and ooze-admixed) sample color varies considerably. We note a good correlation exists between ash composition and color: all rhyolites are light gray in color (hue 2.5Y, value 7 or 8, chroma 1 or 2) or grayish yellow (hue 2.5Y, value 7, chroma 2); dacite-rhyolite (mixtures of the two compositions) are yellowish gray (hue 2.5Y, value 6, chroma 1); most andesite-dacite (mixtures of the two compositions) are yellowish gray (hue 2.5, value 4, 5, and 6, chroma 1); and basaltic andesites are yellowish gray (hue 2.5Y, value 3, 4, and 5, chroma 1 or 2).

## GEOCHEMISTRY

### Major Element Geochemistry

About 2000 major element analyses of vitric shards were obtained by EMP-EDS (Tables 5, 6, 7, and 8). In general, a single analysis of an individual shard was made because of the relatively small sizes involved. Although the compositional spectrum ranges from basaltic andesite to rhyolite, the latter are volumetrically predominant (Fig. 4A). Low-, medium-, and high-K series are identified based on Gill's (1981) classification boundaries (Fig. 4B). On the basis of Miyashiro's (1974) criterion, the overwhelming majority of these are tholeiitic (Fig. 4C). We note a general coincidence of occurrence of compositional types between the southern (881) and northern (882-883-884) sites. Low-K rhyolites do, however, occur predominantly at Site 881 with only sparse representation at the Detroit Seamount sites. In view of the somewhat random sampling technique employed for the ash layers at Sites 882 through 884, it is encouraging that the same compositional groupings appear for all of these Sites. We assume as a result that the sampling strategy has successfully recovered the full range of compositions that exist within the ash population.

In Figure 3 are presented some aspects of the variations of major element geochemistry of the Neogene ashes as a function of time for Sites 881 through 884. A number of observations can be made with respect to these data:

1. Recognizing the likelihood of a variable geographic source of these ashes, there is no regularity in the development of more alkaline (for example, higher K) compositions with the passage of time;
2. In fact, high-K compositions appear at various times in the combined temporal record including a prominent pulse at about 6–7.5 Ma;
3. Recalling that the sampling effort was designed originally for comprehensive coverage but not specifically for correlative purposes, we note that a comparison of the compositional variations between 0

and 3.5 Ma of ashes recovered from Sites 881 and 882 show a number of similarities including a period of explosive quiescence between 1.5 and 1.1 Ma and a general similarity of compositional fluctuations, possibly indicative of fallout from the Kurile-Kamchatka system generally reaching both the southern and northern sites.

In the framework of the global correlation of Plank and Langmuir (1988) of levels of wt% CaO at specific MgO content as a function of arc crustal thickness, we show the relevant data in Figure 6. First, we note no obvious spread of values as a function of time, and, second, a crustal thickness of about 12–15 km would be inferred for the sources of the ashes.

### Trace Element Geochemistry

Trace element abundances were determined by ICP-MS for about 100 ash samples, primarily from Sites 881 and 882 (Tables 9 and 10), and for Paleogene ashes from Sites 883 and 884 (Table 11). A considerable range in abundances of elements such as the REE at any given wt% SiO<sub>2</sub> are present. Within the rhyolites, there is generally a positive correlation between K content and the degree of light REE enrichment. A variety of REE fractionations is present in these ashes from light REE-depleted through relatively unfractionated to light REE-enriched, and 12 groups (A to L) are recognized on the basis of the similarities of these fractionations in combination with other trace element variations (Fig. 7). Negative Eu anomalies of varying magnitude developed in the majority of the groups are indicative of feldspar fractionation, and in most of the dacite and rhyolite compositions, a concave-upward pattern between Gd and Lu is developed. This style of medium-to-heavy REE fractionation is characteristic of the fractional crystallization of amphibole, or the persistence of residual amphibole in a source rock if these felsic rocks represent crustal partial melts. We discern no temporal consistency in terms of REE fractionations (Fig. 5).

In Figure 8, we contrast the variations of a range of trace elements (of contrasted crystal-melt distribution coefficients) within these ash groups. Taking a distinctive group of upper Miocene, high-K, light REE-enriched ashes as a normalizing group (UNE layer numbers 81 to 86), a number of prominent element abundance fractionations and ratios are apparent. Published accounts of subaerial explosive volcanism present in Kamchatka in the upper Miocene (Fedotov and Masurenkov, 1991) indicate the most probable source of this particular group of high-K ashes was the alkaline (including absarokite-shoshonite) volcanism in the SR.

In addition to the fractionation of the REE apparent in Figure 7, abundances of highly incompatible large ion lithophile trace elements such as Rb, Ba, and Th vary by an order of magnitude relative to these high-K ashes. In addition, Rb/Ba and Th/U ratios range from values strongly less than to more than those of the high-K ashes (~0.17 and 2.5, respectively). The high-K Miocene ashes are also characterized by distinctively lower Nb/Ta than the majority of the ashes (Fig. 9). We are in the process of compiling a geochemical data base for comparison of the ash groups with the five, major subaerial volcanic belts of the Kurile-Kamchatka arc system (Kurile Islands, South Kamchatka, EK, CKD and SR). The apparent presence of some geographically diagnostic and temporally persistent trace element fractionations may allow assignment of specific ash layers to sources in the arc.

The <sup>143</sup>Nd/<sup>144</sup>Nd vs. <sup>87</sup>Sr/<sup>86</sup>Sr values for selected ash layers from Sites 881 and 882 are listed in Tables 9 and 10 and displayed in Figure 10. Most of the samples overlap the range we have obtained for active volcanoes in the CKD and EK, and values reported for the Kuriles by Zhuravlev et al. (1985) with  $\epsilon_{\text{Nd}} \sim +8$  and  $^{87}\text{Sr}/^{86}\text{Sr} = 0.7031$  to 0.7038, but some samples range to lower  $\epsilon_{\text{Nd}}$  of +3 and  $^{87}\text{Sr}/^{86}\text{Sr}$  of ~0.7045. Furthermore, many of the highly explosive and active volcanoes of the CKD and the Kurile arc are currently characterized by distinctly higher  $\epsilon_{\text{Nd}}$  (+9 to 10) than the ashes, which is perhaps indicative of the

general insignificance of the CKD as a major source of the offshore ashes sampled to date.

Chondrite-normalized REE abundances for the Paleogene ashes recovered from the base of the sedimentary sections in Holes 883B and 884B, are shown in Figure 11. Given the extensive alteration of these materials, it is not clear to what extent the pristine igneous geochemistry can be recovered. However, the relatively unfractionated patterns with slight negative Eu anomalies are similar to the ejecta of many of the active volcanoes of the Izu-Bonin-Mariana and Kurile arcs of the western Pacific. The high Ba/Nb (>200), Sc/Ga (>1), and low TiO<sub>2</sub> of these basaltic and andesitic ashes are consistent with derivation from an arc rather than mid-ocean ridge basalt (MORB) or ocean island (hot spot) source. The negative Ce anomalies of these ashes may be the result of seawater alteration.

### MINERALOGY

#### Plagioclase

Feldspar microlites were analyzed where present in each ash layer (Tables 12 and 13). A ternary plot (Fig. 12) of albite, anorthite, and orthoclase shows a continuum of plagioclase compositions from ~An<sub>96</sub> to An<sub>38</sub> with <Or<sub>5</sub> mole %. We are surprised by the absence of potassium feldspar given the prominent occurrences of high-K rhyolitic compositions. It is possible that selective winnowing of different mineral fragments has occurred, but a renewed search of the microlites in Site 192 ashes may prove instructive in this regard in view of the relative proximity of this site to Kamchatka.

#### Fe-Ti Oxides

A total of 120 iron-titanium oxide microlites was analyzed from 46 ash layers recovered from Sites 881, 882, 883, and 884. Of these, 23 were identified as a rhombohedral phase and the rest were recognized as spinels. Twelve magnetite-ilmenite pairs were found co-existing with vitric shards ranging from basaltic-andesite to rhyolite. Analyses of the iron-titanium oxides are presented in Table 14. The ferric and ferrous iron contents are calculated by an approach modified from Carmichael (1967). In order to calculate temperature and oxygen fugacity ( $f\text{O}_2$ ) with the Fe-Ti oxide geothermometer/oxygen barometer developed by Ghiorso and Sack (1991), we assume that each ash layer originated from a single source, and the average compositions of the different ilmenite and magnetite pairs are utilized to derive T- $f\text{O}_2$  data. The values are close to the synthetic fayalite-magnetite-quartz (FMQ  $\pm 0.5 \log_{10}$  units) buffer in the range 850°–1100°C. This is, in fact, relatively reduced compared with the majority of island arcs (Ballhaus, 1993).

#### Clinopyroxene and Amphibole

Clinopyroxene microlites are present in ash layers of a wide compositional spectrum but are more common in basaltic andesite to dacite. Most clinopyroxene (Table 15) is in the Wo<sub>40</sub>En<sub>45</sub>Fs<sub>15</sub> ~ Wo<sub>30</sub>En<sub>55</sub>Fs<sub>25</sub> range, with a single microlite of Wo<sub>17</sub>En<sub>53</sub>Fs<sub>30</sub>. Pargasitic amphibole occurs rarely as a microlitic phase, so far discovered only at Site 881.

### DISCUSSION

On the basis of results obtained from geochemical and petrological study of the ash layers from Sites 881 to 884, we can attempt some qualified response to the questions relating to subduction zone petrogenesis posed in the introduction to this paper. For example, it is clear both from this study as well as others pursued recently on the explosive products of the Izu-Bonin-Mariana (IBM) system, that the temporal changes in the eruptive products of island arcs that occur are not in a monotonic sense of increasing alkalinity with time (Gill et al., 1994; Arculus et al., 1995). In fact, in the case of the Kurile-

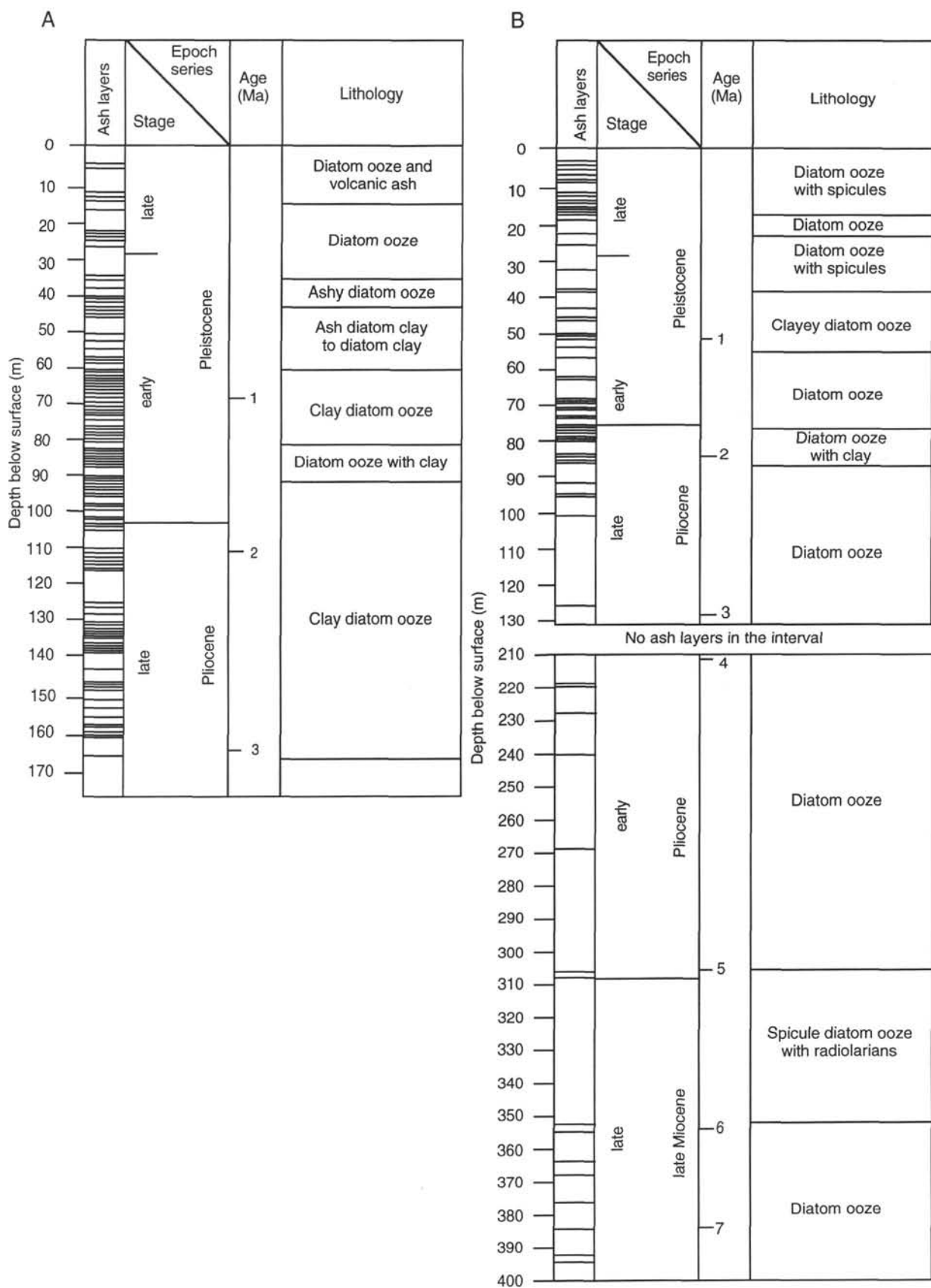
**Table 1.** Stratigraphic and lithological characteristics of volcanic ash layers from Site 881.

UNE number	Group number	Age (Ma)	Depth (mbsf)	Thickness (cm)	Size of vitric shard (0.01 mm)	Color (dry sample)	Color (shipboard estimate)	Composition	Lithology
<b>Hole 881A</b>									
1	d		6.8		1 × 10	Light gray (2.5Y 8/2)	5Y, 10Y, and 10YR	Rhyolite	Diatom ooze and volcanic ash
			7.9				5Y, 10Y, and 10YR	—	Diatom ooze and volcanic ash
2	b	9.2	110 (3–6)		2 × 2	Light gray (2.5Y 8/1)	5Y, 10Y, and 10YR	Rhyolite	Diatom ooze and volcanic ash
		9.5	110 (3–6)				5Y, 10Y, and 10YR	—	Diatom ooze and volcanic ash
		9.8	110 (3–6)				5Y, 10Y, and 10YR	—	Diatom ooze and volcanic ash
		10.1	110 (3–6)				5Y, 10Y, and 10YR	—	Diatom ooze and volcanic ash
		10.6	—				5Y, 10Y, and 10YR	—	Diatom ooze and volcanic ash
3	d	12.1	—	5 × 0	Light gray (2.5Y 8/1)	5Y, 10Y, and 10YR	Rhyolite	Diatom ooze and volcanic ash	
4		12.5	30	1 × 3	Light gray (2.5Y 8/1)	5Y, 10Y, and 10YR	Rhyolite	Diatom ooze and volcanic ash	
<b>Hole 881B</b>									
		0.33	8.7	—			—	—	Diatom ooze with quartz silt
		0.34	8.9	—			—	—	Diatom ooze with quartz silt
7		0.35	12.6	—	1 × 5	Light gray (2.5Y 8/1)	—	Rhyolite	Diatom ooze with quartz silt
		0.36	13.2	—			—	—	Diatom ooze with quartz silt
8		0.38	15.5	—	1 × 8	Light gray (2.5Y 7/1)	—	Rhyolite	Diatom ooze
		0.40	18.6	—			—	—	Diatom ooze
10	g	0.45	22.4	—	1 × 3	Light gray (2.5Y 7/1)	—	Rhyolite	Diatom ooze
11	b	0.46	23.9	—	1 × 5	Light gray (2.5Y 8/1)	—	Rhyolite	Diatom ooze
12	b	0.49	25.8	—	1 × 3	Light gray (2.5Y 8/2)	—	Rhyolite	Diatom ooze
		0.51	26.2	—			—	—	Diatom ooze
		0.53	29.6	—			—	—	Diatom ooze
		0.57	35.1	—			—	—	Ashy diatom ooze
13	j	0.63	38.1	—	4 × 8	Grayish yellow (2.5Y 7/2)	(3.2GY 3.1/1.3)–(5.5YR 3.2/0.8)	Basaltic andesite	Ashy diatom ooze
		0.65	39.3	—			(3.2GY 3.1/1.3)–(5.5YR 3.2/0.8)	—	Ashy diatom ooze
		0.66	41.0	—			(3.2GY 3.1/1.3)–(5.5YR 3.2/0.8)	—	Ashy diatom ooze
		0.67	41.2	—			(3.2GY 3.1/1.3)–(5.5YR 3.2/0.8)	—	Ashy diatom ooze
		0.68	42.6	—			(3.2GY 3.1/1.3)–(5.5YR 3.2/0.8)	—	Ashy diatom ooze
		0.69	42.9	—			(3.2GY 3.1/1.3)–(5.5YR 3.2/0.8)	—	Ashy diatom ooze
		0.70	44.3	—			(3.2GY 3.1/1.3)–(5.5YR 3.2/0.8)	—	Ashy diatom clay to diatom clay
14	e	0.71	45.7	—	0.5 × 5	Yellowish gray (2.5Y 6/1)	(9GY 1.3/1.9)–(2.5Y 5.0/1.0)	Andesite-dacite	Ashy diatom clay to diatom clay
15	c	0.73	46.9	—	1 × 3	Grayish yellow (2.5Y 7/2)	(9GY 1.3/1.9)–(2.5Y 5.0/1.0)	Rhyolite	Ashy diatom clay to diatom clay
16	k	0.76	51.3	—	1 × 5	Light gray (2.5Y 8/1)	(9GY 1.3/1.9)–(2.5Y 5.0/1.0)	Rhyolite	Ashy diatom clay to diatom clay
		0.78	53.2	—			(5.3Y 3.5/1.1)	—	Ashy diatom clay to ashy diatom ooze
		0.80	56.8	—			(5.3Y 3.5/1.1)	—	Ashy diatom clay to ashy diatom ooze
		0.82	59.0	—			(5.3Y 3.5/1.1)	—	Ashy diatom clay to ashy diatom ooze
		0.83	59.2	—			(5.3Y 3.5/1.1)	—	Ashy diatom clay to ashy diatom ooze
		0.85	59.8	—			(5.3Y 3.5/1.1)	—	Ashy diatom clay to ashy diatom ooze
17	a	0.87	60.2	—	2 × 4	Light gray (2.5Y 8/1)	(5.3Y 3.5/1.1)	Rhyolite	Ashy diatom clay to ashy diatom ooze
		0.88	60.6	—			(5.3Y 3.5/1.1)	—	Ashy diatom clay to ashy diatom ooze
		0.88	60.8	—			(5.3Y 3.5/1.1)	—	Ashy diatom clay to ashy diatom ooze
		0.89	61.2	—			(5.3Y 3.5/1.1)	—	Ashy diatom clay to ashy diatom ooze
18	a	0.89	61.5	—	3 × 5	Light gray (2.5Y 8/1)	(5.3Y 3.5/1.1)	Rhyolite	Ashy diatom clay to ashy diatom ooze
		0.89	61.8	—			(5.3Y 3.5/1.1)	—	Ashy diatom clay to ashy diatom ooze
		0.91	62.1	—			(5.3Y 3.5/1.1)	—	Ashy diatom clay to ashy diatom ooze
		0.95	64.5	—			(6.5Y 4.2/1.0)	—	Clayey diatom ooze
		0.96	64.9	—			(6.5Y 4.2/1.0)	—	Clayey diatom ooze
		0.96	65.2	—			(6.5Y 4.2/1.0)	—	Clayey diatom ooze
		0.99	69.1	—			(6.5Y 4.2/1.0)	—	Clayey diatom ooze
		1.00	71.0	—			(6.5Y 4.2/1.0)	—	Clayey diatom ooze
19	a	1.01	72.5	—		Light gray (2.5Y 8/1)	(7.9YR 3.9/1.2)–(9.9YR 3.9/1.2)	Rhyolite	Clayey diatom ooze
		1.03	73.0	—			(7.9YR 3.9/1.2)–(9.9YR 3.9/1.2)	—	Clayey diatom ooze
		1.04	73.4	—			(7.9YR 3.9/1.2)–(9.9YR 3.9/1.2)	—	Clayey diatom ooze
		1.05	74.1	—			(7.9YR 3.9/1.2)–(9.9YR 3.9/1.2)	—	Clayey diatom ooze
		1.11	77.1	—			(7.9YR 3.9/1.2)–(9.9YR 3.9/1.2)	—	Clayey diatom ooze
		1.12	77.3	—			(7.9YR 3.9/1.2)–(9.9YR 3.9/1.2)	—	Clayey diatom ooze
		1.13	78.2	—			(7.9YR 3.9/1.2)–(9.9YR 3.9/1.2)	—	Clayey diatom ooze
		1.14	79.3	—			(7.9YR 3.9/1.2)–(9.9YR 3.9/1.2)	—	Clayey diatom ooze
		1.15	79.7	—			(7.9YR 3.9/1.2)–(9.9YR 3.9/1.2)	—	Clayey diatom ooze
		1.17	80.2	—			(7.9YR 3.9/1.2)–(9.9YR 3.9/1.2)	—	Clayey diatom ooze
		1.21	82.0	—			(7.9YR 3.9/1.2)–(9.9YR 3.9/1.2)	—	Diatom ooze with clay
		1.22	82.2	—			(7.9YR 3.9/1.2)–(9.9YR 3.9/1.2)	—	Diatom ooze with clay
		1.23	82.8	—			(7.9YR 3.9/1.2)–(9.9YR 3.9/1.2)	—	Diatom ooze with clay
		1.23	83.2	—			(7.9YR 3.9/1.2)–(9.9YR 3.9/1.2)	—	Diatom ooze with clay
		1.24	83.8	—			(7.9YR 3.9/1.2)–(9.9YR 3.9/1.2)	—	Diatom ooze with clay

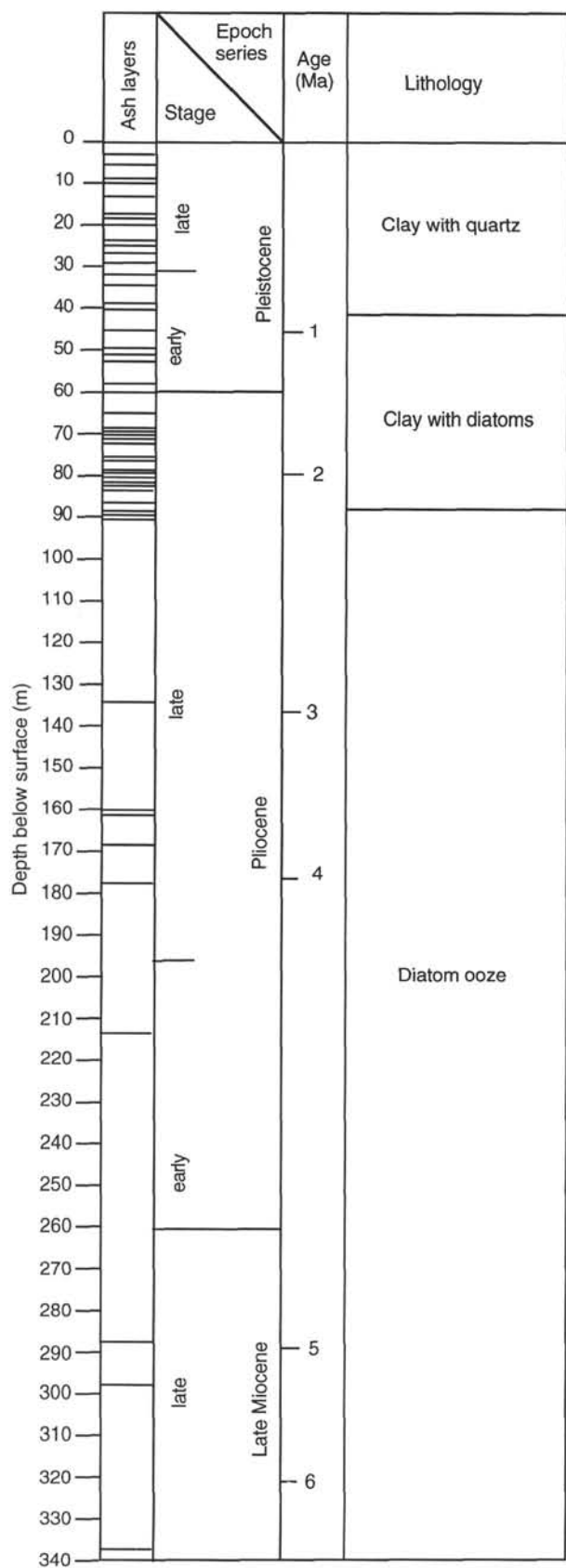
Table 1 (continued).

UNE number	Group number	Age (Ma)	Depth (mbsf)	Thickness (cm)	Size of vitric shard (0.01 mm)	Color (dry sample)	Color (shipboard estimate)	Composition	Lithology
20		1.24 1.34	84.2 85.9	— —	1 × 6	Grayish yellow (2.5Y 6/2)	— —	— —	Diatom ooze with clay Diatom ooze with clay
21-24	f	1.45 1.55 1.60	90.1 90.6 90.8	— — —	1 × 3	Light gray (2.5Y 7/1)	— — —	Andesite-dacite — —	Diatom ooze with clay Diatom ooze with clay Diatom ooze with clay Diatom ooze with clay
25	d	1.62	92.2	—	1 × 10	Light gray (2.5Y 7/1)	(5Y 3/1) (5Y 3/1)	Rhyolite	Clayey diatom ooze
26		1.65 1.68	93.9 94.6	— —	1 × 8	Light gray (2.5Y 7/1)	(5Y 3/1)	—	Clayey diatom ooze
27	d	1.72	96.0	—	1 × 5	Light gray (2.5Y 8/1)	(5Y 3/1)	Rhyolite	Clayey diatom ooze
28	k	1.73 1.79 1.81 1.82	96.2 98.2 98.6 99.0	— — — —	1 × 3	Light gray (2.5Y 8/1)	(5Y 3/1) (5Y 3/1) (5Y 3/1)	Rhyolite —	Clayey diatom ooze Clayey diatom ooze Clayey diatom ooze Clayey diatom ooze
29, 30	g	1.84	101.1	—	1 × 3	Light gray (2.5Y 7/1)	—	Rhyolite	Clayey diatom ooze
31		1.87	101.8	—	0.5 × 8	Light gray (2.5Y 8/2)	—	Rhyolite	Clayey diatom ooze
32	b	1.90 1.92 1.94 1.98	102.2 103.8 104.3 110.0	— — — —	3 × 10	Light gray (2.5Y 7/1)	—	Rhyolite	Clayey diatom ooze Clayey diatom ooze Clayey diatom ooze Clayey diatom ooze
33		2.07 2.09 2.10 2.11	112.7 113.8 114.1 115.8	— — — —	2 × 4	Yellowish gray (2.5Y 4/1)	—	Andesite-rhyolite	Clayey diatom ooze Clayey diatom ooze Clayey diatom ooze Clayey diatom ooze
34		2.12	116.4	—	1 × 5	Light gray (2.5Y 8/2)	—	Rhyolite	Clayey diatom ooze
35		2.13	116.7	—	1 × 6	Light gray (2.5Y 7/1)	—	—	Clayey diatom ooze
36	h	2.22 2.23	125.5 126.0	— 2	2 × 4	Light gray (2.5Y 7/1)	—	Rhyolite	Clayey diatom ooze Clayey diatom ooze
37		2.25 2.29 2.31 2.32 2.33 2.35 2.37 2.40 2.41 2.42 2.43 2.43	128.7 130.3 131.2 132.5 132.8 133.3 133.6 133.9 137.2 137.8 138.1 138.3	— — — — — — — — — — — — —	2 × 3	Yellowish gray (2.5Y 4/1) (1.8Y 1.6/5)	—	—	Clayey diatom ooze Clayey diatom ooze
41		2.43 2.43	139.4 144.5	— —	1 × 8	Light gray (2.5Y 7/1)	Dark green-black Dark green-black	— —	Clayey diatom ooze Clayey diatom ooze
43	b	2.44	147.1	7		Light gray (2.5Y 8/1)	Dark green-black	Rhyolite	Clayey diatom ooze
44		2.44	147.8	—	1 × 2	Light gray (2.5Y 7/1)	Dark green-black	Andesite-rhyolite	Clayey diatom ooze
45		2.45	148.1	—	2 × 3	Dark grayish yellow (2.5Y 4/2)	Dark green-black	Andesite-dacite	Clayey diatom ooze
46	c	2.46 2.48 2.50 2.52 2.54	148.2 151.8 153.6 155.7 157.6	18 7 4 6 10	1 × 3	Light gray (2.5Y 8/1)	Black-light gray Black-light gray Black-light gray Black-light gray Black-white	Andesite-dacite	Clayey diatom ooze Clayey diatom ooze Clayey diatom ooze Clayey diatom ooze Clayey diatom ooze
47, 48, 49		2.60 2.80 2.81 2.82 3.00	158.9 159.1 159.4 160.7 164.1	— 1 — 2 14	1 × 5	Grayish yellow (2.5Y 6/2)	Black-white Black-white Black-white Black-white Black-white	Andesite	Clayey diatom ooze Clayey diatom ooze Clayey diatom ooze Clayey diatom ooze Clayey diatom ooze

Note: — = data not available.

Figure 2. Representation of ash layer occurrence, age and lithology. **A.** Site 881. **B.** Site 882. **C.** Site 883. **D.** Site 884.

C



D

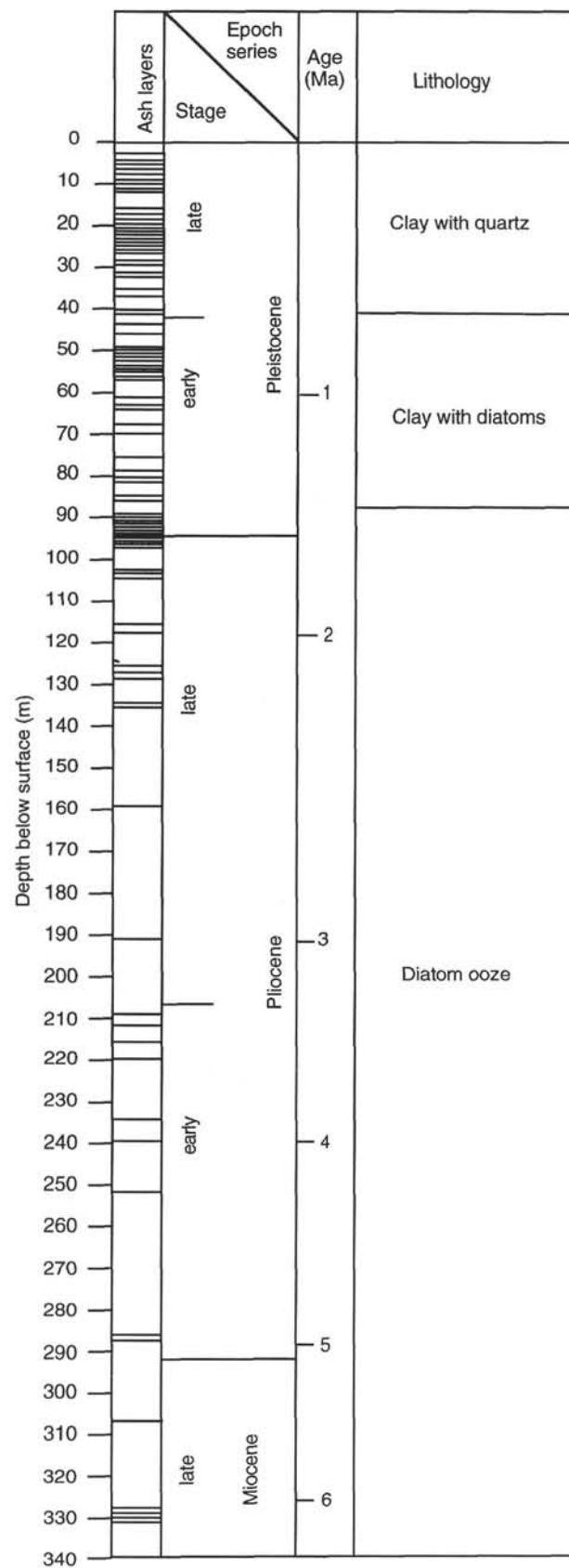


Figure 2 (continued).

Table 2. Stratigraphic and lithological characteristics of volcanic ash layers from Hole 882A.

UNE number	Group number	Age (Ma)	Depth (mbsf)	Thickness (cm)	Size of vitric shard (0.01 mm)	Color (dry sample)
52		0.100	2.0	1	1 × 5	Light gray (2.5Y 7/1)
		0.150	2.9	1		
		0.200	4.4	12		
54	1	0.350	8.1	8	0.5 × 5	Light gray (2.5Y 7/1)
		0.370	9.6	5		
		0.390	9.9	13		
		0.420	12.3	6		
		0.450	13.4	5		Light gray (2.5Y 8/1)
55	1	0.450	14.3	7	1 × 5	Light gray (2.5Y 8/1)
		0.450	14.6	1		
		0.451	16.3	—		Yellowish gray (2.5Y 6/1)
		0.452	16.5	—		Light gray (2.5Y 7/1)
		0.455	17.0	4		
58	i	0.460	17.4	3	1 × 8	Grayish yellow (2.5Y 7/2)
		0.465	19.2	6		
		0.470	22.9	4		Light gray (2.5Y 7/1)
		0.472	25.0	3		
		0.480	32.4	6		
60	e	0.580	37.3	5	1 × 5	Light gray (2.5Y 7/1)
		0.600	38.1	12		
		0.670	43.2	3		
		0.850	46.9	18		Light gray (2.5Y 7/1)
		0.890	47.8	5		
61	g	1.000	49.7	9	0.5 × 2	Light gray (2.5Y 7/1)
		1.020	49.9	5		
		1.050	51.4	6		
		1.140	54.9	20		
		1.230	57.0	1		
63	d	1.350	51.3	5	1 × 7	Light gray (2.5Y 7/1)
		1.370	61.8	8		
		1.500	68.0	2		
		1.510	68.7	6		
		1.550	68.9	9		Light gray (2.5Y 8/2)
65	b	1.590	70.6	8	2 × 5	Yellowish gray (2.5Y 5/1)
		1.610	71.1	1		
		1.650	73.7	3		
		1.690	73.9	10		Light gray (2.5Y 8/2)
		1.720	74.9	4		Light gray (2.5Y 7/1)
67	b	1.790	76.3	2	1.5 × 4	Light gray (2.5Y 6/1)
		1.800	76.5	1		
		1.810	76.9	5		
		1.830	78.0	1		
		1.850	79.1	11		
70	f	1.860	79.5	1	3 × 5	Light gray (2.5Y 6/1)
		1.980	82.0	10		
		1.980	82.8	2		
		2.050	83.3	4		
		2.060	84.1	4		Light gray (2.5Y 7/1)
71	d	2.300	91.0	2	2 × 2	Dark olive brown (2.5Y 3/3)
		2.550	94.8	16		
		2.600	95.3	4		
		2.710	100.2	8		
		3.000	128.4	2		
77	g	4.030	216.2	14	1 × 3	Yellowish gray (2.5Y 6/1)
		4.050	218.8	13		
		4.100	223.8	6		
		4.300	237.6	3		
		4.700	260.9	5		
78	j	5.000	297.8	1	3 × 5	Light gray (2.5Y 8/1)
		5.100	300.4	1		
		5.200	302.8	3		
		5.700	344.9	14		
		6.100	347.9	5		Light gray (2.5Y 8/1)
81	c	6.370	356.3	19	1 × 5	Grayish yellow (2.5Y 6/2)
		6.800	360.0	6		
		6.850	369.1	14		
		7.000	380.7	13		
		7.150	391.6	4		
82	b	7.200	393.8	17	2 × 10	Light gray (2.5Y 7/2)
		7.200	393.8	17		
		7.200	393.8	17		
		7.200	393.8	17		
		7.200	393.8	17		
83	b	7.200	393.8	17	2.5 × 15	Light gray (2.5Y 7/1)
		7.200	393.8	17		
		7.200	393.8	17		
		7.200	393.8	17		
		7.200	393.8	17		
84	a	7.200	393.8	17	1 × 4	Light gray (2.5Y 8/1)
		7.200	393.8	17		
		7.200	393.8	17		
		7.200	393.8	17		
		7.200	393.8	17		
85	a	7.200	393.8	17	2 × 5	Light gray (2.5Y 7/1)
		7.200	393.8	17		
		7.200	393.8	17		
		7.200	393.8	17		
		7.200	393.8	17		
86	a	7.200	393.8	17	6 × 20	Light gray (2.5Y 7/1)
		7.200	393.8	17		
		7.200	393.8	17		
		7.200	393.8	17		
		7.200	393.8	17		

Kamchatka system, pulses of alkaline activity appear at different times in the evolution of the arc with a particularly prominent episode in the late Miocene. Of course, these episodes may be more related to geographic position, the nature of the subjacent arc crust and lithosphere, and tectonic events than a straightforward effect of crustal (or lithospheric) thickening at one locus of magma emission.

In the case of the IBM system, we know that the eruptive products of the Izu-Bonin arc changed subsequent to the development (~25 to 15 Ma) of the backarc Shikoku Basin, leading to decreasing alkalinity from 15 Ma to the present (Gill et al., 1994). It is postulated that melt extraction from a mantle source supplying the backarc basin leaves a refractory mantle that is then advected by coupled drag with the sub-

ducted lithosphere toward the trench. Ingress of slab-derived fluids triggers renewed melting, leading to arc magmatism with the distinctive characteristics of derivation from refractory mantle sources, such as strongly light REE-depleted patterns. In contrast, despite a greater extent of backarc spreading (Parece Vela and Mariana Trough), no such effect is observed in the Marianas (Arculus et al., 1995).

It is possible that the documented along-strike variation in geochemical characteristics of the Kurile arc (Leonova, 1979) may be related to the differential south to north opening in the Miocene of the South Kurile backarc basin, but no such effects are possible in Kamchatka. We believe that knowledge of time-chemical relations of eruptive products in Kamchatka is not yet sufficient to recognize

Table 2 (continued).

UNE number	Group number	Age (Ma)	Depth (mbsf)	Thickness (cm)	Color (shipboard estimate)	Composition	Lithology
52		0.100	2.0	1	Dark	—	Diatom ooze with spicules
		0.150	2.9	1	Dark	—	Diatom ooze with spicules
		0.200	4.4	12	(9Y 0.3/0.2)	—	Diatom ooze with spicules
54	I	0.350	8.1	8	Light brown-dark green	Andesite-dacite	Diatom ooze with spicules
		0.370	9.6	5	Dark	—	Diatom ooze with spicules
		0.390	9.9	13	Light	—	Diatom ooze with spicules
		0.420	12.3	6	Dark	—	Diatom ooze with spicules
55	I	0.450	13.4	5	Dark	Rhyolite	Diatom ooze with spicules
		0.450	14.3	7	Light	—	Diatom ooze with spicules
		0.450	14.6	1	Light	—	Diatom ooze with spicules
56	e	0.451	16.3	—	Light	Dacite-rhyolite	Diatom ooze with spicules
57	I	0.452	16.5	—	Light	Andesite-dacite	Diatom ooze with spicules
		0.455	17.0	4	Light	—	Diatom ooze with spicules
		0.460	17.4	3	Dark green	—	Diatom ooze with spicules
		0.465	19.2	6	Dark green	—	Diatom ooze
58	i	0.470	22.9	4	Dark green	Rhyolite	Diatom ooze
		0.472	25.0	3	Dark green	—	Diatom ooze
60	e	0.480	32.4	6	Dark green	Rhyolite	Calcareous diatom ooze with spicules
		0.580	37.3	5	Dark green	—	Calcareous diatom ooze with spicules
		0.600	38.1	12	Dark green	—	Diatom ooze with calcite
61	g	0.670	43.2	3	Dark green	Andesite-dacite	Diatom ooze with calcite
62	e	0.850	46.9	18	Dark green	Andesite-dacite	Clayey diatom ooze
		0.890	47.8	5	Dark green	—	Clayey diatom ooze
		1.000	49.7	9	Dark green	—	Clayey diatom ooze
		1.020	49.9	5	Dark green	—	Clayey diatom ooze
63	d	1.050	51.4	6	Dark green	Rhyolite	Clayey diatom ooze
		1.140	54.9	20	Light gray(2.9Y 4.0/1.1)	—	Clayey diatom ooze
		1.230	57.0	1	Dark green	—	Diatom ooze with clay
		1.350	51.3	5	Dark green	—	Diatom ooze with clay
		1.370	61.8	8	Dark green	—	Diatom ooze with clay
64	e	1.500	68.0	2	Light brown(8.3YR 3.7/1.5)	Rhyolite	Diatom ooze
		1.510	68.7	6	~Dark brown(5.1YR 1.8/0.6)	—	Diatom ooze
65	b	1.550	68.9	9	Light brown(8.3YR 3.7/1.5)	Rhyolite	Diatom ooze
66		1.590	70.6	8	~Dark brown(5.1YR 1.8/0.6)	—	Diatom ooze
		1.610	71.1	1	Light brown(8.3YR 3.7/1.5)	—	Diatom ooze
		1.650	73.7	3	~Dark brown(5.1YR 1.8/0.6)	—	Diatom ooze
67	b	1.690	73.9	10	Light brown(8.3YR 3.7/1.5)	Rhyolite	Diatom ooze
68	g	1.720	74.9	4	~Dark brown(5.1YR 1.8/0.6)	Rhyolite	Diatom ooze
		1.790	76.3	2	Gray(2.5Y 1.6/1.1)	—	Diatom ooze with clay
		1.800	76.5	1	Gray(2.5Y 1.6/1.1)	—	Diatom ooze with clay
69	e	1.810	76.9	5	Gray(2.5Y 1.6/1.1)	Dacite-rhyolite	Diatom ooze with clay
		1.830	78.0	1	Brown(9.4YR 2.4/1.1)	—	Diatom ooze with clay
70	f	1.850	79.1	11	Gray(2.5Y 1.6/1.1)	Andesite-dacite	Diatom ooze
		1.860	79.5	1	Gray(2.5Y 1.6/1.1)	—	Diatom ooze with clay
71	d	1.980	82.0	10	Gray(2.5Y 1.6/1.1)	Rhyolite	Diatom ooze with clay
72		1.980	82.8	2	Brown(9.4YR 2.4/1.1)	—	Diatom ooze with clay
73	e	2.050	83.3	4	Gray(2.5Y 1.6/1.1)	Rhyolite	Diatom ooze with clay
74	f	2.060	84.1	4	Gray(2.5Y 1.6/1.1)	Andesite	Diatom ooze with clay
		2.300	91.0	2	(0.9YR 2.6/0.9)	—	Diatom ooze with clay and ash
75,76	j	2.550	94.8	16	(0.9YR 2.6/0.9)	—	Diatom ooze
		2.600	95.3	4	(0.9YR 2.6/0.9)	—	Diatom ooze
77	g	2.710	100.2	8	(0.9YR 2.6/0.9)	Dacite-rhyolite	Diatom ooze
		3.000	128.4	2	Light gray	—	Diatom ooze with spicules
78	j	4.030	216.2	14	—	Basalt-andesite	Diatom ooze
79	j	4.050	218.8	13	Dark	Basalt-andesite	Diatom ooze
80		4.100	223.8	6	Dark	—	Diatom ooze
		4.300	237.6	3	—	—	Diatom ooze
		4.700	260.9	5	(5.8Y 4.4/0.7)	—	Diatom ooze
		5.000	297.8	1	Dark green	—	Spicule diatom ooze with radiolarians
		5.100	300.4	1	Dark green	—	Spicule diatom ooze with radiolarians
		5.200	302.8	3	Dark green	—	Spicule diatom ooze with radiolarians
		5.700	344.9	14	Light gray(3.1Y 5.0/0.9)	—	Diatom ooze
81	c	6.100	347.9	5	Brown(7.7YR 2.8/0.8)	Rhyolite	Diatom ooze
82	b	6.370	356.3	19	Dark green(8.5YR 3.2/0.8)	Rhyolite	Diatom ooze
		6.800	360.0	6	Dark green(8.5YR 3.2/0.8)	—	Diatom ooze
83	b	6.850	369.1	14	Gray(2.6YR 3.4/0.7)	Rhyolite	Diatom ooze
84	a	7.000	380.7	13	Dark gray(2.2Y 3.8/0.6)	Rhyolite	Diatom ooze
85	a	7.150	391.6	4	Dark	Rhyolite	Diatom ooze
86	a	7.200	393.8	17	Light	Rhyolite	Diatom ooze

Note: — = data not available.

patterns or cyclicity in composition. It is interesting to note, however, two general features of occurrence and distribution of arc magmatism that merit further study. The first is the remarkable increase in the across-strike distribution of volcanism in sectors of the Izu-Bonin-Honshu-Hokkaido-Kurile-Kamchatka arc, which is underlain in part by continental lithosphere. In the case of northeastern Honshu, there are currently two active chains of volcanoes (Nasu and Chokai zones) and in Kamchatka, there are three (EK, CKD, and SR). The across-strike spread of magmatism (~400 km) contrasts strongly with the apparently restricted geographic spread of magma emission in the Izu-Bonin and Kurile sectors of the arc. Direct chemical involvement of ancient continental lithosphere may be traced in the future with Pb

isotopic studies in combination with Th/U disequilibria studies. But in addition, the physical factors controlling migration and channeling of melts in the mantle beneath subarc continental vs. oceanic lithosphere deserve further attention (Spiegelman and McKenzie, 1987).

The second feature of note is the apparent absence of an explosive record at Site 881 during the period of South Kurile backarc basin opening in the early to middle Miocene (Kimura and Tamaki, 1985). The question of synchronicity of arc vs. backarc magmatism has been controversial since the results of DSDP efforts in the Philippine plate became known. It has been argued by some (Scott and Kroenke, 1980) that arc activity ceases during backarc spreading, whereas others (Karig, 1974, 1983; Hussong and Uyeda, 1982) assert a continuity of

Table 3. Stratigraphic and lithological characteristics of volcanic ash layers from Hole 883B.

Leg 145 number	UNE number	Age (Ma)	Depth (mbfs)	Thickness (cm)	Size of vitric shard (0.01 mm)	Color (dry sample)	Color (shipboard estimate)	Composition	Lithology
1	87	0.10	2.6	7	2 × 5	Light yellow (2.5Y 7/3)	Tan(6.6Y 3.3/0.6)	Rhyolite	Clay with quartz
2		0.25	6.3	6		Black(3.9YR 2.7/0.5)	—		Clay with quartz
3	89	0.30	8.5	6	1 × 8	Light gray (2.5Y 7/1)	Black(3.9YR 2.7/0.5)	Rhyolite	Clay with quartz
4		0.30	8.8	3		Black(3.9YR 2.7/0.5)	—		Clay with quartz
5		0.31	11.5	3		Black(3.9YR 2.7/0.5)	—		Clay with quartz
6		0.33	15.5	1		Black(3.9YR 2.7/0.5)	—		Clay with quartz
7	90	0.36	16.4	15	5 × 10	Yellowish gray (2.5Y 5/1)	Black(3.9YR 2.7/0.5)	Andesite-dacite	Clay with quartz
8		0.37	17.5	5		Black(3.9YR 2.7/0.5)	—		Clay with quartz
9		0.42	21.4	5		Gray(2.5Y 4.0/0.5)	—		Clay with quartz
10	91	0.45	22.9	4	3 × 5	Yellowish gray (2.5Y 4/1)	Black(1.2RP 2.1/0.7)	Andesite-dacite	Clay with quartz
11		0.46	24.0	4		Gray(2.5Y 4.0/0.5)	—		Clay with quartz
12	92	0.47	26.0	8	3 × 5	Light gray (2.5Y 8/1)	Gray(2.5Y 4.0/0.5)	Rhyolite	Clay with quartz
13	93	0.60	29.3	4	2 × 4	Yellowish gray (2.5Y 6/1)	Gray green(0.5 3.3/0.5)	Andesite-dacite	Clay with diatoms
14		0.70	31.6	4		Gray green(0.5 3.3/0.5)	—		Clay with diatoms
15		0.80	36.9	16		Green(3.0Y 2.8/0.9)	—		Clay with quartz
16		0.90	38.9	8		Green(3.0Y 2.8/0.9)	—		Clay with quartz
17	94	1.06	41.5	4	1 × 3	Yellowish gray (2.5Y 6/1)	Green(3.0Y 2.8/0.9)	Dacite-rhyolite	Clay with diatoms
18	95	1.13	46.4	2	2 × 7	Light gray (2.5Y 7/1)	Dark gray(0.9Y 3.0/0.7)	Rhyolite	Clay with diatoms
19	96	1.15	48.0	10	0.5 × 10	Yellowish gray (2.5Y 6/1)	Dark gray(0.9Y 3.0/0.7)	Rhyolite	Clay with diatoms
20	97	1.20	49.7	7	1 × 15	Yellowish gray (2.5Y 6/1)	Dark gray(0.9Y 3.0/0.7)	Rhyolite	Clay with diatoms
21		1.30	54.3	2		Dark gray(0.9Y 3.0/0.7)	—		Clay with diatoms
22		1.40	56.4	10			—		Clay with diatoms
23		1.50	60.2	2			—		Clay with diatoms
24	98	1.70	63.2	18	1 × 2	Light gray (2.5Y 7/1)		Rhyolite	Clay with diatoms
25		1.71		9			—		Clay with diatoms
26	99	1.71	63.6	9	2 × 15	Light gray (2.5Y 8/2)		—	Clay with diatoms
27		1.72	64.2	8			—		Clay with diatoms
28		1.74	65.9	1			—		Clay with diatoms
29		1.76	66.7	1			—		Clay with diatoms
30	100	1.79	69.6	10	1 × 3	Yellowish gray (2.5Y 6/1)		Rhyolite	Clay with diatoms
31	101	1.80	70.9	8	1 × 3	Yellowish gray (2.5Y 5/1)			Clay with diatoms
32	102	1.96	72.9	1	1 × 5	Light gray (2.5Y 7/1)		Rhyolite	Clay with diatoms
33		2.01	73.2	2			—		Clay with diatoms
34		2.02	73.6	1			—		Clay with diatoms
35		2.16	76.8	1			—		Clay with diatoms
36		2.21	77.0	1			—		Clay with diatoms
37		2.26	79.9	5			—		Clay with diatoms
38		2.30	80.9	1			—		Clay with diatoms
39	103	2.46	82.2	7	1 × 6	Grayish yellow (2.5Y 6/2)		Rhyolite	Clay with diatoms
40	104	2.55	84.2	4	1 × 5	Yellowish gray (2.5Y 6/1)		Dacite-rhyolite	Diatom ooze
41		2.56	84.9	1			—		Diatom ooze
42	106	2.87	122.6	8	1 × 10	Light gray (2.5Y 7/1)		Rhyolite	Diatom ooze
43	107	3.79	188.7	9	2 × 2	Yellowish gray (2.5Y 5/1)	Black(1.8R 2.2/0.5)	Basaltic andesite	Diatom ooze
44		3.80	190.0	1		Black	—		Diatom ooze
45	108	3.82	195.8	7	3 × 10	Light gray (2.5Y 8/1)	Light gray	Rhyolite	Diatom ooze
46		3.90	203.0	1		Light gray	—		Diatom ooze
47	109	4.41	239.7	5	2 × 3	Light gray (2.5Y 7/1)	Dark brown(6.0Y 3.3/1.2)	Andesite	Diatom calcareous ooze
48	110	5.63	312.8	21	1 × 5	Light gray (2.5Y 7/1)		Rhyolite	Diatom ooze
49	111	5.88	324.6	6	1 × 5	Light gray (2.5Y 7/1)		Rhyolite	Diatom ooze
50	112	6.30	376.2	4	0.5 × 5	Light gray (2.5Y 7/1)		Rhyolite	Diatom ooze
51	113	34.10	685.3	12	3 × 4	Light gray (2.5Y 7/1)		Rhyolite	Nannofossil chalk
52		34.25	713.5	2			Black(2.8Y 2.8/1.1)	—	Nannofossil chalk
53	115	34.30	716.1	7	2 × 4	Yellowish gray (2.5Y 4/1)	Black(2.8Y 2.8/1.1)	Andesite	Nannofossil chalk
54	114	34.40	718.1	7	2 × 4	Yellowish gray (2.5Y 4/1)	Black(2.8Y 2.8/1.1)	Andesite	Nannofossil chalk
55	116	37.70	722.1	5	1 × 2	Yellowish gray (2.5Y 5/1)	Dark brown	Basaltic andesite	Nannofossil chalk
56		37.90	722.4	4		Dark brown	—		Nannofossil chalk
57		38.00	722.7	1		Dark brown	—		Nannofossil chalk
58		38.20	723.6	1		Dark brown	—		Nannofossil chalk
59		38.30	723.9	1		Dark brown	—		Nannofossil chalk
60		38.40	724.5	4		Dark brown	—		Nannofossil chalk
61		38.50	724.6	2		Dark brown	—		Nannofossil chalk
62		38.60	725.8	2		Dark brown	—		Nannofossil chalk
63	117	38.70	726.7	5	2 × 3	Yellowish gray (2.5Y 4/1)	Dark brown	Basaltic andesite	Nannofossil chalk
64		38.90	726.8	3		Dark brown	—		Nannofossil chalk
65		40.00	732.0	2		Dark brown	—		Nannofossil chalk
66		40.10	733.0	9		Dark brown	—		Nannofossil chalk
67		40.80	733.7	6		Dark brown	—		Nannofossil chalk
68	118	45.00	747.4	7	3 × 5	Yellowish gray (2.5Y 4/1)	Black	Basaltic andesite	Nannofossil chalk
69		45.20	748.4	8		Black	—		Nannofossil chalk
70		46.00	752.4	4			—		Nannofossil chalk
71		46.20	753.9	1			—		Nannofossil chalk
72	119	49.90	783.0	3			Dark brown	—	Nannofossil chalk
73		50.00	783.3	3			Dark brown	—	Nannofossil chalk
74		>50	795.1	1			Brown	—	Nannofossil chalk

Note: — = data not available.

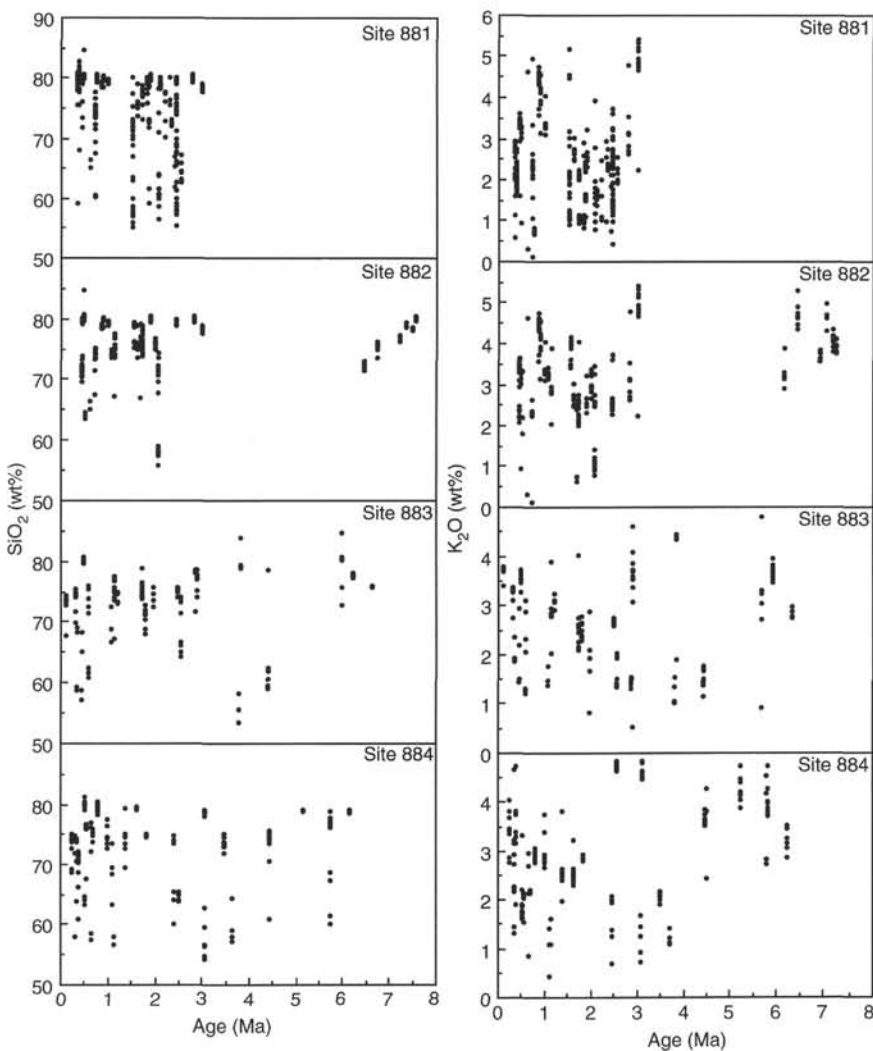


Figure 3. Variation of wt%  $\text{SiO}_2$  and  $\text{K}_2\text{O}$  as a function of age of the ash layers from Sites 881–884, for the past 8 m.y.

activity in the arc. Cambray (1991) has suggested major increases in explosive activity accompany the initial stages of opening in the Izu-Bonin-Mariana system, but that this activity disappears during maximum spreading. In part, of course, the explosive record may not reflect the continuance of arc activity in the event of subsidence of the structure. In the case of the Izu-Bonin system, even the deposition of volcaniclastic-rich turbidites ceases at the initiation of true spreading in the Shikoku Basin (Taylor, 1992), but similar effects have not been documented in the Mariana system. Recovery of a temporal record of activity by drilling in the South Kurile Basin would resolve this issue for the Kurile situation.

Correlations of geochemical parameters of MORB with physical factors such as ridge crest depths and inferred percentages of melting in the mantle have proved to be successful on a global scale (Klein and Langmuir, 1987) even if problematic in detail. In a survey of the geochemistry of the world's arc systems, Plank and Langmuir (1988) discovered a remarkable degree of overlap between MORB and arc basalts, and suggested degrees of melting are controlled at least in part by arc crustal (or lithospheric) thicknesses. Given that island arcs are believed to be the locus of continental crustal growth, we might anticipate some indication of crustal thickening as a function of arc longevity (e.g., decreasing wt% CaO and increasing Na<sub>2</sub>O at specific MgO). At the least, a comparison of the ash data from Leg 145 with the available on-land data and with other arc systems is of interest.

In Figure 6, the covariation wt% CaO with MgO is shown for the ashes in comparison with our data from EK and CKD and our data

from the Izu-Bonin and Mariana systems. Some important features of note are:

1. A relatively restricted spread of ash compositions is apparent with no discernible trend toward lower CaO at fixed MgO with time;
2. Although samples with 6 wt% MgO are sparse, a reasonable extrapolation of the data indicates ~12 wt% CaO at this level of MgO indicative of a crustal thickness of ~14 km;
3. The offset of the ash data to distinctly higher CaO contents than the currently active EK and CKD volcanoes possibly indicates recent crustal thickening. However, we note that the CKD is a major graben structure dominated overwhelmingly by basaltic activity, both of which seem unlikely consequences of crustal thickening;

4. We have found that the Izu-Bonin and Mariana ash data are essentially and remarkably coincident with the 881-884 ashes in terms of CaO vs. MgO characteristics, implying at face value an identity of crustal thicknesses between these diverse systems.

We suspect that part of the reason for the coincidence of the ash compositions from these different arc systems may be the phase chemical control of crystal-melt equilibria at equivalent, and probably relatively low, pressures within the arc crusts (Fig. 13). At a comparitor of 6 wt% MgO for example, it is possible that the melts are already sufficiently evolved for multiple phase (olivine-clinopyroxene-plagioclase-spinel) saturation. Contrasts in the nature of mantle source and melting regimes may have to be sought in the trace element systematics

**Table 4.** Stratigraphic and lithological characteristics of volcanic ash layers from Hole 884B.

UNE number	Age (Ma)	Depth (mbfs)	Thickness (cm)	Size of vitric shard (0.01 mm)	Color (dry sample)	Color (shipboard estimate)	Composition	Lithology
121	0.10	0.3	1		Green	—	Clay with diatoms	
	0.70	2.6	2		Green	—	Clay with diatoms	
	0.10	3.5	1		Green	—	Clay with diatoms	
	0.12	4.1	10		Green	—	Clay with diatoms	
	0.18	5.1	6		Green	—	Clay with diatoms	
	0.22	7.3	7			—	Diatom silty clay	
	0.24	8.7	10	0.5 × 5	Light gray (2.5Y 7/1)		Dacite-rhyolite	Diatom silty clay
	0.25	9.7	17			—	Diatom silty clay	
	0.26	9.9	10			—	Diatom silty clay	
	0.30	12.2	7			—	Diatom silty clay	
122	0.33	14.5	15	0.5 × 5	Light gray (2.5Y 7/1)		Rhyolite	Diatom silty clay
	0.35	15.8	18	0.5 × 3	Light gray (2.5Y 7/1)		Dacite-rhyolite	Diatom silty clay
	0.35	16.1	29			—	Clay with diatoms	
	0.36	16.5	6			—	Clay with diatoms	
	0.36	17.8	20			—	Clay with diatoms	
	0.37	18.1	1			—	Clay with diatoms	
	0.38	18.4	4			—	Clay with diatoms	
	0.38	19	6			—	Clay with diatoms	
	0.39	20	12			—	Clay with diatoms	
	0.39	20.3	6	1 × 3	Light gray (2.5Y 7/1)		Rhyolite	Clay with diatoms
124	0.40	20.6	1			—	Clay with diatoms	
	0.45	24.3	5			—	Clay with diatoms	
	0.47	25.1	4			—	Clay with diatoms	
	0.51	28	11	1 × 5	Light gray (2.5Y 7/1)	Light	Rhyolite	Diatom silty clay
	0.52	28.4	12	2 × 2	Dark grayish yellow (2.5Y 4/2)	Dark	Basaltic andesite	Diatom silty clay
	0.55	30.1	4	1 × 10	Light gray (2.5Y 7/1)	Light	Rhyolite	Diatom silty clay
	0.56	31.8	12			—	Diatom silty clay	
	0.62	36.5	1			—	Clay with diatoms	
	0.63	36.7	7			—	Clay with diatoms	
	0.66	38.3	6	2 × 3	Yellowish gray (2.5Y 6/1)		Andesite-dacite	Clay with diatoms
128	0.69	40.6	11	0.5 × 4	Grayish yellow (2.5Y 7/2)		Rhyolite	Clay with diatoms
	0.75	44.4	4			—	Clay with diatoms	
	0.75	44.7	3			—	Clay with diatoms	
	0.76	44.6	6			—	Clay with diatoms	
	0.76	44.8	8			—	Diatom ooze with clay, spicules and volcanic ash	
	0.78	46	118 (36–40)			—	Diatom ooze with clay, spicules and volcanic ash	
	0.78	46.3	118 (36–40)			—	Diatom ooze with clay, spicules and volcanic ash	
	0.79	46.6	118 (36–40)			—	Diatom ooze with clay, spicules and volcanic ash	
	0.79	46.9	118 (36–40)			—	Diatom ooze with clay, spicules and volcanic ash	
	0.80	47.3	118 (36–40)	2 × 20	Light gray (2.5Y 7/1)		Rhyolite	Diatom ooze with clay, spicules and volcanic ash
130	0.81	48.5	1			—	Diatom ooze with clay, spicules and volcanic ash	
	0.82	49.3	24			—	Diatom ooze with clay, spicules and volcanic ash	
	1.00	53.7	5	1 × 3	Light gray (2.5Y 7/1)		Dacite-rhyolite	Diatom ooze with clay, spicules and volcanic ash
	1.01	56.2	41(44–45)			—	Diatom ooze with clay, spicules and volcanic ash	
	1.02	56.7	41(44–45)	1 × 5	Light gray (2.5Y 7/1)		Rhyolite	Diatom ooze with clay, spicules and volcanic ash
	1.05	60.7	15		Grayish yellow (2.5Y 6/2)		—	Diatom ooze with clay, spicules and volcanic ash
	1.07	62.6	5			—	Diatom ooze with clay, spicules and volcanic ash	
	1.10	68.1	2			—	Diatom ooze with clay, spicules and volcanic ash	
	1.16	70.4	13	3 × 5	Dark grayish yellow (2.5Y 5/2)		Basaltic andesite	Diatom ooze with clay, spicules and volcanic ash
	1.20	72.9	48 (50–51)			—	Diatom ooze with clay, spicules and volcanic ash	
134	1.22	73.2	48 (50–51)			—	Diatom ooze with clay, spicules and volcanic ash	
	1.28	76.6	3		White	—	Diatom ooze with clay, spicules and volcanic ash	
	1.30	77.4	5		White	—	Diatom ooze with clay, spicules and volcanic ash	
	1.32	80.3	370(54–64)		Dark brown (4.2YR 3.4/0.9)	—	Diatom ooze with clay, spicules and volcanic ash	
	1.33	80.6	370(54–64)		Dark brown (4.2YR 3.4/0.9)	—	Diatom ooze with clay, spicules and volcanic ash	
	1.33	80.9	370(54–64)		Dark brown (4.2YR 3.4/0.9)	—	Diatom ooze with clay, spicules and volcanic ash	
	1.37	81.2	370(54–64)		Dark brown (4.2YR 3.4/0.9)	—	Diatom ooze with clay, spicules and volcanic ash	
	1.38	81.5	370(54–64)		Dark brown (4.2YR 3.4/0.9)	—	Diatom ooze with clay, spicules and volcanic ash	
	1.39	81.8	370(54–64)		Dark brown (4.2YR 3.4/0.9)	—	Diatom ooze with clay, spicules and volcanic ash	
	1.40	82	370(54–64)	1 × 10	Light gray (2.5Y 7/1)	Dark brown (4.2YR 3.4/0.9)	Rhyolite	Diatom ooze with clay, spicules and volcanic ash
135	1.42	82.1	370(54–64)		Dark brown (4.2YR 3.4/0.9)	—	—	Diatom ooze with clay, spicules and volcanic ash
	1.45	82.6	370(54–64)		Brown (9.4YR 3.3/1.3)	—	—	Diatom ooze with clay, spicules and volcanic ash
	1.50	83	370(54–64)		Brown (9.4YR 3.3/1.3)	—	—	Diatom ooze with clay, spicules and volcanic ash
	1.55	83.4	370(54–64)		Brown (9.4YR 3.3/1.3)	—	—	Diatom ooze with clay, spicules and volcanic ash
	1.56	86.5	22			—	—	Diatom ooze with clay
136	1.63	93.5	28	1 × 4	Light gray (2.5Y 8/1)		Rhyolite	Diatom clay

Table 4 (continued).

UNE number	Age (Ma)	Depth (mbsf)	Thickness (cm)	Size of vitric shard (0.01 mm)	Color (dry sample)	Color (shipboard estimate)	Composition	Lithology
137	1.64	93.8	8				—	Diatom clay
	1.83	94.9	5				Rhyolite	Diatom clay
	1.89	105.9	11	0.5 × 7	Yellowish gray (2.5Y 6/1)		—	Diatom clay
	2.13	108.1	3				—	Diatom clay
	2.22	116	4				—	Diatom clay
	2.35	118.8	2				—	Diatom clay
138	2.45	119.4	2				—	Diatom clay
	2.55	123.7	5	1 × 7	Grayish yellow (2.5Y 6/2)		Rhyolite	Diatom clay
	2.75	124.9	3	2 × 3	Yellowish gray (2.5Y 6/1)		Dacite	Diatom clay
	2.90	147.7	14		Light gray (7.4YR 4.3/0.8)		—	Clayey calcareous diatom ooze
	3.08	176.4	6				—	Calcareous ooze with diatom
	3.10	191.2	13	1 × 2	Yellowish gray (2.5Y 4/1)	Black (2.9RP 2.1/1.0)	Basaltic andesite	Clay diatom ooze or diatom ooze
140	3.50	196.4	10	1 × 3	Light gray (2.5Y 7/1)	Light gray (6.8YR 4.5/0.5)	Rhyolite	Clay diatom ooze or diatom ooze
	3.70	199.9	5	1 × 6	Grayish yellow (2.5Y 7/2)		Rhyolite	Clay diatom ooze or diatom ooze
	3.84	204.7	5	2 × 3	Yellowish gray (2.5Y 5/1)		Basaltic andesite	Clay diatom ooze or diatom ooze
	3.89	218.8	15				—	Clay diatom ooze or diatom ooze
	4.02	223.5	3				—	Clay diatom ooze or diatom ooze
	4.35	236.1	6				—	Clay diatom ooze or diatom ooze
144	4.36	269.1	6				—	Clay diatom ooze or diatom ooze
	4.48	269.3	6				—	Clay diatom ooze or diatom ooze
	4.50	271.3	5	0.5 × 6	Light gray (2.5Y 7/1)		Rhyolite	Clay diatom ooze or diatom ooze
	5.23	272.6	5	2.5 × 5	Yellowish gray (2.5Y 6/1)		Andesite-dacite	Clay diatom ooze or diatom ooze
	5.80	296.5	4	2 × 10	Grayish yellow (2.5Y 7/2)		Rhyolite	Clay diatom ooze or diatom ooze
	5.81	320	8	2 × 3	Yellowish gray (2.5Y 5/1)		Dacite	Clay diatom ooze or diatom ooze
145	5.85	321.3	4	2 × 5	Light gray (2.5Y 8/1)		Rhyolite	Clay diatom ooze or diatom ooze
	5.87	323.1	5				—	Clay diatom ooze or diatom ooze
	6.22	324	5				—	Clay diatom ooze or diatom ooze
	150	~35	344.1	—	1 × 5	Light gray (2.5Y 7/1)		Andesite-dacite
	~35	711	8				—	Claystone
	~35	711.8	6				—	Claystone
152	35.00	713.9	11				—	Claystone
	>35	719.4	6	1 × 3	Brownish black (2.5Y 3/1)		Basaltic andesite	Claystone
	>35	720.1	15	3 × 5	Yellowish gray (2.5Y 4/1)	Dark gray (1.5Y 2.5/1)	Andesite-dacite	Claystone
	>35	721.5	7		Dark gray (1.5Y 2.5/1)		—	Claystone
	>35	721.9	55		Dark gray (1.5Y 2.5/1)		—	Claystone
	>35	723	6		Dark gray (1.5Y 2.5/1)		—	Claystone
153	>35	724.8	13		Dark gray (1.5Y 2.5/1)		—	Claystone
	>35	726.5	52		Dark gray (1.5Y 2.5/1)		—	Claystone
	>35	729.9	32		Dark gray (1.5Y 2.5/1)		—	Claystone
	>35	730.3	32				—	Claystone
	>35	788.5	51		Light brown~brown	Black (2.3Y 2.8/0.5)	—	Claystone
							—	Claystone

Note: — = data not available.

Table 5. Representative analyses of vitric shards from Site 881.

Hole: UNE number: Core, section: Interval (cm):	881A 1 1H-2 116-117	881A 1 1H-2 116-117	881A 1 1H-2 116-117	881A 1 1H-2 116-117	881A 1 1H-2 116-117	881A 1 1H-2 116-117	881A 2 1H-4 44-45	881A 2 1H-4 44-45	881A 2 1H-4 44-45	881A 3 1H-6 52-53	881A 3 1H-6 52-53	881A 3 1H-6 52-53	881A 4 1H-6 109-110		
SiO <sub>2</sub>	79.46	79.48	79.67	79.3	79.82	79.72	74.03	79.12	79.23	79.4	79.33	75.94	75.82	76.32	77.74
TiO <sub>2</sub>	0.25	0.29	0	0.31	0.16	0	0	0	0	0	0	0.26	0.42	0.32	0.24
Al <sub>2</sub> O <sub>3</sub>	11.98	11.91	11.98	12.05	11.81	12.08	18.9	12.2	12.51	12.13	12.31	14.81	14.59	14.48	12.88
FeO*	1.8	1.84	1.92	1.85	1.74	0.76	0.73	0.47	0.5	0.44	0.44	2.48	2.36	2.32	1.51
MnO	0	0	0	0	0	0	0	0	0	0	0	0	0	0	0
MgO	0	0	0	0	0	0.78	0	0	0	0	0	0.13	0.18	0	0
CaO	1.53	1.59	1.5	1.57	1.56	1.5	2.15	0.34	0.37	0.42	0.38	2.43	2.37	2.3	1.7
K <sub>2</sub> O	2.07	1.93	2.06	1.92	1.9	2.02	1.13	4.12	4.07	4.12	4.06	1.2	1.4	1.38	1.9
Na <sub>2</sub> O	2.91	2.97	2.87	3	2.9	2.95	1.97	3.49	3.35	3.44	3.47	2.74	2.86	2.88	4.03
Total	98.1	96.86	96.05	98.34	96.23	97.02	96.45	99.43	98.62	98.76	99.67	98.51	99.02	98.61	96.69
Hole: UNE number: Core, section: Interval (cm):	881A 4 1H-6 109-110	881A 4 1H-6 109-110	881A 4 1H-6 109-110	881B 6 2H-3 56-57	881B 6 2H-3 56-57	881B 6 2H-3 56-57	881B 6 2H-3 56-57	881B 6 2H-3 56-57	881B 7 2H-5 149-150	881B 7 2H-5 149-150	881B 7 2H-5 149-150	881B 7 2H-5 149-150	881B 7 2H-5 149-150	881B 7 2H-5 149-150	
SiO <sub>2</sub>	78.34	78.51	76.06	79.87	79.98	79.76	80.37	80.02	80.59	80.29	59.19	77.80	78.40	80.47	79.05
TiO <sub>2</sub>	0.22	0.18	0.34	0.13	0.24	0.21	0.00	0.27	0.00	0.00	1.31	0.39	0.16	0.00	0.17
Al <sub>2</sub> O <sub>3</sub>	12.57	12.6	13.25	11.96	12.24	12.32	12.29	12.34	12.30	12.44	15.34	12.79	12.90	12.00	12.51
FeO*	1.4	1.37	2.1	1.15	0.91	1.01	0.90	0.87	0.95	0.89	10.80	1.54	1.63	1.06	1.50
MnO	0	0	0	0	0.00	0.00	0.00	0.00	0.00	0.00	0.16	0.35	0.00	0.00	0.15
MgO	0	0	0	0	0.00	0.00	0.00	0.00	0.00	0.00	2.04	0.00	0.00	0.00	0.00
CaO	1.49	1.5	1.97	1.18	1.10	1.14	1.17	1.25	1.06	1.13	7.43	1.43	1.63	1.18	1.57
K <sub>2</sub> O	2.09	2.08	1.83	2.1	2.90	2.94	2.67	2.79	2.56	2.72	1.15	2.28	2.04	2.16	2.04
Na <sub>2</sub> O	3.89	3.77	4.46	3.61	2.65	2.62	2.61	2.47	2.54	2.53	2.59	3.42	3.25	3.12	3.02
Total	96.29	96.21	98.61	95.13	93.75	94.29	93.48	93.50	93.34	93.49	98.75	96.15	94.12	94.70	94.98
Hole: UNE number: Core, section: Interval (cm):	881B 7 2H-5 149-150	881B 7 2H-5 149-150	881B 8 3H-1 2-3	881B 8 3H-1 2-3	881B 8 3H-1 2-3	881B 8 3H-1 2-3	881B 9 3H-1 2-3	881B 9 3H-1 2-3	881B 9 3H-1 2-3	881B 9 3H-1 35-36	881B 9 3H-1 35-36	881B 9 3H-1 35-36	881B 9 3H-1 35-36	881B 9 3H-1 35-36	
SiO <sub>2</sub>	77.96	78.54	81.93	79.65	80.47	79.99	79.13	81.15	81.10	77.69	78.20	79.78	79.96	79.88	79.95
TiO <sub>2</sub>	0.19	0.27	0.00	0.27	0.00	0.25	0.27	0.16	0.13	0.23	0.15	0.16	0.27	0.15	0.00
Al <sub>2</sub> O <sub>3</sub>	12.71	12.74	12.53	13.09	12.37	12.72	12.97	12.07	12.19	12.90	12.97	11.84	11.63	11.65	11.96
FeO*	1.56	1.51	0.99	1.45	0.98	1.47	1.58	1.32	1.04	1.57	1.58	1.10	1.23	1.13	1.01
MnO	0.22	0.00	0.00	0.00	0.00	0.00	0.00	0.00	0.00	0.00	0.00	0.00	0.00	0.00	0.00
MgO	0.00	0.00	0.00	0.00	0.00	0.00	0.00	0.00	0.00	0.00	0.00	0.00	0.00	0.00	0.00
CaO	1.84	1.69	1.06	1.70	1.14	1.57	1.81	1.16	1.21	1.78	1.59	1.24	1.17	1.15	1.01
K <sub>2</sub> O	2.08	2.07	2.24	1.89	2.65	1.85	1.92	2.05	2.00	2.08	1.90	2.15	2.17	2.44	2.75
Na <sub>2</sub> O	3.44	3.19	1.25	1.95	2.39	2.13	2.31	2.10	2.32	3.75	3.60	3.74	3.57	3.60	3.31
Total	95.14	94.83	94.14	94.63	94.05	93.82	92.00	93.86	93.70	94.42	97.72	99.29	97.96	97.49	95.75
Hole: UNE number: Core, section: Interval (cm):	881B 10 3H-5 19-20	881B 10 3H-5 19-20	881B 11 3H-6 144-145	881B 11 3H-6 144-145	881B 11 3H-6 144-145	881B 11 3H-6 144-145	881B 12 3H-6 144-145	881B 12 3H-6 144-145	881B 12 3H-6 71-12	881B 12 3H-6 71-12	881B 12 3H-6 71-12	881B 12 3H-6 71-12	881B 13 4H-1 71-12	881B 13 4H-1 71-12	881B 14 5H-3 98-99
SiO <sub>2</sub>	76.11	71.64	79.86	79.32	79.33	80.09	79.47	79.77	80.42	80.32	80.72	79.75	66.39	69.25	76.55
TiO <sub>2</sub>	0.53	0.29	0.00	0.15	0.00	0	0	0	0.22	0.18	0	0.19	0.39	0.73	0.23
Al <sub>2</sub> O <sub>3</sub>	13.25	14.72	12.52	12.58	12.58	12.32	12.64	12.25	11.96	12.25	12.02	12.36	19.61	16	13.56
FeO*	2.73	3.00	0.78	1.05	0.88	0.74	0.89	0.93	0.95	0.94	0.89	1.07	1.14	3.43	1.84
MnO	0.00	0.00	0.00	0.00	0.00	0	0	0	0	0	0	0	0	0	0
MgO	0.00	0.16	0.00	0.00	0.00	0	0	0	0	0	0	0	0	0	0
CaO	1.98	1.59	0.97	0.89	0.90	0.9	0.88	0.96	0.96	1.02	0.87	1.15	0.71	2.98	1.29
K <sub>2</sub> O	1.60	3.46	3.28	3.39	3.48	3.43	3.46	3.36	3.31	3.14	3.13	3.02	4.61	2.48	2.12
Na <sub>2</sub> O	4.17	5.15	2.59	2.62	2.84	2.52	2.73	2.73	2.18	2.14	2.38	2.46	7.15	5.13	4.41
Total	96.65	98.40	96.28	96.62	96.11	94.57	95.01	97.25	96.74	97.53	97.46	97.99	100.22	98.54	98.14

Table 5 (continued).

Hole:	881B														
UNE number:	14	14	15	15	15	15	15	16	16	16	16	16	16	16	16
Core, section:	6H-2	6H-2	6H-3	6H-3	6H-3	6H-3	6H-3	6H-6							
Interval (cm):	103–104	103–104	102–103	102–103	102–103	102–103	102–103	106–107	106–107	106–107	106–107	106–107	106–107	106–107	106–107
SiO <sub>2</sub>	77.61	75.57	74.8	74.07	74.35	75.13	74.22	73.43	79.71	80.19	79.37	79.4	80.39	79.4	79.58
TiO <sub>2</sub>	0	0.31	0.59	0.49	0.63	0.56	0.54	0.51	0.31	0.35	0.36	0.35	0.23	0.34	0.28
Al <sub>2</sub> O <sub>3</sub>	12.84	13.61	14.51	14.55	14.54	13.84	14.59	14.47	12.23	12.17	12.16	11.8	12.03	11.95	12.04
FeO*	1.21	2.08	2.62	2.7	2.85	3.02	2.88	3.05	1.96	2.13	2.15	2.23	1.96	2.24	1.99
MnO	0	0	0	0	0.15	0.13	0.14	0.2	0	0	0	0	0	0	0
MgO	0	0	0.23	0.3	0.32	0.13	0.29	0.36	0.16	0	0.15	0.14	0	0.26	0.19
CaO	1.28	1.33	2.03	2.09	2.05	1.65	2.11	2.31	2.35	2.32	2.38	2.53	2.26	2.4	2.38
K <sub>2</sub> O	3.32	2.44	2.35	2.31	2.22	2.61	2.26	2.33	0.67	0.75	0.79	0.75	0.69	0.75	0.82
Na <sub>2</sub> O	3.74	4.65	2.87	3.49	2.91	2.93	2.96	3.34	2.61	2.1	2.63	2.8	2.38	2.67	2.71
Total	99.41	96.35	97.03	96.2	96.33	96.66	97.57	97.7	95.66	94.83	95.57	94.94	95.47	96.1	95.95
Hole:	881B														
UNE number:	17	17	17	17	17	18	18	18	18	18	18	19	19	19	19
Core, section:	7H-5	7H-5	7H-5	7H-5	7H-5	7H-6	7H-6	7H-6	7H-6	7H-6	7H-6	7H-1	9H-1	9H-1	9H-1
Interval (cm):	115–116	115–116	115–116	115–116	115–116	116–117	116–117	116–117	116–117	116–117	116–117	116–117	43–44	43–44	43–44
SiO <sub>2</sub>	78.95	78.39	78.74	78.38	78.43	79.14	78.5	79.64	79.6	79.83	79.84	79.62	79.65	79.37	79.29
TiO <sub>2</sub>	0	0	0	0	0	0	0	0.14	0	0	0	0	0	0	0
Al <sub>2</sub> O <sub>3</sub>	12.45	12.66	12.68	12.81	12.81	12.59	12.62	12.89	12.71	12.87	12.79	12.82	11.85	12.36	12.17
FeO*	0.36	0.66	0.8	0.44	0.5	0.43	0.42	0.5	0.48	0.53	0.57	0.59	0.87	0.97	0.95
MnO	0	0	0	0	0	0	0	0	0	0	0	0	0	0	0
MgO	0	0	0	0	0	0	0	0	0	0	0	0	0	0	0
CaO	0.45	0.49	0.81	0.54	0.43	0.39	0.46	0.43	0.38	0.38	0.47	0.42	1.07	1	1.08
K <sub>2</sub> O	4.62	4.5	3.56	4.48	4.63	4.4	4.53	4.12	4.22	4.17	3.86	4.22	3.29	3.31	3.27
Na <sub>2</sub> O	3.16	3.3	3.41	3.34	3.21	3.05	3.46	2.28	2.61	2.22	2.47	2.32	3.27	2.99	3.24
Total	96.59	97.05	96.68	97.1	96.41	95.36	99.63	96.65	97.53	97.08	97.49	97.25	96.09	96.49	95.24
Hole:	881B														
UNE number:	19	19	19	19	21	21	21	23	23	23	23	23	25	25	25
Core, section:	9H-1	9H-1	9H-1	9H-1	9H-5	10H-5	10H-5	10H-6	10H-6	10H-6	10H-6	10H-6	10H-6	11H-1	11H-1
Interval (cm):	43–44	43–44	43–44	43–44	69–70	69–70	69–70	8–9	8–9	8–9	8–9	8–9	8–9	110–111	110–111
SiO <sub>2</sub>	79.26	78.99	79.03	79.07	71.09	63.43	69.9	66.89	72.04	77.42	70.36	80.08	73.01	78.95	73.58
TiO <sub>2</sub>	0	0	0	0	0.61	1.55	0.72	0.99	0.61	0.28	0.78	0.2	1.32	0.42	0.74
Al <sub>2</sub> O <sub>3</sub>	12.11	12.18	12.33	12.17	15.05	14.47	15.33	14.37	14.18	12.86	14.47	12.23	13.24	11.87	13.76
FeO*	0.93	0.9	1.08	1.01	3.7	7.28	4.09	5.92	4.52	2.65	4.16	1.66	3.61	1.9	2.94
MnO	0	0	0	0	0	0.16	0	0	0	0	0	0	0	0	0
MgO	0	0	0	0	0.5	2.98	0.7	0.99	0.49	0	0.76	0.14	0	0	0.4
CaO	1.04	1.18	1.06	1.07	2.93	5.48	3.08	3.4	3.32	1.77	3.15	2.1	2.11	0.54	2.69
K <sub>2</sub> O	3.33	3.36	3.29	3.28	2.12	1.55	2.05	4.46	1.68	1.91	2.81	0.91	3.18	3.02	2.46
Na <sub>2</sub> O	3.34	3.39	3.21	3.4	4.01	3.1	4.12	2.99	3.17	3.11	3.5	2.68	3.53	3.29	3.43
Total	96.64	96.1	95.74	96.27	95.04	98.15	96.55	97.81	96.94	96.77	96.08	96.28	97.76	96.35	96.53
Hole:	881B														
UNE number:	25	25	25	25	27	27	27	27	28	28	28	29	29	29	29
Core, section:	11H-1	11H-1	11H-1	11H-1	11H-1	11H-4	12H-1	12H-1	12H-1						
Interval (cm):	110–111	110–111	110–111	110–111	110–111	49–50	49–50	49–50	49–50	49–50	49–50	59–60	59–60	5–7	5–7
SiO <sub>2</sub>	75.38	75.79	74.84	74.84	74.98	78.16	78.75	78.27	75.56	77.77	76.9	76.76	76.83	78.88	79.59
TiO <sub>2</sub>	0.62	0.47	0.62	0.56	0.56	0.24	0.29	0.28	0.51	0.23	0.23	0.24	0.2	0.34	0.31
Al <sub>2</sub> O <sub>3</sub>	13.42	13.39	13.51	13.59	13.6	12.75	12.6	12.97	13.52	12.51	13.61	13.73	13.89	12.37	11.96
FeO*	2.48	2.32	2.57	2.64	2.64	1.82	1.82	1.7	2.59	1.67	3.19	2.96	2.74	2.25	2.18
MnO	0	0	0	0	0	0	0	0	0	0	0	0	0	0	0
MgO	0.25	0	0.26	0.19	0	0	0	0	0.18	0	0	0	0	0	0
CaO	2.06	1.85	2.01	2.23	2.09	1.69	1.75	1.65	2.39	1.63	2.76	2.8	2.76	2.24	2.2
K <sub>2</sub> O	2.52	2.64	2.69	2.51	2.73	2.02	2.01	2.11	2.09	2.22	1	1.14	0.95	0.96	1.04
Na <sub>2</sub> O	3.26	3.53	3.5	3.43	3.4	3.32	2.79	3.02	3.17	3.97	2.32	2.37	2.63	2.96	2.72
Total	95.68	96.83	96.05	95.65	96.16	95.48	94.84	96.43	95.37	97.19	92.73	92.95	92.17	96.76	94.14

Table 5 (continued).

Hole: UNE number: Core, section: Interval (cm):	881B 29 12H-1 5-7	881B 29 12H-1 5-7	881B 29 12H-1 5-7	881B 29 12H-1 5-7	881B 30 12H-1 62-63	881B 30 12H-1 62-63	881B 30 12H-1 62-63	881B 30 12H-1 62-63	881B 31 12H-1 140-141	881B 31 12H-1 140-141	881B 31 12H-1 140-141	881B 31 12H-1 140-141	881B 31 12H-1 140-141	
SiO <sub>2</sub>	78.95	80.14	75.65	78.32	79.29	72.43	72.88	73.12	72.56	72.65	71.84	78.85	79.19	
TiO <sub>2</sub>	0.14	0.26	0.37	0.47	0.38	0.45	0.42	0.46	0.52	0.45	0.37	0.44	0.49	
Al <sub>2</sub> O <sub>3</sub>	13.26	11.78	14.34	12.41	12.23	14.11	14.09	14.21	14.02	14.12	15.91	12.29	12.06	
FeO*	1.63	2.41	2.83	2.39	2.43	3.66	3.43	3.38	3.71	3.69	3.24	2.19	2.23	
MnO	0	0	0	0	0	0	0	0	0	0	0	0	0	
MgO	0	0	0.31	0.18	0	0.38	0.19	0.22	0.22	0.25	0	0.18	0	
CaO	2.15	1.99	2.9	2.3	2.04	2.77	2.68	2.56	2.93	2.76	2.58	1.98	2.2	
K <sub>2</sub> O	0.95	1.02	0.82	1.14	1.02	2.37	2.31	2.31	2.43	2.26	2.21	1.63	1.62	
Na <sub>2</sub> O	2.92	2.38	2.77	2.79	2.61	3.82	3.99	3.73	3.62	3.81	3.85	2.44	2.2	
Total	95.59	94.31	95.07	96.25	94.74	96.11	95.66	94.75	94.3	96.49	94.18	97.55	97.35	
												96.21	96.88	
Hole: UNE number: Core, section: Interval (cm):	881B 31 12H-1 140-141	881B 32 12H-2 19-20	881B 32 12H-2 19-20	881B 32 12H-2 19-20	881B 33 13H-2 118-119	881B 33 13H-2 118-119	881B 33 13H-2 118-119	881B 33 13H-2 118-119	881B 34 13H-5 118-119	881B 34 13H-5 118-119	881B 34 13H-5 118-119	881B 34 13H-5 118-119	881B 34 13H-5 118-119	
SiO <sub>2</sub>	79.67	80.2	79.8	80.11	79.97	60.63	78.22	71.03	64.04	74.21	78.58	78.42	79.62	
TiO <sub>2</sub>	0.27	0	0	0	0	1.42	0.23	0.78	0.89	0.5	0.4	0.4	0.51	
Al <sub>2</sub> O <sub>3</sub>	12.49	12.36	12.41	12.26	12.52	16.44	12.9	15.6	16.19	13.12	12.09	12.07	12.36	
FeO*	2	0.99	0.89	1.05	0.93	7.63	1.71	4.37	5.66	3.2	2.23	2.25	2.04	
MnO	0	0	0	0	0	0	0	0	0.15	0	0	0	0	
MgO	0	0	0	0	0	2.18	0	0.47	1.11	0	0	0	0.22	
CaO	1.98	0.95	0.94	0.93	0.97	6.59	1.09	2.91	6.02	1.35	2.16	2.13	1.96	
K <sub>2</sub> O	1.51	2.47	2.48	2.31	2.53	1.43	2.77	1.98	1.68	3.94	1.64	1.76	1.61	
Na <sub>2</sub> O	2.07	3.04	3.49	3.35	3.07	3.67	3.07	2.87	4.25	3.67	2.92	2.96	1.47	
Total	97.38	95.99	97.1	95.37	96.38	97.67	94.67	95.41	98.52	97.23	94.64	96.05	95.62	
												95.46	95.94	
Hole: UNE number: Core, section: Interval (cm):	881B 34 13H-5 42-43	881B 34 13H-5 42-43	881B 34 13H-5 42-43	881B 34 13H-5 42-43	881B 36 14H-5 44-45	881B 36 14H-5 44-45	881B 38 15H-4 129-130	881B 38 15H-4 129-130	881B 39 15H-6 73-74	881B 39 15H-6 73-74	881B 39 15H-6 73-74	881B 39 15H-6 73-74	881B 39 15H-6 73-74	881B 41 16H-1 84-85
SiO <sub>2</sub>	79.56	78.77	78.65	78.41	72.95	76.08	75.56	80	71.94	72.98	72.8	72.58	73.12	
TiO <sub>2</sub>	0.23	0.39	0.45	0.41	0.7	0.9	0.34	0	0.5	0.35	0.42	0.45	0.39	
Al <sub>2</sub> O <sub>3</sub>	11.91	12.21	12.13	12.08	15.01	12.45	13.64	12.51	14.31	14.02	13.51	14.19	14.58	
FeO*	2.21	2.14	2.28	2.14	3.57	3.49	3.17	1.03	3.45	3.24	3.79	3.54	3.14	
MnO	0	0	0	0	0	0	0	0	0	0	0	0	0	
MgO	0	0	0	0.17	0.36	0	0	0	0.32	0.24	0.17	0.24	0	
CaO	1.81	1.92	1.98	1.99	3.44	2.08	2.68	0.95	2.83	2.53	2.64	2.39	2.62	
K <sub>2</sub> O	1.54	1.75	1.64	1.67	1.6	2.48	0.99	2.53	2.4	2.37	2.36	2.26	1.86	
Na <sub>2</sub> O	2.75	2.81	2.88	3.14	2.38	2.53	3.62	2.98	4.25	4.27	4.31	3.86	3.9	
Total	95.29	96.55	96.71	96.79	91.53	92.1	95.85	94.52	98.82	98.73	98.71	96.81	98.04	
												102.33	101.38	
Hole: UNE number: Core, section: Interval (cm):	881B 43 16H-6 145-146	881B 43 16H-6 145-146	881B 43 16H-6 145-146	881B 43 16H-6 145-146	881B 44 16H-6 145-146	881B 44 16H-6 145-146	881B 44 16H-7 30-31	881B 44 16H-7 30-31						
SiO <sub>2</sub>	79.99	79.6	79.18	79.19	79.14	78.96	74	75.2	74.74	55.25	77.18	68.56	74.43	
TiO <sub>2</sub>	0	0	0	0	0.17	0.18	0.37	0.31	0.47	0.96	0.16	1.36	0.35	
Al <sub>2</sub> O <sub>3</sub>	12.44	12.68	12.83	12.9	12.86	12.61	14.13	14.16	13.72	15.15	13.46	13.7	13.91	
FeO*	0.96	1.31	1.41	1.42	1.46	1.47	3.05	1.55	3.06	12.64	1.41	6.72	2.99	
MnO	0	0	0	0	0	0	0.48	0.4	0.31	0.29	0	0.34	0.28	
MgO	0	0	0	0	0	0	0.34	0	0.19	4.44	0	0.61	0.22	
CaO	0.94	1.26	1.47	1.52	1.5	1.49	2.72	1.36	2.67	7.41	1.02	3.45	2.8	
K <sub>2</sub> O	3.73	2.68	2.54	2.57	2.53	2.55	1.43	3.27	1.48	1.33	3.22	2.12	1.51	
Na <sub>2</sub> O	1.94	2.47	2.58	2.4	2.35	2.74	3.46	3.74	3.35	2.53	3.55	3.14	3.52	
Total	93.25	94.73	95.36	94.37	94.82	95.93	95.83	95.56	95.12	97.35	94.28	94.99	95.78	
												95.14	95.22	

**Table 5 (continued).**

Hole:	881B	881B	881B	881C	881C						
UNE number:	45	45	45	46	46	46	47	47	47	50	50
Core, section:	17H-1	17H-1	17H-1	17H-1	17H-1	17H-1	18H-1	18H-1	18H-1	21X-6	21X-6
Interval (cm):	11–12	11–12	11–12	22–23	22–23	22–23	148–149	148–149	148–149	40–41	40–41
SiO <sub>2</sub>	59.12	66.21	65.56	69.83	71.24	69.15	67.63	62.95	67.13	65.85	80.56
TiO <sub>2</sub>	0.89	1.57	1.21	0.62	0.65	0.71	0.81	1.08	0.82	0.94	0.16
Al <sub>2</sub> O <sub>3</sub>	15.69	14.17	17.44	14.38	14.17	14.63	14.83	15.38	14.74	15.06	11.76
FeO*	10.59	8.85	4.39	5.04	4.64	5.32	5.76	7.25	5.48	6.04	1.19
MnO	0	0	0	0	0	0	0	0	0	0	0
MgO	2.64	1	0	0.66	0.36	0.87	1.12	1.75	0.94	1.23	0
CaO	7	4.51	5.2	3.76	3.18	4.07	4.28	6	4.19	4.71	0.97
K <sub>2</sub> O	0.99	1.65	1.76	2.58	2.73	2.47	2.38	1.95	2.53	2.29	3.11
Na <sub>2</sub> O	3.09	2.04	4.44	3.12	3.03	2.77	3.19	3.63	4.17	3.87	2.25
Total	99.07	93.97	98.05	96.67	97.82	97.94	99.88	101.79	99.97	101.76	97.85
											97.23
Hole:	881C	881C	881C	881C	881C						
UNE number:	50	50	50	50	50	51	51	51	51	51	51
Core, section:	21X-6	21X-6	21X-6	21X-6	21X-6	23X-7	23X-7	23X-7	23X-7	23X-7	23X-7
Interval (cm):	40–41	40–41	40–41	40–41	40–41	26–27	26–27	26–27	26–27	26–27	26–27
SiO <sub>2</sub>	80.18	80.43	80.03	79.81	79.62	78.39	78.14	78.25	78.08	78.14	78.99
TiO <sub>2</sub>	0.13	0	0.14	0.25	0	0	0	0	0	0	0
Al <sub>2</sub> O <sub>3</sub>	11.81	11.79	11.75	11.85	12.57	12.56	12.51	12.54	12.69	12.46	11.89
FeO*	1.31	1.2	1.41	1.54	0.59	0.3	0.45	0.35	0.42	0.41	1.5
MnO	0	0	0	0	0	0	0	0	0	0	0
MgO	0	0	0	0	0	0	0	0	0	0	0
CaO	1.18	1	1.46	1.41	0.14	0.49	0.46	0.5	0.58	0.54	1.33
K <sub>2</sub> O	2.82	3.15	2.71	2.62	4.77	4.81	5.41	5.35	5.14	4.93	2.22
Na <sub>2</sub> O	2.58	2.43	2.5	2.51	2.31	3.44	3.03	3.01	3.09	3.53	4.07
Total	98.62	97.27	98.51	98.6	98.01	96.85	95.99	97.43	98.03	97.2	96.7
											97.7

Notes: Major elements reported as wt% oxides. UNE number refers to the ash layer number analyzed at UNE (see Table 1). Total = the original analytical total. Individual oxide values sum to 100%. Zero values indicate that the element abundances are less than the detection limit of EDS. All Fe reported as FeO\*.

**Table 6.** Representative analyses of vitric shards from Hole 882A.

UNE number:	53	53	53	53	53	54	54	54	54	54	54	55	55	55	55
Core, section:	1H-4	1H-4	1H-4	1H-4	1H-4	1H-6	1H-6	1H-6	1H-6	1H-6	1H-6	2H-5	2H-5	2H-5	2H-5
Interval (cm):	145–146	145–146	145–146	145–146	145–146	83–84	83–84	83–84	83–84	83–84	83–84	21–22	21–22	21–22	21–22
SiO <sub>2</sub>	77.02	76.8	77.1	77.43	77.53	68.02	73.59	73.75	72.99	56.51	73.27	71.17	72	70.77	71.52
TiO <sub>2</sub>	0.28	0.3	0.22	0.31	0.31	0.85	0.53	0.41	0.51	3.41	0.34	0.37	0.53	0.77	0.6
Al <sub>2</sub> O <sub>3</sub>	13.44	13.71	13.42	13.49	13.59	16.28	14.96	14.92	14.92	18.5	15.1	16.44	15.18	15.54	15.44
FeO*	2.01	1.96	1.98	1.88	1.66	4.14	2.14	1.99	2.08	8.03	2.02	1.98	2.43	2.71	2.54
MnO	0	0	0	0	0	0	0	0	0	0	0	0	0	0	0
MgO	0	0	0	0	0	1.01	0	0	0.14	1.97	0	0	0.35	0.4	0.34
CaO	1.43	1.43	1.48	1.38	1.07	3.11	1.39	1.24	1.32	5.77	1.24	2.45	1.65	1.9	1.82
K <sub>2</sub> O	2.86	2.86	2.86	2.82	2.98	2.66	3.49	3.54	3.6	1.01	3.41	3.08	3.65	3.34	3.48
Na <sub>2</sub> O	2.96	2.95	2.94	2.69	2.86	3.94	3.91	4.14	4.43	4.8	4.63	4.51	4.2	4.56	4.35
Total	97.32	98.14	98.61	97.8	98.08	97.26	92.18	98.12	96.87	97.19	96.14	97.73	96.66	99.02	97.65

UNE number:	55	56	57	57	57	57	58	58	58	58	58	58	59	59	59
Core, section:	2H-5	2H-6	2H-7	2H-7	2H-7	2H-7	3H-4	3H-4	3H-4						
Interval (cm):	21–22	148–149	17–18	17–18	17–18	17–18	18–19	18–19	18–19	18–19	18–19	18–19	118–120	118–120	118–120
SiO <sub>2</sub>	72.2	81.58	70.83	64.79	70.78	73.26	71.83	77.6	79.28	79.82	79.14	79.4	80.34	77.53	79.96
TiO <sub>2</sub>	0.56	0	0.64	1.33	0.77	0.58	0.68	0.21	0	0	0.19	0.17	0.21	0.2	0
Al <sub>2</sub> O <sub>3</sub>	15.46	12.17	16.16	13.8	15.94	15.82	15.74	13.73	12.98	13.01	13.09	13.07	12.43	13.15	12.81
FeO*	2.24	1.03	3.25	7.88	3.1	2.5	2.71	1.73	1.49	1.45	1.47	1.43	1.35	2.93	0.34
MnO	0	0	0	0	0	0	0	0	0	0	0	0	0	0	0
MgO	0	0	0.4	2.69	0.38	0	0.36	0	0	0	0	0	0	0	0
CaO	1.76	0.23	2.32	4.62	2.36	1.62	2.02	2.04	1.68	1.61	1.62	1.67	1.5	2.28	0.58
K <sub>2</sub> O	3.48	2.87	3.33	2.47	3.4	3.61	3.45	1.61	1.78	1.74	1.81	1.76	1.71	1.78	3.92
Na <sub>2</sub> O	4.29	2.12	3.09	2.44	3.27	2.6	3.21	3.08	2.79	2.37	2.67	2.5	2.47	2.13	2.62
Total	97.27	97.65	97.92	97.95	99.26	97.18	98.75	97.5	97.88	96.07	98.31	97.02	97.5	96.98	98.82

UNE number:	60	60	60	60	60	61	61	61	62	62	62	62	63	63	63
Core, section:	4H-5	4H-5	4H-5	4H-5	4H-5	5H-4	5H-4	5H-4	6H-1	6H-1	6H-1	6H-1	6H-4	6H-4	6H-4
Interval (cm):	12–13	12–13	12–13	12–13	12–13	149–150	149–150	149–150	32–33	32–33	32–33	32–33	29–30	29–30	29–30
SiO <sub>2</sub>	73.72	73.36	73.26	73.85	73.86	74.03	73.59	70.09	75.01	75.24	75.06	77.75	74.53	73.63	74.24
TiO <sub>2</sub>	0.67	0.46	0.59	0.46	0.55	0.49	0.44	0.71	0.53	0.4	0.48	0.6	0.52	0.44	0.32
Al <sub>2</sub> O <sub>3</sub>	14.36	14.34	14.08	14.18	14.04	14	13.94	14.83	13.97	14.37	13.98	12.51	14.15	14.06	14.12
FeO*	3.01	3.17	3.15	3.25	2.99	3.86	3.94	5.29	2.45	2.34	2.41	2.03	2.61	3.68	3.28
MnO	0	0	0	0	0	0	0	0	0	0	0	0	0	0	0
MgO	0	0.18	0.28	0	0	0.3	0.29	1.02	0.22	0	0.2	0	0.25	0	0
CaO	1.78	2.01	1.9	1.83	1.76	2.79	3.13	4.03	2.04	2	2.05	1.09	2.34	1.79	1.86
K <sub>2</sub> O	2.25	2.35	2.39	2.18	2.48	1.73	1.8	1.44	2.93	2.85	2.83	3.38	2.92	3.41	3.31
Na <sub>2</sub> O	4.26	4.14	4.34	4.24	4.31	2.8	2.87	2.6	2.87	2.8	2.98	2.63	2.68	2.98	2.86
Total	97.69	98.07	98.34	97.45	96.89	97.62	98	97.38	98.52	97.91	97.65	97.31	98.11	95.66	96.6

UNE number:	63	63	63	63	64	64	64	64	65	65	65	65	65	65	65
Core, section:	6H-4	6H-4	6H-4	6H-4	8H-2	8H-2	8H-2	8H-2	8H-3						
Interval (cm):	29–30	29–30	29–30	29–30	133–135	133–135	133–135	133–135	12–13	12–13	12–13	12–13	12–13	12–13	12–13
SiO <sub>2</sub>	73.83	74.2	74.82	74.43	73.54	73.58	73.71	73.31	73.63	76.17	79.37	79.03	78.48	79.19	76.09
TiO <sub>2</sub>	0.48	0.47	0.34	0.45	0.67	0.56	0.62	0.69	0.66	0.25	0	0.2	0.15	0.2	0.3
Al <sub>2</sub> O <sub>3</sub>	14.02	14	14.08	13.91	14.2	14.24	13.93	14.35	14.3	14.14	12.12	12.41	12.5	12.29	13.99
FeO*	3.33	3.44	3.38	3.27	3.2	3.4	3.28	3.12	3.1	1.28	0.66	0.58	0.86	0.6	1.24
MnO	0	0	0	0	0	0	0	0	0	0	0	0	0	0	0
MgO	0	0	0	0	0.35	0.26	0.36	0.48	0.51	0	0	0	0	0	0.13
CaO	1.9	1.86	1.73	1.9	2.87	3.1	3.02	3.07	2.75	1.18	0.37	0.47	0.45	0.4	1.27
K <sub>2</sub> O	3.17	3.31	3.14	3.21	2.3	2.02	2.1	2.12	2.22	3.41	4.01	4.09	3.96	3.89	3.48
Na <sub>2</sub> O	3.27	2.72	2.51	2.85	2.88	2.84	2.97	2.85	2.83	3.57	3.48	3.42	3.56	3.48	4.23
Total	97.94	97.92	96.12	96.49	96.83	96.57	97.29	97.51	97.54	97.49	96.59	97.8	97.51	97.1	96.56

Table 6 (continued).

UNE number:	65	67	68	68	68	69	70	70	71	71	71	71	73	73	73	73
Core, section:	8H-3	8H-6	8H-7	8H-7	8H-7	9H-2	9H-3	9H-3	9H-5	9H-5	9H-5	9H-5	9H-6	9H-6	9H-6	9H-6
Interval (cm):	12–13	54–55	12–13	12–13	12–13	14–15	89–91	89–91	76–77	76–77	76–77	76–77	58–59	58–59	58–59	58–59
SiO <sub>2</sub>	78.89	76.26	74.26	74.66	75.12	72.49	72.42	70.36	76.16	75.9	76.28	76.68	71.6	74.3	73.55	71.31
TiO <sub>2</sub>	0	0.17	0.37	0.39	0.45	0.67	0.51	0.85	0.35	0.44	0.35	0.38	0.66	0.34	0.74	0.59
Al <sub>2</sub> O <sub>3</sub>	12.47	13.71	13.35	13.15	13.16	14.28	14.75	14.65	14.22	14.3	14.06	13.59	15.07	14.91	14.57	15.25
FeO*	0.68	1.47	4.63	4.41	4.37	3.79	3.17	4.32	1.99	1.94	1.86	1.59	3.4	1.06	2.96	3.75
MnO	0	0	0	0	0	0	0	0	0	0	0	0	0	0.12	0	0
MgO	0	0	0.2	0.13	0.22	0.17	0.31	0.53	0	0	0	0.56	0	0.35	0.7	0.7
CaO	0.38	1.84	3.02	2.79	2.73	1.93	2.36	2.67	1.56	1.54	1.49	1.18	2.69	1.43	2.09	2.96
K <sub>2</sub> O	4.16	2.52	1.69	1.83	1.72	2.99	2.6	2.68	2.81	2.97	2.83	3.28	2.59	3.44	2.73	2.47
Na <sub>2</sub> O	3.41	4.04	2.48	2.65	2.23	3.67	3.89	3.94	2.9	2.9	3.13	3.3	3.43	4.53	2.89	2.98
Total	98.12	98.87	97.19	98.83	98.54	97.42	98.11	98.6	95.7	94.68	95.16	95.46	97.81	98.45	98.43	97.73
UNE number:	74	76	76	76	77	77	77	77	78	79	80	80	80	80	80	80
Core, section:	9H-6	11H-1	11H-1	11H-1	11H-4	11H-4	11H-4	11H-4	11H-4	23H-6	24H-1	24H-4	24H-4	24H-4	24H-4	24H-4
Interval (cm):	135–136	63–65	63–65	63–65	133–134	133–134	133–134	133–134	133–134	39–40	100–101	144–145	144–145	144–145	144–145	144–145
SiO <sub>2</sub>	58.82	58.77	66.87	56.09	73.72	73.1	76.02	64.96	65.01	67.73	64.06	71.91	71.9	72.97	72.29	72.84
TiO <sub>2</sub>	1.24	1.25	1.13	1.27	0.43	0.57	0.36	0.77	0.77	2.39	1.25	0.61	0.57	0.49	0.64	0.7
Al <sub>2</sub> O <sub>3</sub>	15.23	15.76	15.73	16.05	13.35	13.49	13.06	15.19	15.23	11.21	16.11	16.05	15.97	15.92	15.92	15.77
FeO*	11.47	9.37	6.16	11.07	4.02	4.28	3.59	7.31	7.36	10.06	7.38	2.7	2.86	2.46	2.53	2.5
MnO	0.17	0	0	0	0	0	0	0	0.14	0	0	0	0	0	0	0
MgO	2.12	2.8	0.86	3.19	0	0	0	1.75	1.65	0.32	1.53	0.36	0.45	0.22	0.38	0.21
CaO	6.7	7.26	3.89	8.04	2.41	2.68	2.15	5.71	5.58	2.2	4.93	2.22	2.19	1.83	1.84	1.84
K <sub>2</sub> O	1.4	1.34	2.43	1.07	1.97	1.95	2.07	1.22	1.29	2.56	1.67	3.22	2.92	3.12	3.28	3.19
Na <sub>2</sub> O	2.86	3.44	2.93	3.23	4.1	3.92	2.76	3.1	2.98	3.53	3.08	2.93	3.14	2.99	3.12	2.95
Total	98.84	101.88	99.54	103.36	100.76	100.72	98.65	101.08	101.2	99.67	98.5	97.84	96.61	98.43	98.69	96.06
UNE number:	80	82	82	82	82	82	83	83	83	83	83	83	84	84	84	85
Core, section:	24H-4	38H-4	38H-4	38H-4	38H-4	38H-4	39H-7	39H-7	39H-7	39H-7	39H-7	39H-7	41H-1	41H-1	41H-1	42H-2
Interval (cm):	144–145	116–117	116–117	116–117	116–117	116–117	24–25	24–25	24–25	24–25	24–25	24–25	120–121	120–121	120–121	130–131
SiO <sub>2</sub>	73	73.6	74.98	75.76	76.18	75.56	77.22	76.55	76.15	76.56	76.11	76.49	78.72	78.86	79.31	78.4
TiO <sub>2</sub>	0.62	0.29	0.17	0	0	0.15	0.36	0.31	0.25	0.26	0.19	0	0	0	0	0
Al <sub>2</sub> O <sub>3</sub>	15.54	14.73	14.36	14.09	13.91	14	13.41	13	13.04	12.83	12.99	13.11	12.37	11.94	12.01	12.46
FeO*	2.61	1.9	1.6	1.34	1.25	1.4	1.61	1.7	1.79	1.76	1.88	1.7	0.75	0.78	0.55	1
MnO	0	0	0	0	0	0	0	0	0	0	0	0	0	0	0	0
MgO	0.28	0.13	0	0	0	0	0	0	0	0	0	0	0	0	0	0
CaO	1.92	1.45	1.17	0.86	0.7	0.95	1.05	1.06	1.02	1.1	1.09	1.05	0.66	0.59	0.52	0.78
K <sub>2</sub> O	3.22	4.48	4.35	4.63	4.76	4.66	3.81	3.58	3.86	3.83	3.78	3.8	4.32	4.66	4.7	4.16
Na <sub>2</sub> O	2.81	3.41	3.37	3.32	3.19	3.28	2.55	3.8	3.9	3.63	3.89	3.67	3.19	3.17	2.91	3.2
Total	96.69	98.58	97.09	96.57	97.15	97.95	98.22	98.62	98.63	98.27	98.19	97.98	95.92	95.82	94.08	97.83
UNE number:	85	85	85	85	85	86	86	86	86	86	86	86	84	84	84	85
Core, section:	42H-2	42H-2	42H-2	42H-2	42H-2	42H-4	42H-4	42H-4	42H-4	42H-4	42H-4	42H-4	41H-1	41H-1	41H-1	42H-2
Interval (cm):	130–131	130–131	130–131	130–131	130–131	130–131	55–56	55–56	55–56	55–56	55–56	55–56	120–121	120–121	120–121	130–131
SiO <sub>2</sub>	78.36	78.56	78.59	78.54	78.05	78.33	79.57	80.5	80.16	80.2	79.91					
TiO <sub>2</sub>	0	0	0	0	0.15	0	0	0	0	0	0	0				
Al <sub>2</sub> O <sub>3</sub>	12.54	12.3	12.46	12.39	12.49	12.44	12.43	12.6	12.51	12.5	12.57					
FeO*	0.99	1.03	1.05	1.07	1.06	0.99	0.77	0.62	0.55	0.67	0.6					
MnO	0	0	0	0	0	0	0	0	0	0	0					
MgO	0	0	0	0	0	0	0	0	0	0	0					
CaO	0.69	0.81	0.79	0.79	0.69	0.91	0.58	0.45	0.43	0.38	0.45					
K <sub>2</sub> O	4.37	4.07	3.91	3.8	4.18	3.92	4.12	3.77	3.92	3.96	3.82					
Na <sub>2</sub> O	3.05	3.23	3.21	3.4	3.38	3.41	2.53	2.05	2.42	2.29	2.65					
Total	96.28	96.79	95.52	96.48	97.73	96.52	98.22	96.27	97.78	96.8	97.54					

Notes: Major elements reported as wt% oxides. UNE number refers to the ash layer number analyzed at UNE (see Table 2). Total is the original analytical total. Individual oxide values sum to 100%. Zero values indicate the element abundances are less than the detection limit of EDS. All Fe reported as FeO\*.

**Table 7. Representative analyses of vitric shards from Hole 883B.**

UNE number:	87	87	87	89	89	89	89	89	89	91	92	92	92	92	92	92
Core, section:	1H-2	1H-2	1H-2	2H-1	2H-1	2H-1	2H-1	2H-1	2H-1	3H-6	3H-6	3H-6	3H-6	3H-6	3H-6	3H-6
Interval (cm):	107–108	107–108	107–108	67–70	67–70	67–70	67–70	67–70	67–70	102–103	67–68	67–68	67–68	67–68	67–68	67–68
SiO <sub>2</sub>	73.89	74.31	73.92	75.54	74.64	74.39	69.93	74.09	74.88	74.45	65.01	79.61	80.11	79.69	80.64	79.92
TiO <sub>2</sub>	0.50	0.56	0.60	0.58	0.59	0.56	0.90	0.53	0.53	1.42	0.00	0.00	0.00	0.00	0.00	0.00
Al <sub>2</sub> O <sub>3</sub>	15.01	14.95	15.05	15.62	15.13	15.32	16.25	15.17	15.08	15.28	15.39	12.42	12.45	12.43	12.39	12.28
FeO*	2.40	2.38	2.18	2.14	2.04	2.18	3.81	2.41	2.06	2.48	8.55	0.69	0.66	0.74	0.56	0.77
MnO	0.00	0.00	0.00	0.00	0.00	0.00	0.00	0.00	0.00	0.00	0.00	0.00	0.00	0.00	0.00	0.00
MgO	0.00	0.00	0.00	0.00	0.00	0.00	0.61	0.00	0.00	0.36	0.00	0.00	0.00	0.00	0.00	0.00
CaO	1.43	1.37	1.33	1.33	1.35	1.16	2.75	1.37	1.35	1.49	3.59	0.84	0.64	0.78	0.61	0.78
K <sub>2</sub> O	3.72	3.79	3.77	3.26	3.37	3.37	2.73	3.31	3.32	3.10	2.93	3.71	3.47	3.69	3.28	3.57
Na <sub>2</sub> O	3.05	2.65	3.14	1.89	2.87	3.02	3.04	3.12	2.77	2.74	2.73	2.67	2.69	2.53	2.68	2.75
Total	98.12	98.64	98.84	96.48	97.61	98.56	98.15	98.73	97.28	97.16	98.39	95.80	95.36	95.87	95.93	95.68
UNE number:	92	93	93	93	93	94	95	95	95	95	95	95	95	96	96	96
Core, section:	3H-06	4H-03	4H-03	4H-3	4H-3	5H-4	6H-1	6H-1	6H-1	6H-1	6H-1	6H-1	6H-2	6H-2	6H-2	6H-2
Interval (cm):	67–68	25–26	25–26	25–26	25–26	56–57	40–41	40–41	40–41	40–41	40–41	40–41	40–41	70–71	70–71	70–71
SiO <sub>2</sub>	80.00	72.54	75.54	75.87	71.50	72.58	74.82	74.09	75.05	74.90	75.58	73.66	75.73	77.44	76.81	77.07
TiO <sub>2</sub>	0.13	0.60	0.15	0.67	0.67	0.55	0.42	0.54	0.46	0.56	0.45	0.68	0.52	0.00	0.23	0.25
Al <sub>2</sub> O <sub>3</sub>	12.15	14.43	13.59	12.31	14.73	13.91	14.24	14.70	14.27	14.05	14.11	14.61	14.16	13.41	13.33	13.40
FeO*	0.73	3.47	2.23	3.13	3.46	3.77	2.53	2.56	2.36	2.52	2.39	2.88	2.19	2.21	2.63	2.87
MnO	0.00	0.00	0.00	0.00	0.00	0.00	0.00	0.00	0.00	0.00	0.00	0.00	0.00	0.00	0.00	0.00
MgO	0.00	0.29	0.00	0.00	0.37	0.43	0.23	0.28	0.15	0.20	0.15	0.37	0.15	0.00	0.00	0.00
CaO	0.76	2.27	1.27	1.65	2.49	2.83	2.10	2.42	2.03	2.14	2.23	2.05	0.74	1.32	1.43	1.37
K <sub>2</sub> O	3.49	2.33	2.88	3.09	2.07	1.76	2.95	2.83	2.79	2.93	2.81	2.85	2.79	3.88	2.93	2.84
Na <sub>2</sub> O	2.73	4.08	4.34	3.29	4.72	4.18	2.72	2.58	2.88	2.71	2.38	2.72	2.41	2.33	2.74	2.63
Total	96.79	97.19	96.50	99.04	98.59	97.78	97.29	97.85	98.10	98.02	98.00	98.97	97.24	97.96	98.60	96.61
UNE number:	96	96	96	97	97	97	98	98	98	98	99	99	99	99	99	99
Core, section:	6H-2	6H-2	6H-2	6H-3	6H-3	6H-3	6H-3	6H-3	6H-3	7H-6	7H-6	7H-6	7H-6	7H-6	7H-6	7H-6
Interval (cm):	70–71	70–71	70–71	87–88	87–88	87–88	87–88	87–88	28–30	28–30	28–30	28–30	28–30	71–72	71–72	71–72
SiO <sub>2</sub>	76.83	76.84	76.78	73.07	74.82	74.58	74.65	75.06	74.28	74.75	76.38	73.82	73.84	74.32	74.59	74.07
TiO <sub>2</sub>	0.31	0.24	0.23	0.45	0.35	0.40	0.36	0.65	0.68	0.68	0.50	0.51	0.76	0.57	0.56	0.59
Al <sub>2</sub> O <sub>3</sub>	13.44	13.48	13.24	14.49	14.19	14.19	14.20	13.41	13.83	13.83	13.83	13.23	14.21	14.10	14.18	14.24
FeO*	2.58	2.68	2.72	3.36	3.08	3.21	3.17	2.50	2.78	2.74	2.36	3.34	3.40	3.32	3.19	3.41
MnO	0.00	0.00	0.00	0.00	0.00	0.00	0.00	0.00	0.00	0.00	0.00	0.00	0.00	0.00	0.00	0.00
MgO	0.00	0.00	0.00	0.17	0.00	0.00	0.00	0.16	0.23	0.19	0.00	0.22	0.21	0.32	0.00	0.41
CaO	1.32	1.38	1.47	2.37	1.86	1.80	1.96	2.26	2.61	2.47	2.09	2.81	2.82	2.61	2.72	3.11
K <sub>2</sub> O	2.82	2.81	2.80	3.06	3.09	2.91	3.10	2.55	2.56	2.44	2.61	2.11	2.16	2.26	2.09	2.08
Na <sub>2</sub> O	2.70	2.57	2.77	2.74	2.61	2.91	2.56	3.40	3.02	3.08	2.81	2.75	2.91	2.42	2.59	2.33
Total	98.40	96.19	97.84	97.83	96.92	96.81	96.09	97.44	98.22	98.22	96.44	96.92	96.52	98.06	95.56	97.38
UNE number:	99	100	100	100	100	100	100	100	103	103	103	103	103	103	103	104
Core, section:	7H-6	8H-3	9H-6	9H-6	9H-6	9H-6	9H-6	9H-6	10H-1							
Interval (cm):	71–72	129–130	129–130	129–130	129–130	129–130	129–130	129–130	129–130	27–28	27–28	27–28	27–28	27–28	27–28	35–36
SiO <sub>2</sub>	74.13	70.47	67.90	71.13	70.40	71.25	72.69	71.37	71.86	75.26	75.05	75.63	74.82	75.53	74.94	71.40
TiO <sub>2</sub>	0.55	0.67	1.04	0.77	0.80	0.72	0.67	0.67	0.69	0.39	0.52	0.37	0.45	0.46	0.38	0.49
Al <sub>2</sub> O <sub>3</sub>	14.01	14.05	14.52	14.56	14.45	14.54	14.24	14.14	14.35	13.36	13.26	13.39	13.43	12.96	13.11	13.35
FeO*	3.34	4.65	5.78	4.10	4.58	4.72	4.17	4.45	4.81	3.30	3.22	3.14	3.11	3.18	3.38	4.34
MnO	0.00	0.00	0.00	0.00	0.00	0.00	0.00	0.00	0.00	0.00	0.00	0.00	0.00	0.00	0.00	0.00
MgO	0.32	0.44	0.84	0.46	0.48	0.48	0.24	0.40	0.34	0.00	0.00	0.00	0.00	0.00	0.00	0.40
CaO	2.84	3.14	4.05	2.99	3.23	3.26	2.82	3.24	2.91	1.83	1.82	1.99	1.88	1.67	1.92	3.12
K <sub>2</sub> O	2.14	2.61	2.28	2.78	2.65	2.34	2.40	2.50	2.49	2.69	2.70	2.58	2.71	2.66	2.73	1.95
Na <sub>2</sub> O	2.66	3.96	3.59	2.61	3.42	2.68	2.77	3.22	2.55	3.18	3.43	3.08	3.50	3.32	3.48	3.31
Total	97.33	97.48	97.02	79.80	98.40	96.33	95.93	98.32	98.52	97.07	98.50	96.94	98.38	98.33	97.92	98.14

Table 7 (continued).

UNE number:	104	104	104	104	105	105	105	105	105	105	105	106	106	108	108	108	108
Core, section:	10H-1	10H-1	10H-1	10H-1	13H-3	13H-3	13H-3	13H-3	13H-3	13H-3	14H-1	14H-1	21H-5	21H-5	21H-5	21H-5	
Interval (cm):	35–36	35–36	35–36	35–36	19–20	19–20	19–20	19–20	19–20	19–20	67–68	67–68	136–137	136–137	136–137	136–137	
SiO <sub>2</sub>	66.28	66.66	73.18	73.84	78.11	71.83	78.21	78.42	78.02	78.51	78.69	77.12	77.80	79.27	78.97	79.48	79.14
TiO <sub>2</sub>	0.57	0.78	0.41	0.25	0.00	0.94	0.25	0.15	0.21	0.16	0.14	0.20	0.17	0.00	0.00	0.00	0.00
Al <sub>2</sub> O <sub>3</sub>	14.74	14.66	13.04	13.06	13.61	15.43	13.60	13.55	13.69	13.79	13.42	14.04	13.73	12.60	12.90	12.42	12.48
FeO*	6.75	6.33	4.12	3.99	1.84	4.01	1.87	1.66	1.83	1.71	1.89	1.33	1.07	0.42	0.43	0.38	0.48
MnO	0.00	0.00	0.00	0.00	0.00	0.00	0.00	0.00	0.00	0.00	0.00	0.00	0.00	0.00	0.00	0.00	0.00
MgO	1.40	1.25	0.00	0.00	0.00	0.46	0.00	0.00	0.00	0.00	0.00	0.00	0.00	0.00	0.00	0.00	0.00
CaO	5.03	4.75	2.34	2.39	1.74	3.40	1.84	1.78	1.81	1.87	1.75	0.97	0.85	0.51	0.54	0.49	0.55
K <sub>2</sub> O	1.40	1.49	1.99	1.94	1.49	1.30	1.47	1.40	1.47	1.46	1.49	3.53	3.60	4.37	4.37	4.39	4.44
Na <sub>2</sub> O	3.84	4.07	4.92	4.54	3.22	2.64	2.77	3.03	2.97	2.50	2.62	2.80	2.80	2.83	2.79	2.84	2.92
Total	98.53	99.11	98.36	97.58	93.46	96.92	95.94	97.58	96.81	97.47	97.37	95.14	96.33	97.07	95.70	96.33	97.79
UNE number:	108	109	109	110	110	110	110	110	111	111	111	111	111	110	110	110	110
Core, section:	21H-5	26H-3	26H-3	34X-1	34X-1	34X-1	34X-1	34X-1	35X-2	35X-2	35X-2	35X-2	35X-2	34X-1	34X-1	34X-1	34X-1
Interval (cm):	136–137	86–87	86–87	68–69	68–69	68–69	68–69	68–69	132–133	132–133	132–133	132–133	132–133	68–69	68–69	68–69	68–69
SiO <sub>2</sub>	79.35	78.69	61.84	80.42	80.25	80.74	75.68	72.86	77.43	77.69	77.54	77.71	77.66	80.42	80.25	80.74	75.68
TiO <sub>2</sub>	0.00	0.14	1.00	0.22	0.00	0.00	0.23	0.43	0.21	0.28	0.28	0.25	0.20	0.22	0.00	0.00	0.23
Al <sub>2</sub> O <sub>3</sub>	12.56	13.42	19.49	11.96	12.11	11.86	14.09	14.96	13.12	13.29	12.93	13.09	13.23	11.96	12.11	11.86	14.09
FeO*	0.44	1.89	5.06	0.95	1.09	1.01	1.41	3.34	1.74	1.68	1.78	1.76	1.87	0.95	1.09	1.01	1.41
MnO	0.00	0.00	0.00	0.00	0.00	0.00	0.00	0.00	0.00	0.00	0.00	0.00	0.00	0.00	0.00	0.00	0.00
MgO	0.00	0.00	0.60	0.00	0.00	0.00	0.00	0.13	0.00	0.00	0.00	0.00	0.00	0.00	0.00	0.00	0.00
CaO	0.53	1.75	6.31	0.96	1.03	1.10	1.04	1.86	1.04	1.08	1.02	0.99	1.03	0.96	1.03	1.10	1.04
K <sub>2</sub> O	4.35	1.49	1.76	3.31	3.25	3.04	4.79	2.71	3.77	3.71	3.83	3.58	3.72	3.31	3.25	3.04	4.79
Na <sub>2</sub> O	2.77	2.62	3.93	2.18	2.27	2.25	2.75	3.70	2.69	2.28	2.62	2.61	2.29	2.18	2.27	2.25	2.75
Total	95.43	97.37	95.35	96.74	96.54	96.64	96.18	95.98	95.85	95.03	95.93	95.94	94.55	96.74	96.54	96.64	96.18
UNE number:	110	111	111	111	111	111	111	111	111	111	111	112	112	112	112	113	113
Core, section:	34X-1	35X-2	40X-4	40X-4	40X-4	40X-4	72X-2	72X-2									
Interval (cm):	68–69	132–133	132–133	132–133	132–133	132–133	132–133	132–133	132–133	132–133	132–133	143–144	143–144	143–144	143–144	9–10	9–10
SiO <sub>2</sub>	72.86	77.43	77.69	77.54	77.71	77.66	77.80	77.85	77.58	77.30	76.03	75.81	75.62	75.58	74.59	74.34	75.09
TiO <sub>2</sub>	0.43	0.21	0.28	0.28	0.25	0.20	0.26	0.27	0.22	0.22	0.45	0.30	0.38	0.49	0.00	0.22	0.00
Al <sub>2</sub> O <sub>3</sub>	14.96	13.12	13.29	12.93	13.09	13.23	13.15	12.96	13.12	13.01	13.88	13.98	13.93	13.89	15.07	15.48	15.02
FeO*	3.34	1.74	1.68	1.78	1.76	1.87	1.72	1.67	1.77	1.96	1.94	1.84	1.89	1.95	3.04	3.09	2.75
MnO	0.00	0.00	0.00	0.00	0.00	0.00	0.00	0.00	0.00	0.00	0.00	0.00	0.00	0.00	0.00	0.00	0.00
MgO	0.13	0.00	0.00	0.00	0.00	0.00	0.00	0.00	0.00	0.00	0.00	0.00	0.00	0.17	0.00	0.00	0.00
CaO	1.86	1.04	1.08	1.02	0.99	1.03	1.11	1.05	1.12	1.08	1.57	1.70	1.66	1.56	1.14	1.16	1.06
K <sub>2</sub> O	2.71	3.77	3.71	3.83	3.58	3.72	3.54	3.66	3.59	3.94	2.99	2.89	2.78	2.76	3.23	2.88	3.18
Na <sub>2</sub> O	3.70	2.69	2.28	2.62	2.61	2.29	2.42	2.54	2.61	2.48	3.15	3.48	3.74	3.58	2.93	2.83	2.90
Total	95.98	95.85	95.03	95.93	95.94	94.55	95.10	95.52	96.13	95.69	96.51	97.41	98.74	98.23	95.11	95.49	95.66
UNE number:	113	113	114	115	116	116	116	118									
Core, section:	72X-2	72X-2	75X-cc	75X-4	76X-2	76X-2	78X-6										
Interval (cm):	9–10	9–10	25–25	49–50	55–56	55–56	62–63										
SiO <sub>2</sub>	74.40	74.50	57.67	62.40	77.38	77.67	53.82										
TiO <sub>2</sub>	0.14	0.25	1.19	1.07	0.15	0.00	1.00										
Al <sub>2</sub> O <sub>3</sub>	15.27	15.24	16.24	17.05	11.16	11.06	14.73										
FeO*	2.95	2.83	10.06	7.15	3.96	3.56	12.70										
MnO	0.00	0.00	0.00	0.13	0.00	0.00	0.00										
MgO	0.00	0.00	3.06	0.72	0.00	0.00	4.46										
CaO	1.23	1.23	7.62	5.64	1.84	1.95	10.12										
K <sub>2</sub> O	3.21	3.07	1.26	1.76	1.68	1.74	0.71										
Na <sub>2</sub> O	2.80	2.88	2.91	4.09	3.83	4.02	2.45										
Total	96.33	97.40	98.52	98.68	99.60	96.47	96.55										

Notes: Major elements reported as wt% oxides. UNE number refers to the ash layer number analyzed at UNE (see Table 3). Total is the original analytical total. Individual oxide values sum to 100%. Zero values indicate the element abundances are less than the detection limit of EDS. All Fe reported as FeO\*.

**Table 8.** Representative analyses of vitric shards from Hole 884B.

UNE number:	121	121	121	121	121	121	122	122	123	123	123	124	124	124	124	
Core, section:	2H-2	2H-2	2H-2	2H-2	2H-2	2H-2	2H-6	2H-6	2H-7	2H-7	2H-7	3H-3	3H-3	3H-3	3H-3	
Interval (cm):	76-77	76-77	76-77	76-77	76-77	76-77	55-56	55-56	38-39	38-39	38-39	143-144	143-144	143-144	143-144	
SiO <sub>2</sub>	72.7	75	74.07	74.4	73.7	74.23	69.26	74.73	74.81	74.25	71.77	70.44	70.29	71.63	71.8	70.86
TiO <sub>2</sub>	0.57	0.4	0.43	0.36	0.49	0.46	0.85	0.39	0.14	0.34	0.31	0.63	0.65	0.59	1.13	0.64
Al <sub>2</sub> O <sub>3</sub>	15.16	14.4	15.18	15.13	15.18	14.96	15.87	13.62	13.72	14.03	16.49	15.77	15.99	15.46	13.76	15.88
FeO*	2.61	1.79	2.11	1.97	2.19	2.05	3.87	2.75	2.76	1.98	0.97	2.6	3.03	2.38	3.81	2.82
MnO	0	0	0	0	0	0	0	0	0	0	0	0	0	0	0	0
MgO	0.17	0	0	0	0	0	0.66	0	0	0	0	0.19	0.3	0.25	0	0.38
CaO	1.75	0.78	1.34	1.35	1.38	1.26	3.17	1.71	1.77	0.44	1.91	2.41	2.32	1.81	1.46	2.23
K <sub>2</sub> O	3.35	4.04	3.82	3.45	3.47	3.69	2.77	2.23	2.23	4.66	3.21	3.15	3.4	3.75	4.73	3.82
Na <sub>2</sub> O	3.69	3.6	3.06	3.34	3.59	3.35	3.57	4.57	4.57	4.3	5.34	4.81	4.02	4.13	3.3	3.37
Total	97	97.5	95.29	95.74	96.74	96.78	98.99	97.19	97.05	97.5	97.83	97.92	97.77	98.19	97	96.27

UNE number:	124	124	125	125	125	125	125	125	126	127	127	127	127	127	128	128
Core, section:	3H-3	3H-3	4H-2	4H-4	4H-4	4H-4	4H-04	4H-04	5H-03	5H-03						
Interval (cm):	143-144	143-144	119-120	119-120	119-120	119-120	119-120	119-120	119-120	141-142	17-18	17-18	17-18	17-18	38-39	38-39
SiO <sub>2</sub>	72.03	70.6	79.54	79.15	79.85	79.62	80.08	80.36	81.08	64.16	76.05	67.5	76.41	76.65	58.51	72.04
TiO <sub>2</sub>	0.45	0.69	0	0.13	0	0.2	0.16	0	0	1	0.36	0.91	0.43	0.45	1.05	0.65
Al <sub>2</sub> O <sub>3</sub>	15.37	15.66	12.79	13.05	12.84	13.02	12.83	12.85	12.16	15.7	13.56	15.18	13.53	13.34	18.16	14.77
FeO*	2.24	2.77	1.28	1.44	1.41	1.37	1.52	1.36	1.22	6.57	2.48	5.24	2.38	2.57	6.53	3.41
MnO	0	0	0	0	0	0	0	0	0	0	0	0	0	0	0	0
MgO	0.15	0.42	0	0	0	0	0	0	0	1.44	0	1.32	0	0	2.34	0.27
CaO	1.62	2.2	1.55	1.61	1.57	1.62	1.58	1.66	1.3	5.45	1.97	4.32	1.64	1.69	8.31	2.52
K <sub>2</sub> O	3.78	3.76	1.75	1.73	1.71	1.71	1.66	1.62	1.9	1.79	2.08	1.56	2.09	2.05	0.86	2.14
Na <sub>2</sub> O	4.36	3.9	3.09	2.89	2.64	2.46	2.17	2.16	2.35	3.89	3.5	3.96	3.52	3.25	4.24	4.2
Total	98.78	97.75	97.69	98.19	96.93	97.97	97.44	96.71	97.4	102.53	95.48	100.38	96.2	96.34	95.04	98.9

UNE number:	128	129	129	129	129	130	130	130	130	130	130	131	131	132	132	
Core, section:	5H-03	5H-04	5H-04	5H-04	5H-4	6H-2	6H-2	6H-2	6H-2	6H-2	6H-2	6H-7	6H-7	7H-2	7H-2	
Interval (cm):	38-39	120-121	120-121	120-121	120-121	120-121	120-121	120-121	120-121	120-121	120-121	22-23	22-23	115-116	115-116	
SiO <sub>2</sub>	76.11	75.3	75.96	75.93	74.68	78.3	78.3	78.72	79.71	79.34	79.92	80.4	69.4	73.47	74.43	77.45
TiO <sub>2</sub>	0.15	0.58	0.41	0.53	0.49	0.32	0.32	0.16	0.19	0.27	0.15	0.13	0.65	0.14	0.42	0
Al <sub>2</sub> O <sub>3</sub>	13.77	14.52	14.15	14	14.24	12.35	12.35	12.24	12.34	12.39	12.43	12.35	14.56	16.26	14.05	13.36
FeO*	2.04	3.09	3.13	3.03	3.26	1.32	1.32	1.33	1.5	1.55	1.34	1.34	5.22	0.61	2.3	1.46
MnO	0	0	0	0	0	0	0	0	0	0	0	0	0	0	0	0
MgO	0	0	0	0	0	0	0	0	0	0	0	0	0.81	0	0	0
CaO	1.36	1.87	1.73	1.74	1.88	0.77	0.77	0.8	0.82	0.89	0.74	0.78	3.66	3.66	1.73	0.64
K <sub>2</sub> O	2.71	2.15	2.21	2.17	2.19	3.07	3.07	2.98	2.83	2.94	2.9	2.75	1.42	0.44	3.38	3.74
Na <sub>2</sub> O	3.86	2.49	2.41	2.6	3.26	3.87	3.76	2.61	2.62	2.51	2.25	4.28	5.41	3.69	3.36	3.86
Total	97.36	96.25	96.25	95.39	98.47	99.97	99.97	100.82	95.8	95.82	95.26	94.86	94.63	102.77	99.12	96.8

UNE number:	132	132	134	135	135	135	136	136	136	136	136	136	136	136	136	
Core, section:	7H-2	7H-2	8H-5	9H-7	9H-7	9H-7	9H-7	13X-1								
Interval (cm):	115-116	115-116	89-90	2-3	2-3	2-3	2-3	32-33	32-33	32-33	32-33	32-33	32-33	32-33	32-33	
SiO <sub>2</sub>	74.3	74.34	56.8	73.59	79.27	75.15	74.59	79.5	79.73	79.33	79.7	79.66	79.3	79.16	79.71	
TiO <sub>2</sub>	0.51	0.54	1.33	0.59	0	0.51	0.44	0	0	0	0	0	0	0	0	
Al <sub>2</sub> O <sub>3</sub>	14.02	14.39	18.72	14	12.28	13.44	13.63	12.16	12.1	12.31	12.07	12.12	12.12	12.49	12.2	12.19
FeO*	2.27	2.53	8.31	2.74	0.73	2.37	2.54	0.9	1.09	0.93	0.84	1.02	1.02	1.01	1.02	0.86
MnO	0	0	0	0	0	0	0	0	0	0	0	0	0	0	0	0
MgO	0.21	0	1.59	0.18	0	0	0.13	0	0	0	0	0	0	0	0	0
CaO	2.09	1.95	8.09	2.39	0.36	2.07	2.17	0.9	0.98	0.96	0.94	0.86	0.86	0.88	0.91	0.93
K <sub>2</sub> O	2.92	2.81	1.08	2.4	3.83	2.46	2.56	2.59	2.3	2.46	2.53	2.51	2.38	2.62	2.46	
Na <sub>2</sub> O	3.69	3.44	4.07	4.1	3.53	4.01	3.94	3.95	3.81	4.01	3.91	3.82	3.94	4.1	3.86	
Total	97.4	96.86	104.95	99.98	98.96	99.86	98.26	97.17	95.2	96.14	97.12	96.9	96.9	96.07	97.78	95.95

**Table 8 (continued).**

UNE number: Core, section: Interval (cm):	137 14X-2 143–144	137 14X-2 143–144	137 14X-2 143–144	137 14X-2 143–144	137 14X-2 143–144	138 16X-1 141–142	138 16X-1 141–142	138 16X-1 141–142	139 16X-2 116–117	139 16X-2 116–117
SiO <sub>2</sub>	74.91	74.43	75.01	75.15	74.86	73.88	73.43	73.56	65.01	65.02
TiO <sub>2</sub>	0.28	0.46	0.42	0.38	0.41	0.4	0.41	0.42	0.74	0.61
Al <sub>2</sub> O <sub>3</sub>	13.97	13.83	13.77	13.73	13.9	13.11	13.27	13.06	16.46	16.22
FeO*	1.92	1.9	1.96	1.67	1.91	3.99	4.24	4.2	5.36	5.46
MnO	0	0	0	0	0	0	0	0	0	0
MgO	0	0	0	0	0	0	0	0	0.66	0.53
CaO	1.49	1.53	1.48	1.49	1.5	2.44	2.71	2.56	2.93	3.13
K <sub>2</sub> O	2.93	2.93	2.8	2.85	2.85	1.95	2.06	1.97	4.69	4.72
Na <sub>2</sub> O	4.51	4.92	4.57	4.73	4.57	4.23	3.87	4.24	4.14	4.32
Total	96.33	97.22	96.96	96.56	97.35	96.7	96.64	96.5	99.24	97.05

UNE number: Core, section: Interval (cm):	139 16X-2 116–117	139 16X-2 116–117	139 16X-2 116–117	139 16X-2 116–117	140 23X-1 142–143	141 23X-3 30–31	142 23X-5 37–38	142 23X-5 37–38	142 23X-5 37–38	142 23X-5 37–38
SiO <sub>2</sub>	63.98	64.09	65.46	65.25	54.27	62.91	78.8	79.04	79.02	78.87
TiO <sub>2</sub>	0.71	0.79	0.64	0.66	1.055	1.17	0	0	0	0
Al <sub>2</sub> O <sub>3</sub>	16.56	16.52	16.29	16.46	17.01	15.52	12.48	12.41	12.43	12.61
FeO*	5.37	5.55	5.09	5.38	10.88	7.59	0.3	0.37	0.23	0.26
MnO	0	0	0	0	0	0	0	0	0	0
MgO	0.75	0.78	0.62	0.65	3.52	1.46	0	0	0	0
CaO	3.52	3.18	2.93	3.07	8.52	5.22	0.39	0.48	0.39	0.46
K <sub>2</sub> O	4.64	4.72	4.85	4.67	0.92	1.68	4.55	4.55	4.81	4.51
Na <sub>2</sub> O	4.47	4.37	4.12	3.86	3.33	4.45	3.49	3.14	3.11	3.3
Total	98.07	98.25	98.04	96.1	101.37	99.27	96.49	98.87	98.47	98.08

Notes: Major elements reported as wt% oxides. UNE number refers to the ash layer number analyzed at UNE (see Table 4). Total is the original analytical total. Individual oxide values sum to 100%. Zero values indicate the element abundances are less than the detection limit of EDS. All Fe reported as FeO\*.

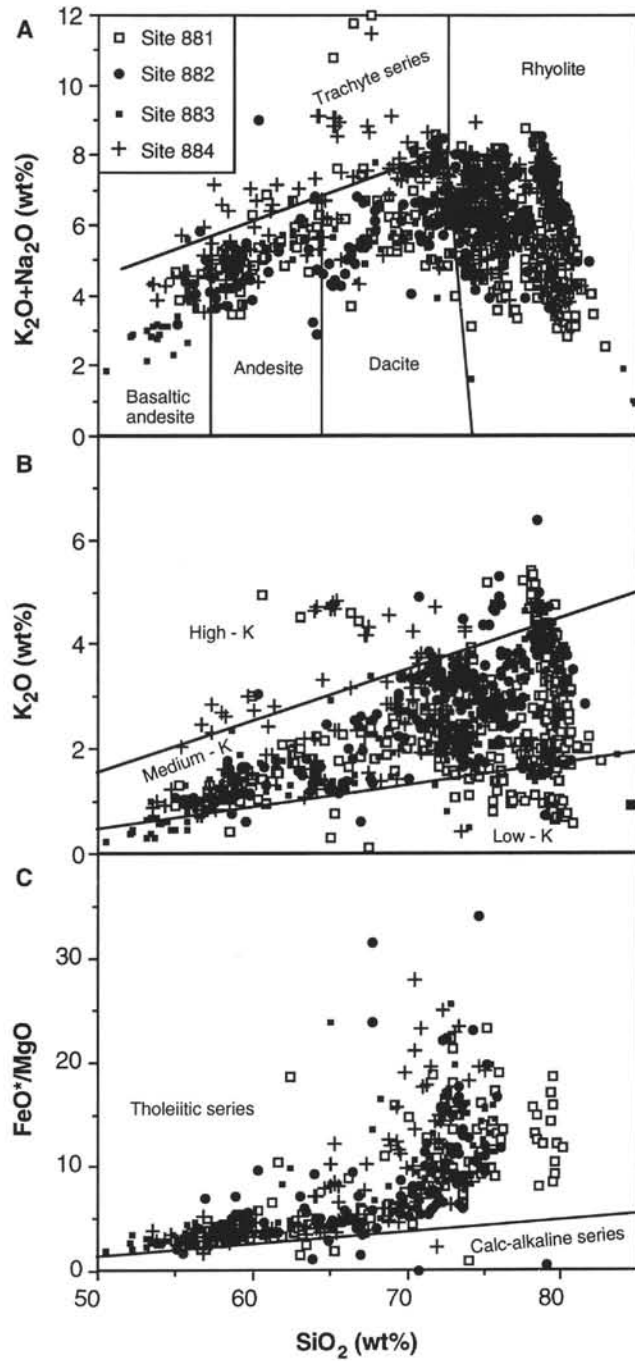


Figure 4. A. Variation of wt%  $K_2O + Na_2O$  vs.  $SiO_2$  for ashes from Sites 881–884. B. Variation of wt%  $K_2O$  vs.  $SiO_2$  for ashes from 881–884. C. Variation of  $FeO^*/MgO$  vs. wt%  $SiO_2$  for ashes from 881–884.

(Pearce and Parkinson, 1993). But our primary conclusion at this stage is that we cannot detect any evidence for crustal thickening from the major element compositions of the Leg 145 ashes.

Whether some level of global synchronicity of explosive volcanism exists and whether such pulses could be climatically significant (Kennett and Thunell, 1977; Ninkovich and Donn, 1976; Kennett et al., 1977) have been controversial issues. Excluding localized effects such as the subduction of adjacent backarc basins in the Philippine region for example, Cambray (1991) advocated synchronicity of explosive activity on the basis of a comprehensive analysis of the principal arcs bordering the Pacific plate. His analysis involved systematic frequency/thickness ash layer determinations, and discrimination

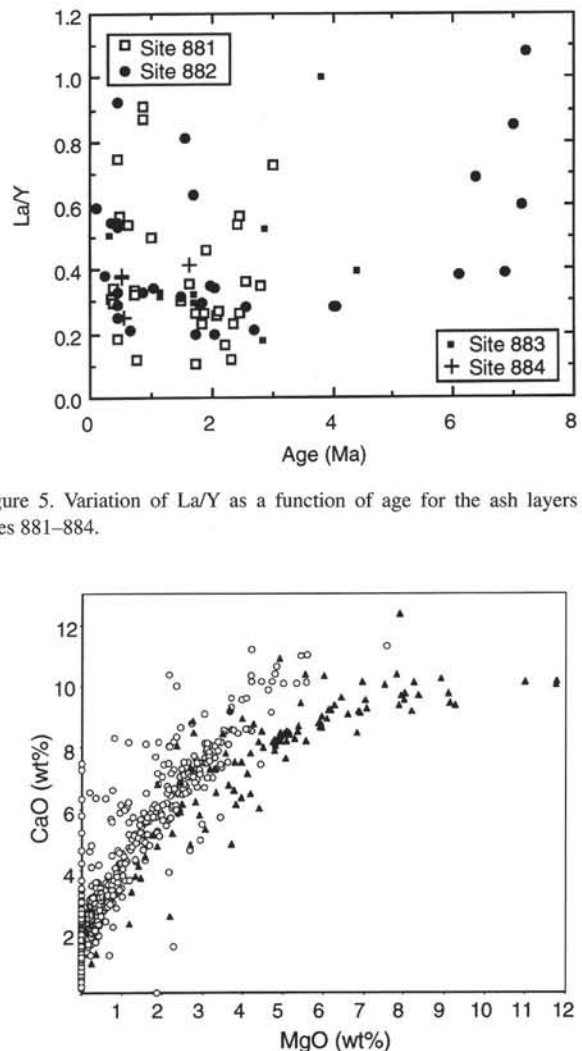


Figure 5. Variation of La/Y as a function of age for the ash layers from Sites 881–884.

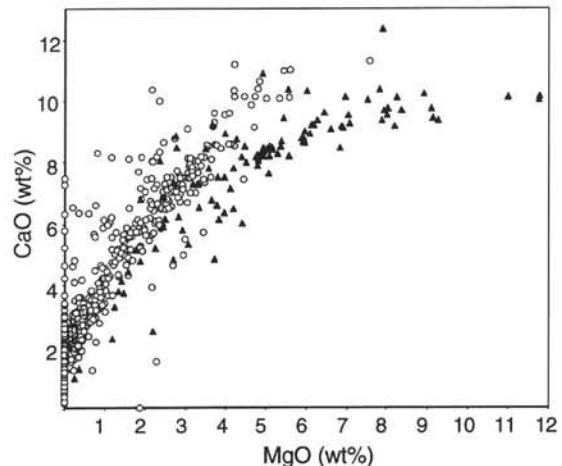


Figure 6. Variation of wt% CaO vs. MgO for ashes from 881–884 (open circles) compared with lavas from the Central Kamchatka Depression and East Kamchatka (solid triangles).

between adjacent arc and remote inputs. Two marked periods emerge of concentrated explosive activity in arcs emerge: (1) lower to middle Miocene (18–13 Ma) and (2) Pliocene–Quaternary (5 Ma–present).

There is no evidence from Leg 145 to substantiate the Miocene pulse, but there is ample evidence to support the claim of increased explosivity in the younger period. We note an increase in volcanism derived from the Aleutian arc at ~5 Ma is also documented at Leg 145 Site 887, with a further increase in intensity at ~2.6 Ma (Cao et al., this volume). The nature of a Pacific plate-wide trigger for these enhanced periods of explosive activity is clearly a matter of prime cross-disciplinary research interest, not the least because of the possible climatic effects.

An important point previously made by Scheidegger et al. (1980) is the contrasts in compositional modes between the rhyolite-dominated ashes and the predominance of basalt in Kamchatka (Leonova, 1979; Fedotov and Masurenkov, 1991). Although individual arc volcanoes such as Fuji and Klyuchevskoy are dominated overwhelmingly by basalt with a large fraction of pyroclastic rock, it is nevertheless common knowledge that far-travelled ash clouds from plinian explosive eruptions are more likely to be composed of rhyolite.

Paleogene volcanism has previously been recognized at a number of central Pacific basins (Rea and Thiede, 1981) and the Hess Rise (Vallier et al., 1983). We suggest an island arc source for the Eocene–

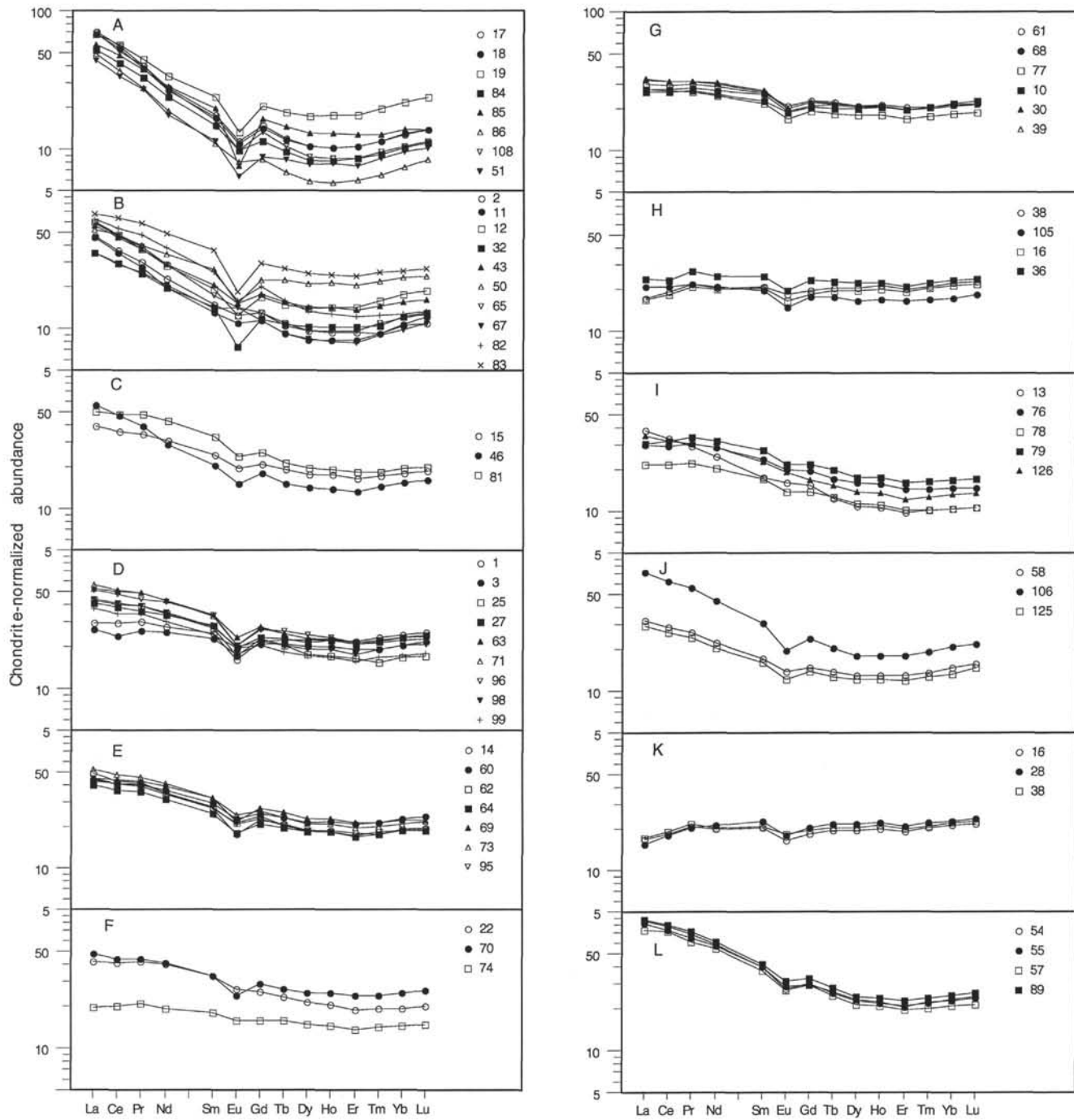


Figure 7. Chondrite-normalized rare earth element abundances for different groups (A–L) of ashes. Numbers by the symbols for each pattern are the UNE layer numbers. Normalizing values from Sun and McDonough (1989).

Oligocene ashes recovered from the Detroit Seamount Sites, which would have been located ~30°–40°N at that time, and possibly downwind from early Aleutian arc activity (Rea and Duncan, 1986; Lonsdale, 1988).

## CONCLUSIONS

1. A Late Miocene increase in explosive activity of the Kurile-Kamchatka arc is apparent (<6.3 Ma) from the number and thickness of ash deposits recovered from Sites 881, 882, 883, and 884. A further major increase of activity occurred at 2.6 Ma lasted to the present. A number of spectacularly thick (~30–250 cm) Pliocene–Pleistocene

rhyolitic layers are present that appear to be plinian airfall, and must represent colossal eruptions.

2. A spectrum of compositions of both major and trace elements in these ashes ranges from basaltic andesite to rhyolite, from low- through medium- to high-K series, and with strongly contrasted trace element abundance patterns. We believe these reflect different source origins that may well prove to be derived from the known distinct volcanic belts in the Kurile-Kamchatka system.

3. Near coincidence of the true liquid compositions (vitric shards) with experimentally determined low-pressure crystal-melt cotectics reflects the significant role of fractional crystallization in the evolution of mafic-to-felsic systems. Coincidence of Sr and Nd isotopic charac-

**Table 9.** Bulk major element and trace element analyses and Sr-Nd isotopic ratios of ash layers from Site 881.

Hole: UNE number: Core, section: Interval (cm):	881A 1	881A 2	881A 3	881A 4	881B 7	881B 8	881B 9	881B 10	881B 12	881B 14	881B 15	881B 16	881B 17	881B 18	881B 19	881B 22	881B 25
SiO <sub>2</sub>	76.31	74.53	76.00	78.39	77.22	80.50	77.66	73.67	81.03	70.18	73.25	79.85	78.83	79.73	79.30	62.81	75.58
TiO <sub>2</sub>	0.30	0.34	0.37	0.18	0.28	0.17	0.21	0.33	0.10	0.52	0.54	0.31	0.02	0.02	0.00	1.03	0.56
Al <sub>2</sub> O <sub>3</sub>	13.69	13.74	14.67	12.67	12.91	12.59	13.23	14.30	12.22	15.26	15.05	12.06	12.58	12.77	12.20	15.81	13.32
FeO*	1.95	2.10	2.38	1.37	2.18	1.34	1.35	2.51	0.98	3.86	2.78	2.02	0.57	0.53	0.95	7.10	2.49
MnO	0.00	0.00	0.00	0.00	0.10	0.00	0.00	0.00	0.00	0.08	0.00	0.00	0.00	0.00	0.00	0.03	0.00
MgO	0.09	0.16	0.11	0.00	0.17	0.00	0.02	0.05	0.00	0.32	0.29	0.09	0.00	0.00	0.00	2.19	0.12
CaO	2.00	2.19	2.32	1.50	2.13	1.43	1.62	1.72	1.00	2.32	1.99	2.40	0.54	0.46	1.05	5.69	1.96
K <sub>2</sub> O	2.15	3.00	1.37	2.09	1.87	2.03	2.13	2.78	2.80	2.49	2.11	0.74	4.36	4.01	3.36	1.52	2.66
Na <sub>2</sub> O	3.49	3.92	2.78	3.78	3.14	1.93	3.81	4.77	1.91	5.10	3.90	2.55	3.12	2.48	3.17	3.84	3.33
Total	98.49	101.15	99.27	95.04	95.13	93.24	97.84	96.57	96.47	100.55	98.40	95.11	95.68	97.40	94.80	98.85	95.66
<sup>143</sup> Nd/ <sup>144</sup> Nd	0.512933			0.513110			0.513065			0.513058							
<sup>87</sup> Sr/ <sup>86</sup> Sr	0.703509			0.703625			0.703403			0.703586							
Sc	23	11	22	12	11	13	11	18	8	14	25	17	3	5	9	24	24
V	60	40	23	13	20	18	14	24	5	33	29	8	0	0	1	106	71
Cr	4	11	2	1	0	3	0	1	1	14	5	0	1	1	1	2	22
Co	6	5	4	3	5	2	2	4	2	4	3	3	1	1	2	11	9
Ni	6	7	8	0	7	3	0	6	0	6	12	0	0	0	0	13	17
Cu	38	17	17	7	6	5	4	11	7	15	8	8	4	4	9	43	50
Zn	50	32	58	43	39	41	31	58	30	59	56	41	23	21	31	89	54
Ga	14	12	14	12	11	11	9	15	31	13	16	11	31	30	28	18	17
Ge	1	1	2	1	4	1	1	1	2	1	5	1	2	2	1	2	
Rb	37.0	53.1	26.9	46.9	50.1	66.2	47.5	23.8	115.6	69.8	38.5	14.9	185.2	188.1	118.5	28.1	65.0
Sr	171	181	216	152	187	160	159	206	86	199	216	165	56	48	73	336	190
Y	51.1	20.1	43.2	46.0	38.3	44.9	41.4	44.5	32.4	44.7	38.0	43.8	24.3	24.0	41.6	42.9	37.9
Zr	178.7	89.2	137.2	162.4	147.2	152.6	145.4	122.0	151.4	185.5	164.3	99.9	63.6	62.4	123.2	145.3	171.4
Nb	2.04	8.62	2.20	2.36	2.08	2.63	1.78	2.08	3.26	5.59	4.72	0.62	7.47	7.49	5.48	3.94	5.20
Mo	2.46	2.84	1.75	2.09	1.97	2.11	1.66	1.65	3.82	1.60	2.01	1.38	1.61	1.66	3.56	1.52	2.00
Sn	2.44	2.08	1.03	2.19	0.96	1.52	0.70	1.92	1.08	1.25	2.55	2.06	1.67	1.68	1.91	2.23	1.16
Ba	417.8	562.3	271.5	597.4	483.3	629.8	489.5	247.7	897.4	611.5	497.9	273.9	870.7	868.1	804.1	480.8	605.2
La	9.18	14.43	8.22	14.56	11.93	15.28	12.37	8.24	18.31	14.98	12.21	5.23	22.08	21.00	20.96	13.11	13.41
Ce	23.81	30.05	19.47	33.84	27.86	35.17	28.82	21.49	38.37	34.90	28.82	14.96	45.00	43.42	45.54	32.88	32.44
Pr	3.69	3.67	3.16	4.62	3.81	4.83	3.90	3.31	4.60	5.11	4.23	2.54	4.93	4.73	5.47	5.07	4.79
Nd	16.52	13.59	15.36	19.63	16.47	19.90	16.90	15.19	16.94	21.17	18.58	12.13	16.61	15.89	20.41	24.04	20.85
Sm	4.89	2.88	4.49	5.14	4.26	5.04	4.42	4.50	3.78	5.33	4.74	4.03	3.40	3.27	4.61	6.44	5.32
Eu	1.18	0.92	1.29	1.45	0.96	1.12	0.97	1.37	0.92	1.28	1.44	1.21	0.84	0.81	0.98	1.94	1.26
Gd	5.67	3.36	5.41	5.81	4.95	5.68	5.13	5.25	4.34	5.74	5.45	4.78	3.81	3.68	5.36	6.61	5.87
Tb	1.05	0.49	0.99	0.98	0.87	0.99	0.90	0.96	0.70	0.99	0.91	0.92	0.56	0.55	0.87	1.11	0.97
Dy	7.13	3.08	6.42	6.44	5.60	6.24	5.72	6.41	4.45	6.10	5.69	6.32	3.39	3.36	5.54	6.82	5.66
Ho	1.62	0.67	1.44	1.45	1.26	1.40	1.29	1.46	1.01	1.34	1.26	1.44	0.74	0.74	1.26	1.47	1.24
Er	4.59	1.95	4.05	4.18	3.62	4.03	3.68	4.12	3.00	3.77	3.46	4.04	2.18	2.20	3.72	3.98	3.44
Tm	0.76	0.30	0.62	0.68	0.56	0.61	0.57	0.67	0.51	0.57	0.56	0.66	0.37	0.37	0.64	0.62	0.50
Yb	5.10	2.20	4.30	4.68	3.94	4.36	4.01	4.52	3.64	3.99	3.73	4.45	2.68	2.69	4.58	4.05	3.55
Lu	0.82	0.35	0.70	0.76	0.64	0.70	0.65	0.73	0.61	0.63	0.60	0.71	0.45	0.45	0.77	0.65	0.56
Hf	5.14	2.80	3.62	4.57	3.89	3.81	3.76	3.43	4.32	4.33	4.25	3.10	2.52	2.50	4.22	3.92	3.92
Ta	0.17	0.83	0.22	0.19	0.21	0.24	0.20	0.17	0.31	0.42	0.35	0.06	0.85	0.88	0.52	0.27	0.39
Pb	18.65	12.40	14.90	14.59	17.80	18.45	18.13	9.47	24.40	17.33	13.55	10.88	22.09	22.29	27.03	8.65	17.62
Th	2.23	3.86	1.69	4.75	4.48	5.32	4.53	1.50	10.65	2.60	2.23	1.04	13.63	13.49	9.66	1.44	2.64
U	1.07	1.64	0.66	1.43	1.39	1.45	1.12	0.60	3.08	1.17	2.69	0.49	4.14	4.32	2.31	0.92	1.27

Table 9 (continued).

Hole: UNE number: Core, section: Interval (cm):	881B 27 11H-04 49-50	881B 28 11H-04 59-60	881B 30 12H-01 62-63	881B 31 12H-01 140-141	881B 32 12H-02 19-20	881B 33 13H-02 118-119	881B 34 13H-05 42-43	881B 36 14H-05 44-45	881B 38 15H-04 129-130	881B 39 15H-06 73-74	881B 43 16H-06 145-146	881B 45 17H-01 11-12	881B 46 17H-01 22-23	881B 47 18H-01 148-149	881C 50 21X-06 40-41	881C 51 23X-07 26-27	
SiO <sub>2</sub>	77.63	75.93	70.17	79.34	80.01	64.14	78.91	74.86	77.27	70.42	79.55	60.10	68.23	64.13	79.97	78.24	
TiO <sub>2</sub>	0.30	0.17	0.53	0.37	0.00	1.00	0.40	0.70	0.57	0.50	0.04	1.44	0.79	1.02	0.12	0.00	
Al <sub>2</sub> O <sub>3</sub>	12.85	14.35	14.60	12.16	12.39	16.21	12.21	12.88	12.93	14.88	12.69	15.91	14.69	15.26	11.94	12.49	
FeO*	1.90	2.37	4.87	2.16	0.97	6.30	2.11	4.07	1.52	3.95	1.38	8.91	5.57	6.69	1.29	0.48	
MnO	0.00	0.00	0.00	0.00	0.00	0.01	0.00	0.00	0.00	0.00	0.00	0.00	0.00	0.00	0.00	0.00	
MgO	0.02	0.00	0.47	0.02	0.00	1.49	0.05	0.19	0.00	0.67	0.00	2.18	0.95	1.59	0.00	0.00	
CaO	1.80	2.88	3.54	2.04	0.91	5.31	1.99	2.70	1.87	2.97	1.32	6.76	4.17	5.26	1.09	0.59	
K <sub>2</sub> O	2.09	1.04	2.12	1.59	2.56	1.75	1.63	1.64	2.16	2.16	2.73	1.26	2.42	2.14	3.13	4.77	
Na <sub>2</sub> O	3.44	3.29	3.69	2.34	3.18	3.79	2.74	2.99	3.66	4.45	2.30	3.44	3.18	3.90	2.47	3.43	
Total	96.71	94.98	95.96	97.35	95.89	99.38	95.59	94.34	90.97	100.03	93.96	99.43	99.50	102.13	98.30	96.77	
<sup>143</sup> Nd/ <sup>144</sup> Nd	0.512991	0.513072	0.513056							0.513073	0.513063		0.512946		0.513054	0.512794	0.513011
<sup>87</sup> Sr/ <sup>86</sup> Sr	0.703482	0.703572	0.703432							0.703649	0.703465		0.703839		0.703131	0.704533	0.704070
Sc	17	20	20	13	11	27	16	17	23	21	6	33	15	27	12	8	
V	26	13	16	33	9	236	42	26	57	20	0	213	7	91	19	0	
Cr	2	0	0	10	4	41	13	2	4	0	2	7	1	6	3	2	
Co	4	4	5	4	2	25	4	5	6	5	2	20	3	12	5	1	
Ni	0	4	0	4	1	26	7	5	0	4	0	25	0	16	0	18	
Cu	16	25	39	11	7	52	21	22	24	34	7	249	8	69	22	4	
Zn	46	59	65	38	29	90	39	68	64	66	34	98	38	75	32	31	
Ga	14	15	15	11	9	18	12	22	16	15	31	21	29	17	12	9	
Ge	1	1	1	1	2	1	1	1	1	1	1	1	1	1	1	0	
Rb	51.5	17.9	43.1	54.8	87.8	40.8	55.5	15.9	18.5	44.2	109.7	27.9	94.3	47.1	81.6	76.7	
Sr	183	200	224	162	117	280	174	177	236	219	102	301	147	300	107	62	
Y	47.9	47.0	43.7	47.9	23.9	38.2	46.5	43.7	44.0	44.2	31.8	40.4	30.2	47.0	46.7	18.7	
Zr	165.4	100.1	149.4	162.0	114.1	144.8	146.9	107.4	88.7	152.2	153.4	148.4	147.3	165.7	186.8	62.7	
Nb	2.13	0.77	1.94	2.24	2.02	3.53	2.20	1.05	0.80	2.08	4.36	3.64	4.17	3.65	5.49	4.19	
Mo	2.50	1.51	2.82	1.80	1.85	0.89	1.66	1.78	1.24	3.05	2.05	1.45	1.98	3.60	3.01	1.83	
Sn	2.21	1.74	2.73	1.00	0.73	0.86	0.89	2.74	2.36	2.07	1.52	2.37	3.57	2.19	2.59	2.49	
Ba	533.3	297.6	496.4	498.3	671.7	233.3	487.7	235.4	281.5	511.6	785.7	234.4	751.9	430.4	552.3	375.5	
La	12.76	4.83	9.98	12.65	11.00	9.93	12.50	7.32	5.34	10.19	17.10	10.78	17.08	16.99	16.31	13.49	
Ce	30.76	14.53	25.31	32.45	24.14	26.37	33.01	18.95	15.56	25.71	36.96	27.64	37.44	40.71	38.39	27.30	
Pr	4.38	2.49	3.82	4.46	3.01	3.92	4.40	3.30	2.64	3.84	4.59	4.23	4.76	5.61	4.88	3.28	
Nd	20.09	12.97	18.18	19.62	11.72	18.30	19.22	15.04	12.21	18.58	17.23	20.68	17.37	26.62	20.79	10.52	
Sm	5.48	4.42	5.17	5.31	2.79	5.03	5.17	4.82	4.11	5.26	3.97	5.81	3.98	6.87	5.21	2.20	
Eu	1.44	1.33	1.48	1.08	0.54	1.49	1.13	1.43	1.36	1.47	1.10	1.68	1.10	1.74	1.10	0.47	
Gd	6.02	5.25	5.73	6.18	3.04	5.87	6.02	6.04	5.11	5.80	4.60	6.07	4.62	7.11	5.73	2.28	
Tb	1.09	1.03	1.02	1.08	0.51	1.00	1.07	1.08	0.97	1.04	0.73	1.09	0.72	1.23	1.06	0.40	
Dy	6.95	7.09	6.60	6.79	3.31	6.11	6.66	7.13	6.56	6.71	4.53	6.84	4.51	7.56	6.80	2.49	
Ho	1.60	1.59	1.48	1.51	0.73	1.32	1.50	1.60	1.52	1.51	1.01	1.44	1.00	1.62	1.54	0.56	
Er	4.41	4.40	4.08	4.34	2.13	3.59	4.35	4.44	4.22	4.11	2.84	3.87	2.81	4.38	4.28	1.59	
Tm	0.71	0.72	0.65	0.65	0.34	0.51	0.63	0.72	0.68	0.66	0.47	0.60	0.47	0.69	0.71	0.28	
Yb	4.90	4.81	4.37	4.65	2.52	3.57	4.71	4.86	4.62	4.44	3.23	3.86	3.20	4.55	4.89	2.01	
Lu	0.78	0.76	0.69	0.75	0.42	0.57	0.76	0.77	0.73	0.69	0.52	0.60	0.52	0.70	0.77	0.33	
Hf	4.72	3.03	4.26	4.17	2.98	3.69	3.91	3.38	2.63	4.35	4.40	3.86	4.32	4.54	5.63	2.03	
Ta	0.17	0.07	0.14	0.24	0.25	0.32	0.24	0.08	0.07	0.16	0.40	0.25	0.38	0.25	0.47	0.45	
Pb	15.84	14.15	16.35	17.46	17.98	16.24	17.18	12.70	11.59	15.78	22.05	5.82	20.88	13.36	14.54	14.87	
Th	4.33	0.62	2.73	4.24	3.51	1.75	4.36	1.00	0.68	2.90	7.45	1.61	6.29	4.30	8.35	5.14	
U	1.35	0.33	1.14	1.23	1.22	0.64	1.24	0.42	0.36	1.18	2.14	0.65	1.98	1.34	2.18	2.18	

Notes: UNE number refers to the ash layer number analyzed at UNE (see Table 1). Major elements are averages of individual shard analyses from the same layer. Major elements reported as wt% oxides and trace elements as parts per million. All Fe reported as FeO\*.

**Table 10.** Bulk major element and trace element analyses and Sr-Nd isotopic ratios of ash layers from Site 882.

UNE number:	54	55	56	57	58	59	60	61	62	63	64	65	67	68	69
Core, section:	1H-6	2H-5	2H-6	2H-7	3H-4	3H-4	4H-5	5H-4	6H-1	6H-4	8H-2	8H-3	8H-6	8H-7	9H-2
Interval (cm):	83-84	21-22	148-149	17-18	18-19	118-120	12-13	149-150	32-33	29-30	133-135	12-13	54-55	12-13	14-15
SiO <sub>2</sub>	69.06	71.2	68.58	67.92	79.58	78.16	73.38	70.03	73.35	74.1	70.71	77.78	75.56	72.49	69.99
TiO <sub>2</sub>	0.93	0.58	0.95	0.93	0.09	0.18	0.63	0.59	0.61	0.4	0.67	0.14	0.07	0.48	0.78
Al <sub>2</sub> O <sub>3</sub>	15.62	15.69	14.21	15.88	12.88	13.17	14.22	14.93	13.98	14.04	13.97	13.01	14.32	13.71	14.26
FeO*	3.82	2.38	6.32	4.68	1.49	1.53	3.16	5.04	3.24	3.38	4.33	0.89	1.32	5.07	5.31
MnO	0.01	0	0	0	0	0	0	0	0	0	0	0	0	0	0
MgO	0.65	0.27	0.8	0.94	0	0.06	0.13	0.73	0.44	0	1.26	0.02	0.19	0.43	0.59
CaO	2.73	1.97	3.89	3.61	1.61	1.29	1.84	4.08	2.44	1.87	4.25	0.73	2.54	3.42	3.38
K <sub>2</sub> O	2.83	3.4	1.82	2.94	1.92	2.89	2.27	1.55	3.09	3.26	1.93	3.83	1.95	1.62	2.33
Na <sub>2</sub> O	4.35	4.5	3.32	3.1	2.43	2.73	4.38	3.07	2.85	2.95	2.89	3.61	3.99	2.79	3.3
Total	99.16	98.04	102.24	99.36	97.85	98.92	98.34	98.95	99.42	97.87	98.42	97.5	98.17	100.14	99.74
<sup>143</sup> Nd/ <sup>144</sup> Nd	0.513037			0.513032				0.513044	0.513067				0.513084	0.513016	
<sup>87</sup> Sr/ <sup>86</sup> Sr	0.703269			0.703828				0.703409	0.70346				0.703575	0.703419	
Sc	10	18	3	17	26	0	6	14	22	18	28	19	13	20	21
V	24	15	6	48	15	36	0	26	65	24	44	0	30	42	58
Cr	5	0	0	3	1	34	0	0	4	2	0	0	1	1	3
Co	4	2	1	8	3	7	3	9	7	5	2	0	5	14	9
Ni	0	0	0	0	18	13	0	0	28	23	4	0	1	10	23
Cu	9	8	3	17	16	27	9	20	15	17	5	7	14	65	27
Zn	67	57	8	64	37	30	73	79	53	63	51	27	28	74	68
Ga	30	18	2	25	13	18	20	16	15	15	16	13	11	15	16
Ge	1	1	0	1	1	0	1	1	1	1	1	1	1	1	1
Rb	60.4	63.4	2.2	51.5	36.1	20.6	41.5	28.1	55.9	59.3	40	76	35.4	28	44
Sr	189	226	26	254	173	309	151	307	226	196	207	147	286	239	206
Y	48.4	46.8	3.3	43.1	30.2	10.2	46	44.8	40.5	47.4	39.9	22.1	17.1	44.4	47.1
Zr	329.1	320.2	11.2	266.8	152.9	35.4	190.3	118.7	216.3	257.4	200.9	197	132.4	121.2	222
Nb	9.18	9.95	0.25	7.52	2.12	2.36	4.57	1.24	5.76	5.91	4.89	5.45	2.61	1.61	4.73
Mo	2.57	2.81	0.11	2.22	1.72	0.21	1.86	2.86	2.06	2.42	2.28	3.12	1.75	2.27	1.51
Sn	3.92	2.68	0.2	2.92	2.06	1.4	2.01	1.36	2.57	3.27	3.08	2.7	1.93	1.91	3.1
Ba	915	946.1	32.2	670.8	468.4	600	496.2	393.3	607.2	666.9	556.3	895.8	724.8	442	418.8
La	26.47	25.71	0.83	22.87	9.96	9.39	13.47	9.32	13.4	16.27	12.54	17.88	10.82	8.67	13.81
Ce	63.14	59.49	2.13	58.13	23.2	19.48	33.22	23.84	32.92	40.64	30.03	38.05	23.45	22.59	35.43
Pr	8.45	7.86	0.33	7.46	3.25	2.67	4.91	3.66	4.82	5.95	4.4	4.76	3.11	3.43	5.24
Nd	35.16	34.41	1.5	32.92	13.34	9.3	22.03	17.23	20.59	25.84	19.01	17.41	12.24	16.46	23.44
Sm	7.84	7.78	0.43	7.39	3.38	2.02	5.76	5.04	5.35	6.59	4.84	3.39	2.68	4.93	6.33
Eu	2.03	2.12	0.14	1.98	1.01	0.77	1.66	1.55	1.56	1.7	1.33	1.04	1.03	1.4	1.62
Gd	7.91	7.6	0.48	7.72	3.82	2.52	6.45	5.9	6.12	7.25	5.41	3.39	2.95	5.4	7.06
Tb	1.22	1.25	0.08	1.19	0.66	0.31	1.11	1.06	0.98	1.18	0.93	0.52	0.43	1.0	21.2
Dy	7.3	7.44	0.52	6.86	4.22	1.76	6.93	6.7	6.03	7.31	5.96	3.09	2.71	6.66	7.41
Ho	1.58	1.61	0.11	1.49	0.94	0.36	1.58	1.52	1.33	1.63	1.32	0.69	0.58	1.49	1.64
Er	4.44	4.34	0.32	4.13	2.75	1	4.41	4.27	3.64	4.47	3.54	1.99	1.66	4.12	4.47
Tm	0.71	0.72	0.05	0.65	0.44	0.15	0.7	0.67	0.59	0.72	0.57	0.35	0.29	0.66	0.7
Yb	4.83	4.78	0.33	4.41	3.1	1.02	4.77	4.56	3.91	4.83	3.94	2.48	2.04	4.49	4.65
Lu	0.78	0.76	0.05	0.69	0.51	0.15	0.77	0.73	0.62	0.77	0.61	0.41	0.35	0.71	0.72
Hf	7.52	7.67	0.31	6.54	3.94	0.94	5.08	3.51	5.44	6.77	5	4.98	3.73	3.54	5.94
Ta	0.59	0.65	0.02	0.53	0.18	0.17	0.33	0.09	0.44	0.44	0.37	0.47	0.23	0.12	0.37
Pb	14.61	12.73	0.58	12.08	13.55	4.93	6.7	10.94	11.41	12.55	11.46	17.9	15.31	14.78	12.55
Th	3.71	4.17	0.12	3.66	1.92	2.23	2.84	2.06	2.85	3.05	2.09	4.74	2.49	1.69	2.6
U	1.58	1.68	0.07	1.55	0.82	0.9	1.51	0.88	1.74	1.95	1.11	1.96	1.15	0.78	1.27

Table 10 (continued).

UNE number:	70	71	73	74	76	77	78	79	81	82	83	84	85	86
Core, section:	9H-3	9H-5	9H-6	9H-6	11H-1	11H-4	23H-6	24H-1	37H-6	38H-4	39H-7	41H-1	42H-2	42H-4
Interval (cm):	89-91	76-77	58-59	135-136	63-65	133-134	39-40	100-101	53-54	116-117	24-25	120-121	130-131	55-56
SiO <sub>2</sub>	65.93	75.84	71.37	58.01	59.14	69.68	61.66	58.95	72.34	75.44	76.57	78.82	78.4	80.07
TiO <sub>2</sub>	0.99	0.43	0.73	1.13	1.19	0.52	1.32	1.39	0.65	0.12	0.26	0	0.03	0
Al <sub>2</sub> O <sub>3</sub>	15.53	14.08	14.95	15.83	16.14	14.63	15.31	16.85	15.74	14.12	13.03	12.08	12.45	12.52
FeO*	6.01	1.98	3.58	10.55	9.03	5.12	8.32	8.83	2.72	1.46	1.72	0.7	1.02	0.64
MnO	0	0	0.02	0.02	0	0.03	0	0	0	0	0	0	0	0
MgO	1	0.02	0.51	2.81	2.47	0.8	2.05	2.68	0.27	0.02	0	0	0	0
CaO	4.44	1.5	2.68	7.6	7.37	4.19	5.74	6.51	1.94	0.96	1.05	0.56	0.79	0.46
K <sub>2</sub> O	2.06	2.99	2.65	1.06	1.43	1.95	1.87	1.38	3.26	4.68	3.76	4.67	4.08	3.92
Na <sub>2</sub> O	4.02	3.16	3.53	3.08	3.23	3.1	3.73	3.42	3.08	3.2	3.61	3.17	3.24	2.39
Total	101.67	94.6	98.15	103.73	102.25	101.16	102.38	101.58	97.53	97.82	97.22	94.75	97.23	97.32
<sup>143</sup> Nd/ <sup>144</sup> Nd		0.513069	0.513075				0.51308							
<sup>87</sup> Sr/ <sup>86</sup> Sr		0.703228	0.703481				0.703187							
Sc	24	25	19	38	41	25	21	29	16	12	21	10	8	8
V	83	21	54	338	289	98	160	245	62	30	33	4	3	6
Cr	4	1	4	4	3	4	6	8	0	8	4	1	2	1
Co	6	12	8	29	22	12	15	21	4	5	6	1	1	2
Ni	8	9	21	54	33	28	29	44	8	7	15	1	0	0
Cu	18	10	24	150	120	37	76	103	19	33	15	8	5	11
Zn	54	53	64	89	85	85	63	84	60	38	44	30	27	23
Ga	15	15	17	18	18	17	14	18	16	16	11	12	11	
Ge	1	1	1	1	2	1	1	1	1	1	1	1	1	
Rb	44.6	52.2	51.8	17.3	21.1	26.8	14.2	20.9	53.3	90.3	83.5	85.1	107.3	72.8
Sr	252	175	263	293	368	244	314	356	277	201	146	84	57	71
Y	50.3	49.3	47	30.7	33.1	40.5	24.3	34.4	40.6	27.9	53.6	19.2	29.1	13.9
Zr	268.1	320.7	207.9	80.9	115.6	111.2	83.4	131	218.8	257.1	334.5	93.3	91.6	67.7
Nb	7.43	8.67	5.76	1.29	2.64	1.48	1.71	2.77	3.7	8.47	7.48	4.71	4.23	4.98
Mo	2.29	3.03	2.09	3.25	1.68	2	0.86	1.34	3	4.07	2.3	4.04	2.46	3.7
Sn	2.96	3.69	2.58	1.8	2.45	2.68	1.89	2.18	3.35	1.69	4.2	1.29	2.13	1.11
Ba	481.7	518.7	468.4	255.9	298.6	318.7	173.6	206.4	798	668.6	674.6	786	605.5	768.9
La	14.92	17.2	15.99	6.11	9.4	8.67	6.82	9.66	15.54	19.04	20.93	16.28	17.55	15.03
Ce	35.43	41.39	39	16.16	24	21.96	17.48	26.37	38.47	43.46	51.04	34.08	38.41	29.5
Pr	5.33	5.96	5.59	2.55	3.76	3.27	2.72	4.25	5.84	5.77	7.05	4.03	4.56	3.39
Nd	24.54	25.54	24.36	11.63	17.33	14.84	12.42	19.49	25.61	22.97	29.22	14.4	16.97	11.2
Sm	6.38	6.4	6.29	3.48	4.62	4.25	3.37	5.37	6.43	5	7.15	2.86	3.79	2.12
Eu	1.74	1.5	1.78	1.17	1.46	1.24	1.01	1.6	1.74	1.16	1.34	0.72	0.56	0.59
Gd	7.46	7.07	6.75	4.12	5.1	4.99	3.61	5.62	6.61	5.23	7.69	2.97	4.24	2.17
Tb	1.26	1.17	1.11	0.74	0.82	0.88	0.6	0.96	1.02	0.75	1.29	0.45	0.69	0.32
Dy	8.05	7.3	6.68	4.73	5.15	5.78	3.67	5.72	6.34	4.24	8.05	2.62	4.15	1.89
Ho	1.79	1.6	1.5	1.05	1.13	1.29	0.8	1.25	1.39	0.91	1.76	0.59	0.94	0.41
Er	4.99	4.39	4.1	2.87	3.06	3.54	2.15	3.36	3.86	2.56	5	1.81	2.67	1.25
Tm	0.78	0.69	0.65	0.46	0.47	0.57	0.33	0.53	0.6	0.4	0.83	0.3	0.41	0.21
Yb	5.24	4.65	4.36	3.03	3.07	3.84	2.19	3.5	4.09	2.65	5.44	2.12	2.87	1.54
Lu	0.83	0.74	0.7	0.48	0.48	0.61	0.34	0.55	0.65	0.43	0.87	0.36	0.45	0.27
Hf	7.27	7.6	4.97	2.27	3.16	3.1	2.16	3.79	6.08	6.3	8.67	2.89	2.86	2.17
Ta	0.59	0.62	0.39	0.11	0.2	0.12	0.13	0.23	0.28	0.61	0.58	0.48	0.45	0.54
Pb	13.66	10.28	12.12	11.46	5.75	12.25	3.19	4.27	15.18	12.06	20.27	14.03	18.69	12.63
Th	2.41	2.7	3.36	1.27	0.92	1.46	0.46	0.97	3.52	5.2	6.02	6.98	8.91	6.33
U	1.32	1.49	1.42	0.65	0.68	0.65	1.03	0.84	1.82	2.41	2.24	2.81	2.84	2.6

Notes: UNE number refers to the ash layer number analyzed at UNE (see Table 2). Major elements are averages of individual shard analyses from the same layer. Major elements reported as wt% oxides and trace elements as parts per million. All Fe reported as FeO\*.

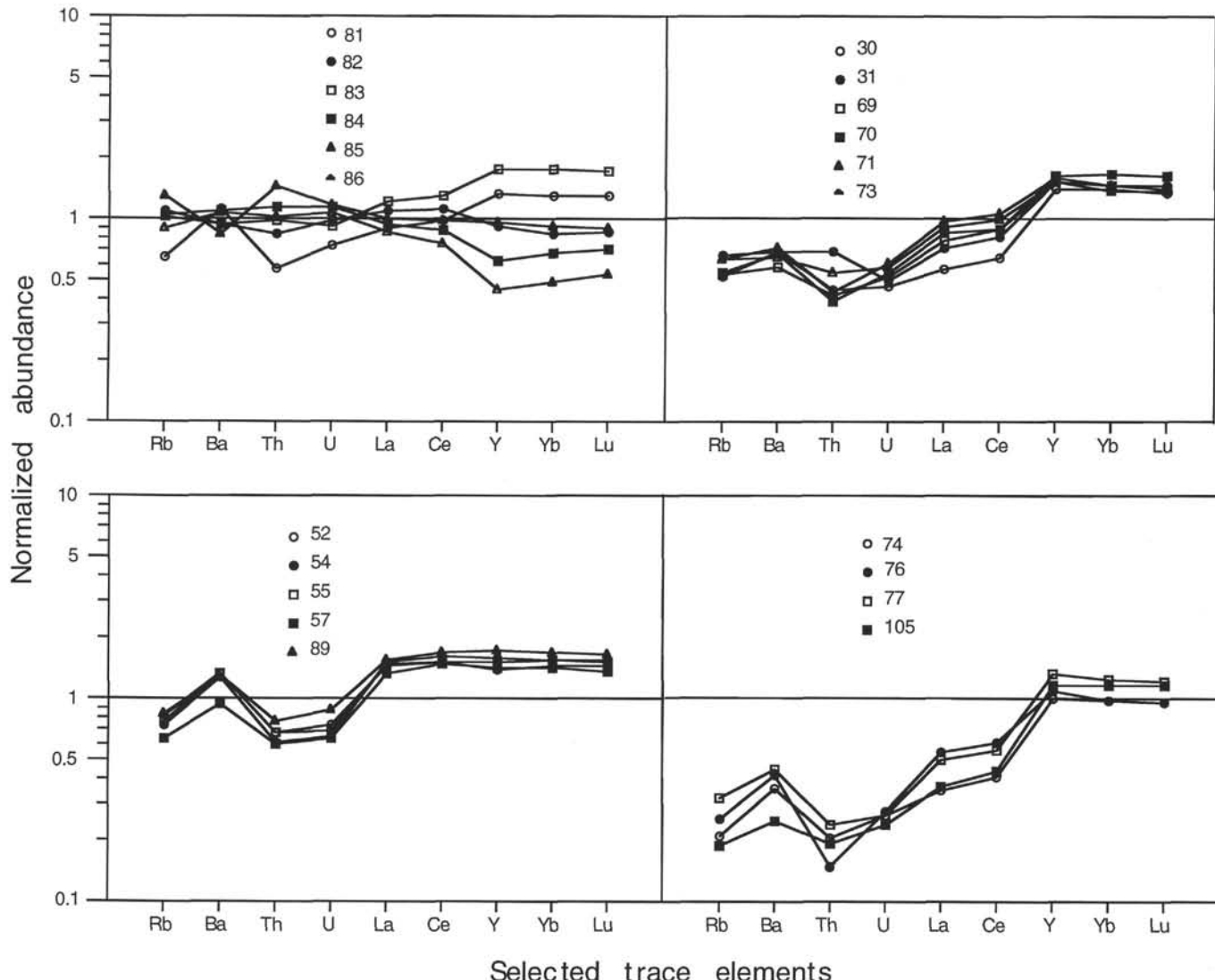


Figure 8. Normalized abundances of selected trace elements for different groups of ashes (UNE layer numbers indicated by specific symbols). Normalizing factors are the averages of element abundances for a group of Miocene high-K ashes.

teristics of a range of compositions is consistent with such processes, but the near isotopic identity of the basement of EK with primary upper mantle-derived arc magmas makes detection of crustal melting and assimilation difficult to detect (B. Castellana, pers. comm., 1994). The ubiquity of negative Eu anomalies and concave-upward Gd to Lu REE patterns in the intermediate-to-felsic compositions signify extensive plagioclase and amphibole fractionation, or the persistence of these phases in a crustal source undergoing partial melting.

4. There is no evidence for any consistent temporal trends in the geochemistry of the ashes. Comparison of major element parameters that are believed to correlate globally with crustal thicknesses in arcs among the Leg 145 ashes, rock samples collected from active volcanoes in Kamchatka, and ashes from the Izu-Bonin-Mariana system lead to some surprising conclusions: (1) no evidence for crustal thickening with time based on the Leg 145 ash compositions; (2) an apparent increase in crustal thickening manifested by a lower CaO content at specific MgO content of the land samples compared with the ashes, which is inconsistent with known tectonic features in Kamchatka; and (3) a coincidence of all of the ash compositions whether from the Kurile-Kamchatka or Izu-Bonin-Mariana arcs.

5. A global increase of explosive activity in arc systems occurred in the period 5 Ma to present, and in the northern Pacific, a further increase in intensity was initiated at 2.6 Ma.

6. Finally, we note the decoupling of characteristics ( $\text{FeO}^*/\text{MgO}$  at specific  $\text{SiO}_2$ , low- vs. medium- to high-K, level of absolute light REE abundances, and the La/Y ratio) commonly believed to be collectively distinguishing features of tholeiitic vs. calcalkaline rock series is demonstrable in these Leg 145 ashes.

#### ACKNOWLEDGMENTS

The support of David Rea for our involvement in this study is greatly appreciated, as is the diligence of the shipboard scientific party in providing representative sampling of critical samples. Our research was funded by a grant from the Australian Research Council (ARC). Peter Garlick and Rick Porter ensured the EMP at UNE was available and functional. Rikki Davidson was responsible for ensuring the consistent productivity of the ion-exchange columns at UNE, and the staff members of the jointly funded (ARC and Commonwealth Scientific Industrial Research Organisation) Center for Isotope Studies are thanked for their outstanding cooperation in the generation of high quality data. The tolerance of Dr. David Lambert at the Monash ICP-MS facility is much appreciated. L.-Q. Cao was supported by Overseas Postgraduate Research and UNE Overseas Student scholarships. We thank Jon Davidson and Ben Castellana for their detailed and constructive reviews.

**Table 11.** Bulk major and trace element analyses of Paleogene ash layers from Sites 883 and 884.

UNE number:	114	116	118	152	153
Core, section:	75X-CC	76X-2	78X-6	77X-CC	78X-1
Interval (cm):	25–24	55–56	62–63	25–26	105–106
SiO <sub>2</sub>	58.17	62.51	54.12	57.5	43.93
TiO <sub>2</sub>	1.14	0.81	0.94	1.19	1.21
Al <sub>2</sub> O <sub>3</sub>	16.19	13.91	14.8	16.54	15.27
FeO*	10.06	9.47	12.91	9.03	9.54
MnO	0	0	0.05	0	0.06
MgO	2.99	2.57	4.31	2.58	2.13
CaO	7.58	6.94	9.68	6.84	6.46
K <sub>2</sub> O	1.15	0.93	0.69	2.57	1.21
Na <sub>2</sub> O	2.71	2.86	2.49	3.75	3.64
Total	103	101.4	100.63	100.03	102.33
Sc	33	40	46	18	31
V	385	342	378	332	258
Cr	17	23	33	19	10
Co	26	33	36	21	25
Ni	13	30	23	16	15
Cu	97	149	129	103	104
Zn	107	103	93	111	105
Ga	19	16	17	21	18
Rb	16.5	12	11.4	42.9	14.5
Sr	333	224	232	649	368
Y	33.5	29.4	23.8	31.6	25.2
Zr	90.9	64.1	50.2	159.6	83
Nb	1.61	0.8	0.55	2.84	1.77
Cs	0.57	0.67	0.62	1.4	0.76
Ba	269.3	235.8	133.1	593.6	207
La	7.04	3.81	3.4	21	6.36
Ce	16.82	8.94	8.56	46.14	16.41
Pr	3.04	1.73	1.52	7.18	2.7
Nd	15.17	8.95	7.87	31.22	13.25
Sm	4.39	2.96	2.55	6.99	3.7
Eu	1.32	0.95	0.86	1.78	1.2
Tb	0.86	0.71	0.6	0.95	0.68
Gd	5.02	3.8	3.23	6.2	4.01
Dy	5.09	4.4	3.68	5.1	4.01
Ho	1.11	0.98	0.82	1.03	0.86
Er	3.18	2.9	2.36	2.93	2.48
Yb	2.97	2.75	2.24	2.7	2.32
Lu	0.45	0.42	0.34	0.4	0.36
Hf	2.56	1.86	1.5	4.16	2.29
Ta	0.12	0.06	0.05	0.19	0.12
Pb	6.66	7.88	2.46	8.5	3.86
Th	0.5	0.32	0.22	3.05	0.39
U	0.25	0.15	0.13	1.43	0.26

Notes: UNE number refers to the ash layer number analyzed at UNE (see Tables 3 and 4). Major elements are averages of individual shard analyses from the same layer. Major elements reported as wt% oxides and trace elements as parts per million. All Fe reported as FeO\*.

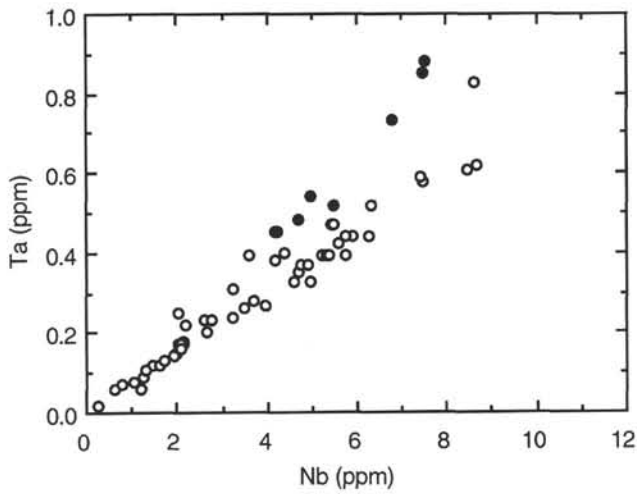


Figure 9. Variation of Ta vs. Nb for ashes from Sites 881–884, with the Miocene high-K samples distinguished by solid circles. Open circles represent all other analyzed samples.

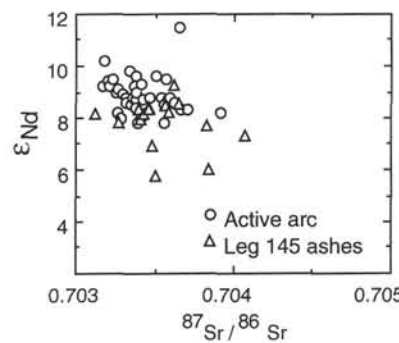


Figure 10.  $\epsilon_{\text{Nd}}$  (deviation in parts per ten thousand of the sample compared with a  $^{143}\text{Nd}/^{144}\text{Nd}$  chondritic standard of 0.512638) vs.  $^{87}\text{Sr}/^{86}\text{Sr}$  for ashes from Sites 881 through 884 compared with active volcanoes from the Central Kamchatka Depression and East Kamchatka.

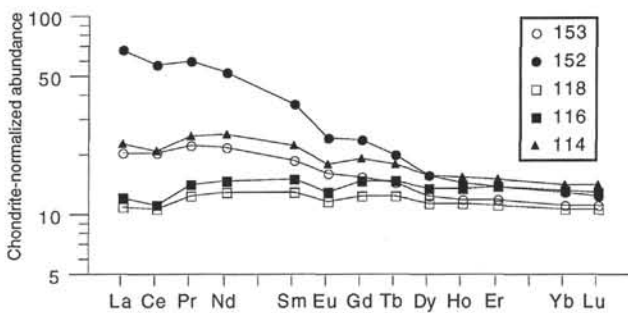


Figure 11. Chondrite-normalized rare earth element abundances for Paleogene ashes from Sites 883 and 884. Numbers by the symbols for each pattern are the UNE layer numbers.

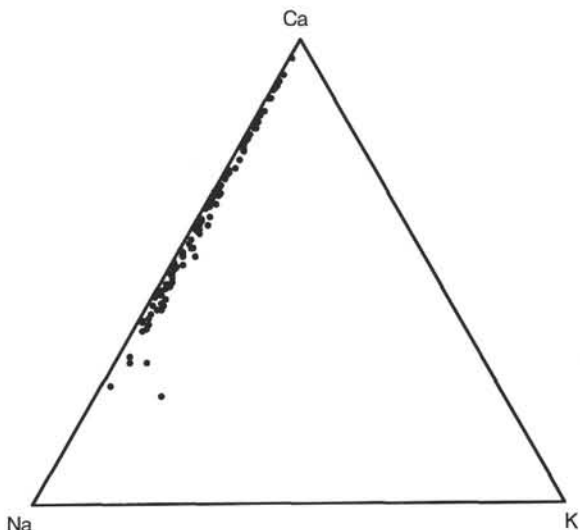


Figure 12. Projections of plagioclase compositions in terms of atomic proportions of Ca, Na, and K.

**Table 12. Representative analyses of plagioclase from Site 881.**

Hole: UNE number:	881A 1	881A 1	881A 2	881A 2	881A 3	881A 3	881A 3	881A 3	881A 4	881A 4	881A 4	881A 4	881B 4	881B 6	881B 6
SiO <sub>2</sub>	55.58	56.65	51.52	50.34	46.02	50.82	57.64	45.82	56.07	52.75	57.53	56.50	56.01	59.75	56.90
Al <sub>2</sub> O <sub>3</sub>	28.14	27.69	30.40	31.68	34.44	31.30	27.09	34.84	27.97	30.18	26.99	27.67	27.85	25.73	27.54
FeO*	0.20	0.14	1.07	0.47	0.78	0.61	0.28	0.50	0.16	0.43	0.23	0.30	0.50	0.15	0.15
CaO	9.89	8.36	12.58	14.15	17.22	13.25	8.15	17.41	9.41	12.03	8.10	9.41	9.52	6.61	8.53
BaO	0.27	0.26	0.28	0.27	0.26	0.26	0.27	0.27	0.27	0.27	0.27	0.27	0.27	0.28	0.27
K <sub>2</sub> O	0.26	0.18	0.39	0.12	0.16	0.20	0.11	0.09	0.16	0.09	0.42	0.16	0.26	0.37	0.28
Na <sub>2</sub> O	5.95	7.11	4.03	3.26	1.28	3.82	6.74	1.33	6.25	4.51	6.75	5.96	5.86	7.54	6.58
Hole: UNE number:	881B 6	881B 7	881B 8	881B 8	881B 9	881B 9	881B 11	881B 12	881B 12	881B 13	881B 13	881B 13	881B 14	881B 14	881B 14
SiO <sub>2</sub>	56.98	53.07	55.66	56.11	51.42	44.83	54.21	53.81	57.01	59.39	47.81	54.55	60.16	48.96	45.50
Al <sub>2</sub> O <sub>3</sub>	27.33	29.54	28.14	27.72	30.79	35.07	29.34	29.71	27.14	25.64	33.07	28.93	25.00	32.74	34.92
FeO*	0.29	0.59	0.36	0.42	0.68	0.64	0.18	0.15	0.39	0.26	0.63	0.26	0.23	0.43	0.79
CaO	8.39	11.65	9.59	9.04	13.09	18.37	11.10	10.74	8.69	6.47	16.01	10.35	5.55	15.29	17.78
BaO	0.27	0.28	0.27	0.27	0.28	0.27	0.27	0.27	0.27	0.27	0.28	0.27	0.26	0.27	0.28
K <sub>2</sub> O	0.28	0.19	0.20	0.19	0.15	0.15	0.09	0.23	0.37	0.47	0.14	0.18	0.32	0.08	0.07
Na <sub>2</sub> O	6.73	4.97	6.06	6.52	3.91	0.94	5.08	5.53	6.40	7.77	2.36	5.73	8.76	2.49	1.02
Hole: UNE number:	881B 14	881B 15	881B 15	881B 16	881B 16	881B 16	881B 16	881B 16	881B 22	881B 22	881B 23	881B 24	881B 24	881B 24	881B 24
SiO <sub>2</sub>	51.27	49.81	56.72	46.26	54.36	49.71	52.25	49.90	53.06	57.44	45.19	51.92	50.83	52.05	49.23
Al <sub>2</sub> O <sub>3</sub>	30.77	31.74	27.38	34.09	29.12	32.05	30.50	32.00	29.64	26.63	34.91	30.00	31.31	30.48	31.76
FeO*	0.74	0.68	0.32	0.65	0.37	0.57	0.58	0.44	0.55	0.62	0.65	0.66	0.55	0.57	0.96
CaO	13.24	13.86	8.66	17.21	10.67	14.37	12.71	13.99	11.80	8.35	17.78	12.70	13.40	12.48	14.82
BaO	0.27	0.27	0.27	0.27	0.27	0.27	0.27	0.27	0.27	0.27	0.29	0.27	0.27	0.27	0.27
K <sub>2</sub> O	0.16	0.27	0.29	0.15	0.07	0.11	0.06	0.09	0.16	0.27	0.16	0.21	0.12	0.18	0.26
Na <sub>2</sub> O	3.80	3.64	6.64	1.64	5.42	3.18	3.95	3.58	4.80	6.67	1.30	4.50	3.78	4.25	2.97
Hole: UNE number:	881B 27	881B 28	881B 29	881B 29	881B 29	881B 30	881B 30	881B 31	881B 33	881B 33	881B 33	881B 34	881B 34	881B 34	881B 34
SiO <sub>2</sub>	56.14	63.32	55.56	53.21	56.71	53.54	55.31	55.30	51.24	50.09	50.24	51.62	44.44	55.62	46.86
Al <sub>2</sub> O <sub>3</sub>	27.73	21.41	28.61	29.25	27.41	28.96	28.08	28.01	30.97	31.35	31.08	30.16	35.38	27.92	33.85
FeO*	0.27	2.05	0.15	0.78	0.41	0.88	0.65	0.56	0.52	0.96	1.03	1.07	0.79	0.40	0.68
CaO	9.41	5.58	9.65	11.42	9.15	11.19	9.88	10.11	13.66	14.03	13.75	12.62	18.20	9.91	16.61
BaO	0.26	0.30	0.28	0.27	0.27	0.26	0.27	0.27	0.27	0.27	0.27	0.27	0.27	0.27	0.27
K <sub>2</sub> O	0.24	0.95	0.39	0.42	0.13	0.21	0.36	0.30	0.06	0.14	0.23	0.20	0.08	0.24	0.12
Na <sub>2</sub> O	6.20	6.38	5.81	4.91	6.20	5.22	5.71	5.71	3.61	3.42	3.67	4.33	1.10	5.95	1.88
Hole : UNE number:	881B 42	881B 42	881B 42	881B 44	881B 44	881B 44	881B 45	881B 45	881B 45	881B 46	881B 46	881B 46	881B 47	881B 47	881B 47
SiO <sub>2</sub>	47.32	44.04	48.31	58.25	54.11	56.00	50.74	55.07	49.43	44.72	50.85	49.41	55.78	51.33	47.04
Al <sub>2</sub> O <sub>3</sub>	33.49	35.85	32.81	26.44	29.51	27.35	31.03	27.10	32.05	35.65	31.12	32.09	27.79	30.32	33.87
FeO*	0.76	0.70	0.82	0.38	0.15	1.19	0.73	1.79	0.76	0.69	0.57	0.73	0.46	1.12	0.66
CaO	16.12	18.54	15.50	7.71	10.69	10.27	13.61	10.28	14.67	17.74	13.35	14.50	9.21	13.14	16.32
BaO	0.26	0.26	0.27	0.27	0.27	0.28	0.27	0.30	0.29	0.28	0.27	0.27	0.25	0.27	0.27
K <sub>2</sub> O	0.14	0.10	0.10	0.44	0.16	0.61	0.16	0.36	0.07	0.06	0.16	0.19	0.39	0.32	0.11
Na <sub>2</sub> O	2.16	0.78	2.46	6.78	5.53	4.59	3.73	5.10	3.09	1.13	3.96	3.09	6.37	3.78	1.98

Notes: UNE number refers to the ash layer number analyzed at UNE (see Table 1). All totals are normalized to 100%, volatile free. All Fe reported as FeO\*.

Table 13. Representative analyses of plagioclase from Hole 882A.

UNE number:	52	52	55	59	60	60	61	61	63	63	66
SiO <sub>2</sub>	52.21	56.32	56.13	45.86	57.71	57.50	53.45	55.19	47.60	48.77	47.63
Al <sub>2</sub> O <sub>3</sub>	30.22	27.40	27.70	35.15	26.50	26.78	29.33	28.48	33.24	32.65	33.10
FeO*	0.50	0.56	0.40	0.14	0.58	0.34	0.61	0.40	0.89	0.72	0.95
CaO	12.20	8.94	9.16	17.19	7.83	8.39	11.31	10.16	16.11	14.92	15.53
BaO	0.27	0.27	0.27	0.26	0.27	0.27	0.27	0.27	0.27	0.27	0.26
K <sub>2</sub> O	0.26	0.52	0.50	0.14	0.34	0.28	0.14	0.23	0.14	0.23	0.22
Na <sub>2</sub> O	4.61	6.25	6.11	1.66	7.06	6.71	5.18	5.54	2.00	2.71	2.56

UNE number:	66	67	67	70	70	70	70	72	72	73	73
SiO <sub>2</sub>	46.21	54.78	47.56	52.46	57.48	52.89	52.06	59.43	54.22	55.12	55.12
Al <sub>2</sub> O <sub>3</sub>	34.10	28.98	33.31	30.40	26.08	29.14	30.28	22.04	29.07	28.46	28.46
FeO*	0.74	0.37	0.74	0.53	1.02	1.29	0.63	3.63	0.61	0.49	0.49
CaO	16.91	10.28	15.69	12.00	8.64	12.04	12.14	4.67	10.75	10.15	10.15
BaO	0.27	0.26	0.27	0.26	0.26	0.27	0.26	1.01	0.27	0.26	0.26
K <sub>2</sub> O	0.19	0.19	0.16	0.10	0.50	0.22	0.32	2.11	0.24	0.21	0.21
Na <sub>2</sub> O	1.86	5.42	2.55	4.51	6.28	4.42	4.56	7.11	5.11	5.56	5.56

UNE number:	74	74	74	76	76	76	78	78	78	95
SiO <sub>2</sub>	46.02	44.53	50.80	48.15	47.05	44.17	46.76	53.01	53.61	52.58
Al <sub>2</sub> O <sub>3</sub>	34.12	35.41	31.18	32.99	33.47	36.07	34.06	29.36	27.50	30.34
FeO*	1.08	0.95	0.86	0.78	1.00	0.57	0.56	0.79	1.71	0.39
CaO	16.90	17.98	13.63	15.69	16.31	18.79	16.58	11.51	12.43	12.04
BaO	0.27	0.27	0.26	0.27	0.27	0.28	0.27	0.26	0.27	0.27
K <sub>2</sub> O	0.14	0.10	0.08	0.12	0.19	0.06	0.11	0.34	0.45	0.23
Na <sub>2</sub> O	1.72	1.04	3.44	2.28	1.99	0.39	1.93	4.99	4.28	4.42

Notes: UNE number refers to the ash layer number analyzed at UNE (see Table 2). All totals are normalized to 100%, volatile free. All Fe reported as FeO\*.

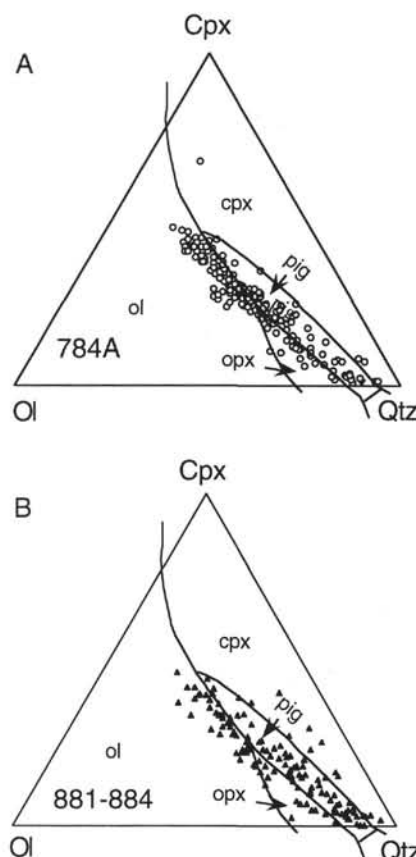


Figure 13. Ash composition projections from plagioclase. A. ODP Leg 125 Hole 784A (Izu-Bonin forearc site) ash compositions in terms of oxygen-weighted, molar proportions in the system: Ol = olivine; Cpx = clinopyroxene; and Qtz = SiO<sub>2</sub>. The atmospheric pressure primary liquidus phase fields for olivine (ol), clinopyroxene (cpx), orthopyroxene (opx), pigeonite (pig), and cotectics are from Grove et al. (1982). B. Sites 881-884 ash compositions, abbreviations as above.

#### REFERENCES\*

- Arculus, R.J., and Bloomfield, A.L., 1992. Major-element geochemistry of ashes from Sites 782, 784, and 786 in the Bonin forearc. In Fryer, P., Pearce, J.A., Stokking, L.B., et al., Proc. ODP, Sci. Results, 125: College Station, TX (Ocean Drilling Program), 277-292.
- Arculus, R.J., Gill, J.B., Cambray, H., Chen, W., and Stern, R.J., 1995. Geochemical evolution of arc systems in the western Pacific: the ash and turbidite record recovered by drilling. In Taylor, B., and Natland, J. (Eds.), *The ODP in the Western Pacific Convergent Margins*. Am. Geophys. Union, 45-65.
- Baker, P.E., 1968. Comparative volcanology and petrology of the Atlantic island arcs. *Bull. Volcanol.*, 32:189-206.
- Baker, P.E., Coltorti, M., Brihuega, L., Hasenaka, T., and Condiffe, E., 1994. Volcanic ash layers from Sites 828, 830, 831, 832, and 833, New Hebrides island arc. In Greene, H.G., Collot, J.-Y., Stokking, L.B., et al., Proc. ODP, Sci. Results, 134: College Station, TX (Ocean Drilling Program), 403-412.
- Ballhaus, C., 1993. Redox states of lithospheric and asthenospheric upper mantle. *Contrib. Mineral. Petrol.*, 114:331-348.
- Cambray, H., 1991. Etude de téphra des sédiments marins: comparaison entre les épisodes d'activité volcanique et l'évolution tectonique [Ph.D. thesis]. Univ. Pierre et Marie Curie, Paris VI.
- Carey, S., and Sigurdsson, H., 1980. The Roseau ash: deep-sea tephra deposits from a major eruption on Dominica, Lesser Antilles arc. *J. Volcanol. Geotherm. Res.*, 7:67-86.
- Carmichael, I.S.E., 1967. The iron-titanium oxides of salic volcanic rocks and their associated ferromagnesian silicates. *Contrib. Mineral. Petrol.*, 14:36-64.
- Creager, J.S., Scholl, D.W., et al., 1973. *Init. Repts. DSDP*, 19: Washington (U.S. Govt. Printing Office).
- Erlich, E.N., 1971. Recent movements and Quaternary volcanic activity within the Kamchatka territory. *Pac. Geol.*, 6:23-39.
- Fedorchuk, A., Kepezhinskis, P., Defant, M.J., Maury, R.C., and Cotten, J., 1993. Two types of granitic melts related to amalgamation of the Ganal metamorphic terrane, Kamchatka, Russia: implications for crustal evolution during collision of island arc systems. *Eos*, 74:681.
- Fedotov, S.A., and Masurenkov, Yu.P., 1991. *Active Volcanoes of Kamchatka*: Moscow (Nauka).

\* Abbreviations for names of organizations and publications in ODP reference lists follow the style given in *Chemical Abstracts Service Source Index* (published by American Chemical Society).

- Fujioka, K., Matsuo, Y., Nishimura, A., Koyama, M., and Rodolfo, K.S., 1992. Tephrae of the Izu-Bonin forearc (Sites 787, 792, and 793). In Taylor, B., Fujioka, K., et al., *Proc. ODP, Sci. Results*, 126: College Station, TX (Ocean Drilling Program), 47–74.
- Ghiorso, M.S., and Sack, R.O., 1991. Fe-Ti oxide geothermometry: thermodynamic formulation and the estimation of intensive variables in silicic magmas. *Contrib. Mineral. Petrol.*, 108:485–510.
- Gill, J.B., 1970. Geochemistry of Viti Levu, Fiji, and its evolution as an island arc. *Contrib. Mineral. Petrol.*, 27:179–203.
- , 1981. *Orogenic Andesites and Plate Tectonics*: New York (Springer).
- Gill, J.B., Hiscott, R.N., and Vidal, P., 1994. Turbidite geochemistry and evolution of the Izu-Bonin arc and continents. *Lithos*, 33:135–168.
- Gnibidenko, H.S., Gorbachev, S.Z., Lebedev, M.M., and Marakhanov, V.I., 1972. Geology and deep structure of Kamchatka Peninsula. *Pac. Geol.*, 7:1–29.
- Grove, T.L., Gerlach, D.C., and Sando, T.W., 1982. Origin of calc-alkaline series lavas at Medicine Lake Volcano by fractionation, assimilation and mixing. *Contrib. Mineral. Petrol.*, 80:160–182.
- Heath, G.R., Burckle, L.H., et al., 1985. *Init. Repts. DSDP*, 86: Washington (U.S. Govt. Printing Office).
- Huang, T.C., 1980. A volcanic sedimentation model: implications of processes and responses of deep-sea ashes. *Mar. Geol.*, 38:103–122.
- Hussong, D.M., and Uyeda, S., 1982. Tectonic processes and the history of the Mariana Arc: a synthesis of the results of Deep Sea Drilling Project Leg 60. In Hussong, D.M., Uyeda, S., et al., *Init. Repts. DSDP*, 60: Washington (U.S. Govt. Printing Office), 909–929.
- Jolivet, L., Cadet, J.-P., and Lalevée, F., 1988. Mesozoic evolution of Northeast Asia and the collision of the Okhotsk microcontinent. *Tectonophysics*, 149:89–109.
- Karig, D.E., 1974. Evolution of arc systems in the western Pacific. *Annu. Rev. Earth Planet. Sci.*, 2:51–75.
- , 1983. Temporal relationships between back-arc basin formation and arc volcanism with special reference to the Philippine Sea. In Hayes, D.E. (Ed.), *The Tectonic and Geological Evolution of Southeast Asian Seas and Islands* (Pt. 2): Geophys. Monogr., Am. Geophys. Union., 27:318–325.
- Kennett, J.P., McBirney, A.R., and Thunell, R.C., 1977. Episodes of Cenozoic volcanism in the Circum-Pacific region. *J. Volcanol. Geotherm. Res.*, 2:145–163.
- Kennett, J.P., and Thunell, R.C., 1977. On explosive Cenozoic volcanism and climatic implications. *Science*, 196:1231–1234.
- Kersting, A.B., and Arculus, R.J., 1994. Klyuchevskoy volcano, Kamchatka, Russia: the role of high-flux, recharged, tapped and fractionated magma chamber(s) in the genesis of high-Al<sub>2</sub>O<sub>3</sub> from high-MgO basalt. *J. Petrol.*, 35:1–42.
- Kimura, G., and Tamaki, K., 1985. Tectonic framework of the Kuril arc since its initiation. In Nasu, N. (Ed.), *Formation of Active Margins*: Tokyo (Terra Publ.), 641–676.
- Kir'yanov, V.Y., and Rozhkov, G.F., 1990. Grain-size distribution of Recent tephra deposited by the largest explosive eruptions of the Kamchatka volcanoes. *Volc. Seis.*, 11:305–324.
- Kir'yanov, V.Y., Zharinov, S.E., and Perepelov, A.B., 1990. Possible geochemical differences of east Kamchatkan volcanic ashes. *Volc. Seis.*, 9:320–328.
- Klein, E.M., and Langmuir, C.H., 1987. Global correlations of ocean ridge basalt chemistry with axial depth and crustal thickness. *J. Geophys. Res.*, 92:8089–8115.
- Kuno, H., 1959. Origin of Cenozoic petrographic provinces of Japan and surrounding areas. *Bull. Volcanol.*, 20:37–76.
- Kyle, P.R., Jezek, P.A., Mosley-Thompson, E., and Thompson, L.G., 1981. Tephra layers in the Byrd station ice core and the dome C ice core, Antarctica, and their climatic importance. *J. Volcanol. Geotherm. Res.*, 11:29–39.
- Leonova, L.L., 1979. Geochemistry of the Quaternary and Recent volcanic rocks in the Kurile islands and Kamchatka. *Geokhimiya*, 2:179–197.
- Lonsdale, P., 1988. Paleogene history of the Kula plate: offshore evidence and onshore implications. *Geol. Soc. Am. Bull.*, 100:733–754.
- Miyashiro, A., 1974. Volcanic rock series in island arcs and active continental margins. *Am. J. Sci.*, 274:321–355.
- Moroz, Y.F., 1988. The deep structure of East Kamchatka from magnetotelluric data. *Volc. Seis.*, 6:769–779.
- Natland, J.H., 1993. Volcanic ash and pumice at Shatsky Rise: sources, mechanisms of transport, and bearing on atmospheric circulation. In Natland, J.H., Storms, M.A., et al., *Proc. ODP, Sci. Results*, 132: College Station, TX (Ocean Drilling Program), 57–66.
- Ninkovich, D., and Donn, W.L., 1976. Explosive Cenozoic volcanism and climatic interpretations. *Science*, 194:899–906.
- Oyama, M., and Takehara, H., 1967. *Revised Standard Soil Colour Charts*: Japan (Res. Coun. Agric. Forest. Fish., Minist. Agric. Forest.).
- Pearce, J.A., and Parkinson, I.J., 1993. Trace element models for mantle melting: application to volcanic arc petrogenesis. In Pritchard, H.M., Alabaster, T., Harris, N.B.W., and Neary, C.R. (Eds.), *Magmatic Processes and Plate Tectonics*. Geol. Soc. Spec. Publ. London, 76:373–403.
- Plank, T., and Langmuir, C.H., 1988. An evaluation of the global variations in the major element chemistry of arc basalts. *Earth Planet. Sci. Lett.*, 90:349–370.
- Pouclet, A., Fujioka, K., Furuta, T., and Ogihara, S., 1992. Data report: Geochemistry and mineralogy of ash layers from Legs 127 and 128 in the Japan Sea. In Tamaki, K., Suyehiro, K., Allan, J., McWilliams, M., et al., *Proc. ODP, Sci. Results*, 127/128 (Pt. 2): College Station, TX (Ocean Drilling Program), 1373–1393.
- Pouclet, A., Pubellier, M., and Spadea, P., 1991. Volcanic ash from Celebes and Sulu Sea basins off the Philippines (Leg 124): petrography and geochemistry. In Silver, E.A., Rangin, C., von Breymann, M.T., et al., *Proc. ODP, Sci. Results*, 124: College Station, TX (Ocean Drilling Program), 467–488.
- Pouclet, A., and Scott, S.D., 1992. Volcanic ash layers in the Japan Sea: tephrochronology of Sites 798 and 799. In Tamaki, K., Suyehiro, K., Allan, J., McWilliams, M., et al., *Proc. ODP, Sci. Results*, 127/128 (Pt. 2): College Station, TX (Ocean Drilling Program), 791–803.
- Rea, D.K., Basov, I.A., Janecek, T.R., Palmer-Julson, A., et al., 1993. *Proc. ODP, Init. Repts.*, 145: College Station, TX (Ocean Drilling Program).
- Rea, D.K., and Duncan, R.A., 1986. North Pacific Plate convergence: a quantitative record of the past 140 m.y. *Geology*, 14:373–376.
- Rea, D.K., and Thiede, J., 1981. Mesozoic and Cenozoic mass accumulation rates of the major sediment components in the Nauru Basin, Western Equatorial Pacific. In Larson, R.L., Schlaeger, S.O., et al., *Init. Repts. DSDP*, 61: Washington (U.S. Govt. Printing Office), 549–555.
- Rodolfo, K.S., Solidum, R.U., Nishimura, A., Matsuo, Y., and Fujioka, K., 1992. Major-oxide stratigraphy of glass shards in volcanic ash layers of the Izu-Bonin Arc-backarc sites (Sites 788/789 and 790/791). In Taylor, B., Fujioka, K., et al., *Proc. ODP, Sci. Results*, 126: College Station, TX (Ocean Drilling Program), 505–517.
- Rose, W.I., and Chesner, C.A., 1987. Dispersal of ash in the great Toba eruption, 75 ka. *Geology*, 15:913–917.
- Scheidegger, K.F., Corliss, J.B., Jezek, P.A., and Ninkovich, D., 1980. Composition of deep-sea ash layers derived from north Pacific volcanic arcs: variations in time and space. *J. Volcanol. Geotherm. Res.*, 7:107–137.
- Scott, R., and Kroenke, L.W., 1980. Evolution of back arc spreading and arc volcanism in the Philippine Sea: interpretation of Leg 59 DSDP results. In Hayes, D.E. (Ed.), *The Tectonic and Geological Evolution of Southeast Asian Seas and Islands*. Geophys. Monogr., Am. Geophys. Union, 23:283–291.
- Shantser, A.E., and Shapiro, M.N., 1988. Evolution of volcanic zones in Kamchatka and tectonic development of the active continental margin. *Volc. Seis.*, 6:195–217.
- Sparks, R.S.J., and Walker, G.P.L., 1977. The significance of vitric enriched air-fall ashes associated with crystal-enriched ignimbrites. *J. Volcanol. Geotherm. Res.*, 2:329–341.
- Spiegelman, M., and McKenzie, D.P., 1987. Simple 2-D models for melt extraction at mid-ocean ridges and island arcs. *Earth Planet. Sci. Lett.*, 83:137–152.
- Sugimura, A., 1960. Zonal arrangement of some geophysical and petrological features in Japan and its environs. *J. Fac. Sci., Univ. Tokyo*, 12:133–153.
- Sun, S.-S., and McDonough, W.F., 1989. Chemical and isotopic systematics of oceanic basalts: implications for mantle composition and processes. In Saunders, A.D., and Norry, M.J. (Eds.), *Magmatism in the Ocean Basins*. Geol. Soc. Spec. Publ. London, 42:313–345.
- Taylor, B., 1992. Rifting and the volcanic-tectonic evolution of the Izu-Bonin-Mariana Arc. In Taylor, B., Fujioka, K., et al., *Proc. ODP, Sci. Results*, 126: College Station, TX (Ocean Drilling Program), 627–651.
- Taylor, S.R., 1967. The origin and growth of continents. *Tectonophysics*, 4:17–34.
- Vallier, T.L., Dean, W.E., Rea, D.K., and Thiede, J., 1983. Geologic evolution of Hess Rise, central North Pacific Ocean. *Geol. Soc. Am. Bull.*, 94:1289–1307.

- Walker, G.P.L., 1980. The Taupo pumice: product of the most powerful known (ultraplinian) eruption? *J. Volcanol. Geotherm. Res.*, 8:69–94.
- Watson, B.F., and Fujita, K., 1985. Tectonic evolution of Kamchatka and the Sea of Okhotsk and implications for the Pacific Basin. In Howell, D.G. (Ed.), *Tectonostratigraphic Terranes*: Houston (Circum-Pac. Counc. Energy Miner. Resour.), 333–348.
- Zhuravlev, D.Z., Tsvetkov, A.A., Zhuravlev, A.Z., Gladkov, N.G., and Chernyshev, I.V., 1985. Petrogenetic significance of lateral variations in neo-

dymium and strontium isotope ratios in Quaternary lavas of the Kurile island arc. *Geokhimiya*, 12:1723–1736.

Date of initial receipt: 26 April 1994

Date of acceptance: 17 October 1994

Ms 145SR-126

**Table 14. Representative analyses of spinel and ilmenite.**

Spinel												
Hole: UNE number:	881B 11	881B 11	881B 11	881B 11	881B 11	881B 13	881B 13	881B 13	881B 24	881B 24	881B 24	881B 25
TiO <sub>2</sub>	2.84	6.89	6.96	7.07	7.09	4.48	5.56	9.45	3.22	13.15	13.33	9.60
Al <sub>2</sub> O <sub>3</sub>	0.70	2.56	2.13	1.71	1.94	0.98	2.12	3.40	1.12	2.40	2.75	1.60
Cr <sub>2</sub> O <sub>3</sub>	0.13	0.14	0.13	0.14	0.13	0.13	0.13	0.13	0.13	0.13	0.13	0.14
V <sub>2</sub> O <sub>3</sub>	0.16	0.40	0.44	0.36	0.39	0.36	0.17	0.95	0.62	0.41	0.45	0.85
FeO*	90.59	88.37	88.09	88.98	88.45	92.45	89.36	81.48	93.87	81.73	80.85	86.55
NiO	2.87	0.30	0.29	0.30	0.29	0.29	0.28	0.28	0.28	0.28	0.28	0.29
MnO	1.42	0.56	0.58	0.74	0.63	1.15	0.89	4.07	0.21	0.49	0.58	0.35
MgO	1.28	0.77	1.37	0.69	1.07	0.16	1.50	0.25	0.55	1.42	1.63	0.64

Hole: UNE number:	881B 36	881B 36	881B 43	881B 47	881B 47	882A 52	882A 52	882A 53	882A 62	882A 62	882A 73	882A 73
TiO <sub>2</sub>	6.87	11.88	15.17	13.06	16.30	11.15	11.68	11.57	10.42	11.32	11.49	11.51
Al <sub>2</sub> O <sub>3</sub>	1.39	2.13	1.17	2.88	2.56	3.45	1.85	2.42	3.33	2.31	2.50	2.66
Cr <sub>2</sub> O <sub>3</sub>	0.14	0.13	0.13	0.13	0.13	0.24	0.13	0.13	0.14	0.13	0.13	0.13
V <sub>2</sub> O <sub>3</sub>	0.19	0.84	0.99	0.97	0.28	0.65	0.54	0.45	0.65	0.48	0.43	0.47
FeO*	88.80	84.35	81.53	80.84	78.75	80.25	82.54	82.90	81.72	82.55	83.18	82.79
NiO	0.29	0.28	0.28	0.28	0.26	0.28	0.27	0.28	0.27	0.28	0.27	0.26
MnO	0.81	0.22	0.35	0.37	0.67	0.49	0.56	0.62	0.40	0.54	0.40	0.47
MgO	1.51	0.16	0.38	1.47	1.04	3.48	2.43	1.63	3.09	2.37	1.61	1.72

Ilmenite												
Höle: UNE number:	881B 11	881B 13	881B 24	881B 25	881B 25	881B 36	881B 43	882A 52	882A 53	882A 53	882A 62	882A 73
TiO <sub>2</sub>	45.15	47.58	47.53	39.18	39.51	42.88	30.39	43.01	44.54	45.45	41.75	46.31
Al <sub>2</sub> O <sub>3</sub>	0.22	0.23	0.38	0.46	0.22	0.38	0.40	0.21	0.37	0.49	0.17	0.15
Cr <sub>2</sub> O <sub>3</sub>	0.29	0.13	0.13	0.13	0.13	0.13	0.13	0.12	0.13	0.13	0.13	0.13
V <sub>2</sub> O <sub>3</sub>	0.29	0.29	0.29	0.27	0.45	0.28	0.25	0.26	0.29	0.28	0.28	0.29
FeO*	50.50	48.03	48.94	56.24	56.61	52.67	67.13	52.26	51.11	50.23	53.98	49.82
NiO	0.28	0.26	0.26	0.26	0.27	0.27	0.28	0.25	0.27	0.26	0.27	0.26
MnO	1.61	0.86	0.85	0.56	0.41	0.92	0.32	0.62	0.65	0.84	0.52	1.00
MgO	1.67	2.61	1.63	2.90	2.39	2.45	1.11	3.27	2.65	2.31	2.91	2.04

Notes: UNE number refers to the ash layer number analyzed at UNE (see Tables 1 and 2). All totals are normalized to 100%, volatile free. All Fe reported as FeO\*.

**Table 15. Representative analyses of clinopyroxene (cpx) and amphibole.**

Hole: UNE number:	cpx 881B 13	cpx 881B 28	cpx 882A 64	cpx 882A 66	cpx 882A 70	cpx 882A 73	cpx 883B 90	cpx 887A 171	amphibole 881A 2	amphibole 881B 11
SiO <sub>2</sub>	51.30	50.86	52.77	50.74	51.33	50.74	51.63	52.03	45.93	55.01
TiO <sub>2</sub>	0.41	0.36	0.38	0.61	0.51	0.69	0.55	0.35	1.05	0.14
Al <sub>2</sub> O <sub>3</sub>	1.89	1.73	2.53	2.68	2.85	3.12	2.13	1.62	12.25	12.26
Cr <sub>2</sub> O <sub>3</sub>	0.13	0.13	0.13	0.13	0.13	0.13	0.13	0.13	0	0
FeO*	12.59	14.24	8.76	10.35	9.56	8.85	18.06	8.94	9.94	14.79
MnO	0.46	0.77	0.55	0.37	0.23	0.31	0.62	0.79	0.12	0.14
MgO	15.52	11.92	14.84	15.17	15.69	15.25	17.00	15.11	16.71	15.69
CaO	17.50	19.79	19.63	19.76	19.50	20.55	9.69	20.77	11.62	1.62
K <sub>2</sub> O	0	0	0	0	0	0	0	0	0.36	0.16
Na <sub>2</sub> O	0.20	0.20	0.41	0.19	0.19	0.34	0.20	0.25	2.02	0.20

Notes: UNE number refers to the ash layer number analyzed at UNE (see Tables 1, 2, 3, and 11). All totals are normalized to 100%, volatile free. All Fe reported as FeO\*.